N-Heterocyclic Olefins: An Investigation into a Developing Class of Ligands

by

Katherine Powers

A thesis submitted in partial fulfillment of the requirements for the degree of

Master of Science

Department of Chemistry
University of Alberta

Abstract

An investigation into the relatively new carbene class, *N*-heterocyclic olefins (NHOs) was completed. An improved synthesis of the ligand was developed. NHOs were tested as ligands for late transition metal complexes. Specifically complexes with rhodium, gold and palladium were synthesized and characterized. The rhodium complex allowed for investigation into the donor strength and bonding mode. It was determined that NHOs are good σ-donors and very poor π-acceptors. Comparing the NHOs to the ubiquitous *N*-heterocyclic carbenes (NHCs) showed NHOs to be weaker donors. The NHO-palladium complexes were tested as catalysts for Suzuki-Miyauri cross-coupling reactions. The complexes were active catalysts, but fell short of the currently used NHC complexes.

Preface

Portions of the work discussed in this Thesis were completed in collaboration with other researching with the Rivard group in the Department of Chemistry at the University of Alberta. Specifically, Dr. Christian Hering-Junghans assisted with the synthesis of compounds in Chapter 2. Dr. Hering-Junghans also completed the theoretical calculations in Chapter 2.

All the X-ray crystallographic studies described in this Thesis were preformed by Dr. Robert (Bob) McDonald and Dr. Michael Ferguson, including mounting of crystals, setup and operation of the diffractometer, refinement of structures and preparation of all crystallographic data tables.

Mr. Mark Miskolzie helped to run deuterium ^{2}H NMR and variable temperature NMR spectra. Elemental analyses were preformed by the Analytical Instrumental Laboratory at the University of Alberta. UV-Vis spectrometry was completed with the assistance of Alyona Shynkaruk.

According to the policy in our research group, each chapter of this Thesis is essentially self-contained, prepared in the form of a paper that is intended for publication in peer-reviewed journals. A portion of this Thesis has been published previously and the publications are listed below:

Chapter 2: Powers, K; Hering-Junghans, C; McDonald, R; Ferguson, M. J.; Rivard, E. *Polyhedron*. **2015**, 10.1016/j.poly.2015.07.070.

Acknowledgements

I would like to acknowledge the support and guidance I have received throughout my path to completing my thesis. First and foremost I must thank David Rauch for his constant support and encouragement, even in the face of strife and conflict. My friends Regina Sinelnikov, Kimberly Hyson, Anton Oliynik and Abshek Iyer helped me immensely, constantly being generous with their support, time and art skills. My past and current labmates, specifically Christian Hering-Junghans, Melanie Lui, Paul Lummis, and Alyona Shynkaruk, for their support and involvement in my research. The staff of the chemistry department, especially Dr. Bob McDonald, Dr. Michael Ferguson, Mark Miskolzie, Jason Dibbs, Ryan Lewis, Bernie Hippel, Andrew Yeung, Wayne Moffat, Jennifer Jones and the machine shop. Without their guidance and expertise it would be nearly impossible for our department to run. Dr. Jon Veinot and Dr. Jason Cooke provided crucial encouragement and mentorship throughout my graduate career, and for that I am grateful. I also thank Prof. Eric Rivard for his commitment and guidance throughout my degree completion. I would like to acknowledge my supervisory committee Prof. Rylan Lundgren, Prof. Michael Serpe and Prof. Mark McDermott for their contributions to my education.

Table of Contents

List of Schemes

List of Tables **Page**

List of Figures

List of Symbols, Nomenclature or Abbreviations

$\{^{n}E\}$	Decoupled ^{n}E nucleus
% Conv.	Percent Conversion
Ad	Adamantyl ($C_{10}H_{16}$)
Å	Angstrom, 10^{-10} m
aNHCs	Abnormal *N*-Heterocyclic Carbenes
Ar	Aryl Group
C_6D_6	Deuterated Benzene
$CDCl_3$	Deuterated Chloroform
Cinnamyl	1-Phenylallyl Ligand
CO	Carbonyl Ligand
Cy	Cyclopentyl Ligand
d	Doublet
D	Deuterium
δ	Chemical Shift
DFT	Density Functional Theory
Dipp	2,6-Diisopropylphenyl
η^3	A ligand coordinated through 3 contiguous atoms
FTIR	Fourier Transform Infrared Spectroscopy
H	Proton
HMBC	Heteronuclear Multiple Bond Correlation
HOMO	Highest Occupied Molecular Orbital
HSQC	Heternoclear Single Quantum Coherance
IAd	N,N'-diadamantyl-imidazol-2-ylidene
IMes	1,3-Dimesityl-imidazol-4,5-dihydro-2-ylidene
IPr	1,3-Bis-(2,6-diisopropylphenyl)-imidazol-2-ylidene ($[(HCNDipp)_2C:]$)
iPr	*Iso*-propyl (Me_2CH)
IPrCH2	1,3-Bis-(2,6-diisopropylphenyl)-2-methyleneimidazoline ($(HCNDipp)_2C=CH_2$)
KOtBu	Potassium *tert*-Butoxide
L_n	n Number of Ligands
LUMO	Lowest Unoccupied Molecular Orbital
m	Multiplet

M	Molar
Me	Methyl (-CH_3)
MeOH	Methanol
mol%	Percent by Mole
μ	Bridging Ligand That Connects Two or More Atoms
NBO	Natural Bond Order
n-BuLi	*n*-butyllithium, tetra-μ_3-butyl-tetralithium
NHC	*N*-Heterocyclic Carbene
NHO	*N*-Heterocyclic Olefin
NMR	Nuclear Magnetic Resonance Spectroscopy
ν	Vibrational Frequency
ORTEP	Oak Ridge Thermal Ellipsoid Plot
PEPPSI	Pyridine-Enhanced Precatalyst Preparation, Stabilization, and Initiation
Ph	Phenyl, (-C_6H_5)
rt	Room Temperature
s	Singlet
t	Triplet
*t*Bu	*Tert*-Butyl (-$C(CH_3)_3$)
THF	Tetrahydrofuran
TOF	Turn Over Frequency
UV/vis	Ultraviolet/Visible Spectroscopy

Chapter One: Introduction

1.1 *N*-Heterocyclic Carbenes

1.1.1 History

Carbenes have been of great interest to chemists for decades. The popularity of carbenes has grown exponentially in the past 25 years since the discovery of stable carbenes in the early 1990's.[1] In its simplest form, a carbene is a divalent species (R_2C) in which the central carbon atom has six electrons in its valence shell. Carbenes range from the simplest, and unstable, methylene (CH_2) to extremely large and complex structures than can be stable in air for days. It is this variety of size and shape that has made carbenes a useful tool in synthesis for the modern chemist. Carbenes can be divided into two general groups, carbenes in the singlet state and carbenes in the triplet state (Scheme 1.1).

Chemists have seen evidence of carbene complexes for nearly a century. Tschugajeff synthesized the Pt complexes **1a** and **1b** in 1925,[2] but it was not until 1970 that the structures of these species were determined by X-ray crystallography (Scheme 1.1 A).[3–5] Fischer was the first to prepare and clearly characterize the first metal carbene complex, $(OC)_5W{=}C(OMe)Ph$ (**2**) (Scheme 1.1 B).[6] A Fischer carbene complex can be viewed as being derived from the interaction of a singlet carbene fragment (*e.g.* :CPh(OMe)) with a metal center; specifically the carbene carbon donates its lone pair into an empty metal d-orbital and there is accompanying π-backbonding from a filled metal d-orbital into the empty

p-orbital of the carbon atom; as a result a π-bond is formed between the carbene carbon and the metal center. Fischer carbene complexes generally form with metals in low formal oxidation states and when strong π-accepting ligands (such as CO) are present (Scheme 1.1 B). The presence of electron withdrawing CO ligands at the metal alters the polarization of the M=C bond so that the carbon center becomes electrophilic.

In the mid 1970s, Richard Schrock discovered a new class of carbene-bound metal complex.[7] These so-called Schrock carbene complexes can be viewed as the interaction of a triplet carbene ligand with a metal center to form two polarized M-C bonds (Scheme 1.1 C); Schrock carbene complexes contain nucleophilic carbene carbon centers and metals with formally high oxidation states.

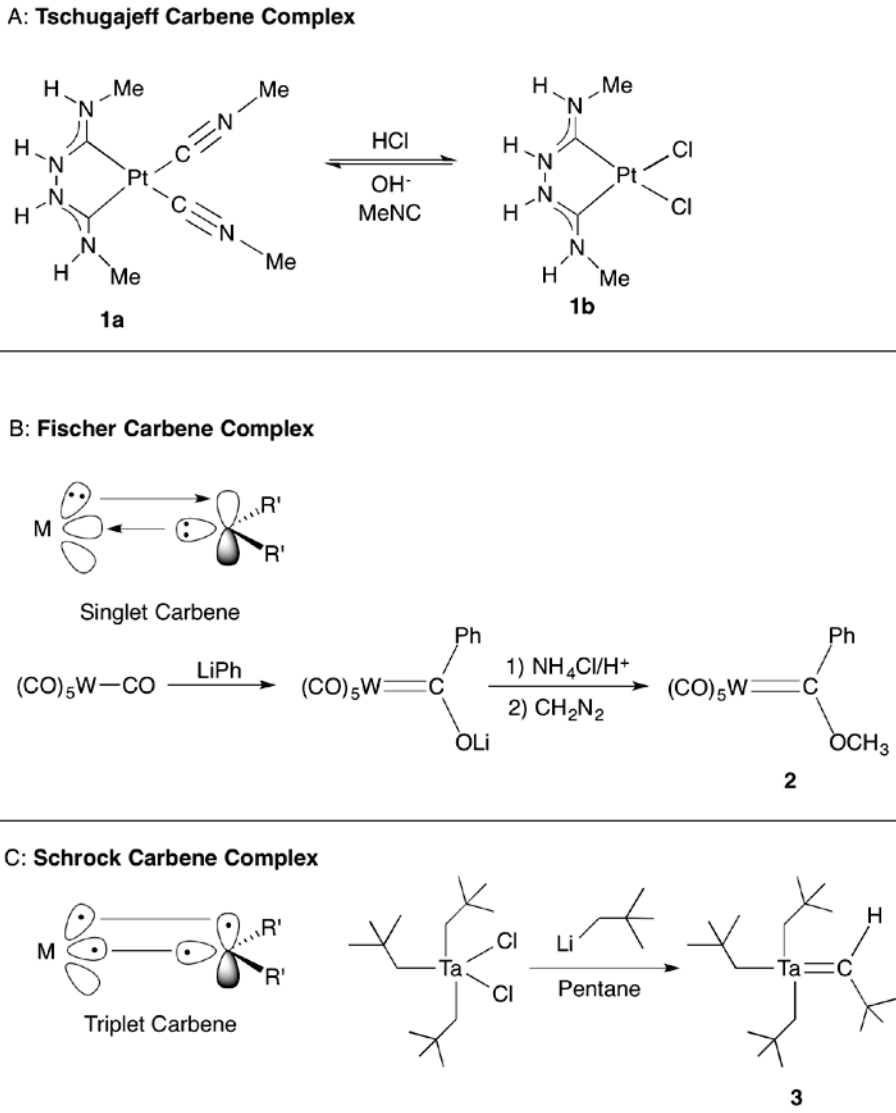

Scheme 1.1: A) The first synthesized carbene-metal complexes 1a and 1b. B) Initial example of a Fischer carbene-metal complex. C) Synthesis of a Schrock carbene complex.

The quest to obtain stable singlet carbenes necessitated both electronic and steric stabilization strategies to prevent their dimerization to alkenes $R_2C{=}CR_2$. Bertrand *et al.* reported the synthesis of a stable free λ^3-phosphino carbene $[(i\text{-}Pr_2N)_2PC(SiMe_3)]$,[8] however this carbene could not act as a ligand due to its weakly nucleophilic character. Soon after the

discovery of Bertrand's carbene, Arduengo reported the first stable *N*-heterocyclic carbene (NHC) bearing adamantyl side groups (Scheme 1.2 B).[1] As will be seen, NHCs are very good electron pair donors and have led to a revolution in coordination chemistry. According to SciFinder, only a few papers were published in the early 1990's, however during 2014 more than 1,000 papers were published in this field. Wanzlick was the first to actively explore the synthesis of potentially stable *N*-heterocyclic carbenes. One synthetic route to transient carbenes involved the α-elimination of chloroform to yield dimerized products (Scheme 1.2 A).[9–11] The key to Arduengo's successful synthesis of a stable NHC was to place bulky NHC adamantyl substituents on the heterocycle to sterically prevent dimerization (Wanzlick's carbene was substituted with less bulky phenyl groups); in addition, the neighboring nitrogen atoms can participate in N-C π-interactions which leads to a carbon center that approaches an octet configuration (Scheme 1.2 C).

A: **Wanzlick's Carbene**

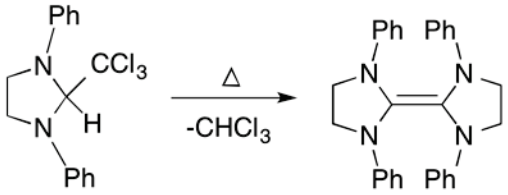

4

B: **Arduengo's Carbene**

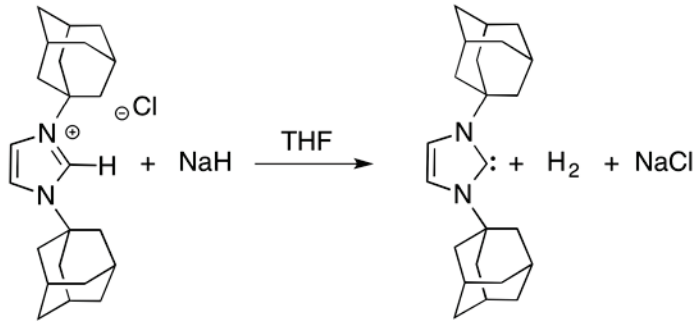

5

Resonance Structures of NHCs

Scheme 1.2: Wanzlick's carbene (**4**) was insufficiently sterically hindered to prevent dimerization. The very sterically demanding adamantyl substituents on Arduengo's carbene (**5**) prevented dimerization, leading to the first stable free carbene. The carbene is further stabilized by the resonance structures shown in C.

1.1.2 Structural Versatility of *N*-Heterocyclic Carbenes

NHCs combine ease of synthesis with a high level of tunability, thus the steric and electronic characteristics can be easily manipulated in several ways, making these donors of great utility to chemists.[12]

NHCs can have singlet ground states and in turn can act as good two-electron, sigma-donors to various electron deficient metals and non-metals. The C_{NHC}-E bonding (E = element) can be depicted using a dative formalism (*i.e.* arrow) that shows that these bonds cleave in a heterolytic fashion.[13] In addition to being very strong σ-donors, NHCs are also weak to moderate π-acceptors.[14] As a result, NHCs can form very strong bonds with metal centers and other types of atoms. The σ-donating and π-accepting electronic properties of NHCs can be tuned easily by changing the nature of the substituents attached to the carbon and nitrogen atoms that make up the heterocyclic core.[15]

The electronic effects of the substituents can be readily quantified via the determination of Tolman Electronic Parameters (TEPs). TEPs measure the electron withdrawing or donating ability of a ligand. Originally these values were derived by preparing various 18-electron Ni(0) complexes L•$Ni(CO)_3$ (L = ligand),[16] and then infrared spectroscopy is used to measure the carbonyl stretching frequencies, ν(CO). As the electron donating power of the ligand increases, the carbonyl stretching frequency decreases as electron density populates C-O π* orbitals. Resonance forms of metal-carbonyl bonding can explain the shift in

frequency. The electron density of the metal center effects the π-backbonding of the carbonyl ligand to the metal center (Scheme 1.3) The electronic effects of installing varying substituents about the NHC can evaluated, with Scheme 1.4 illustrating some examples of electron donating ability series.

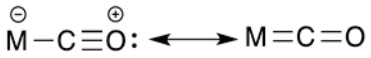

Scheme 1.3: Resonance forms of the M-CO bond. The change in strength of the C-O bond is reflected in a shift of the ν(CO) frequency in the IR spectrum.

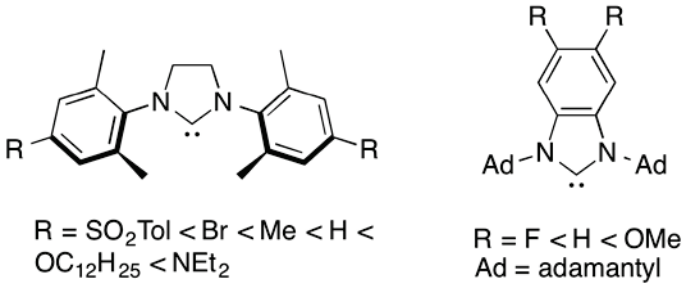

Scheme 1.4: Examples of electronics tuning in NHCs. Below the structure is the electron donating ability of the species, ordered via substituents.

In addition to shifting the electronic properties of the NHCs, substituents on the heterocycle also influence steric effects and in turn their ability to act as co-ligands within various metal-based catalysts; recent examples of sterically encumbered NHCs that are used to support palladium-mediated carbon-nitrogen bond formation can be found in Scheme 1.5.

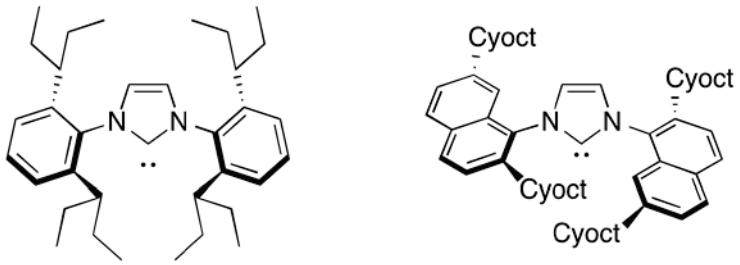

IPent

Anti-(2,7)-ICyoctNap
Cyoct = cyclooctyl

Scheme 1.5: Examples of steric bulk tuning in NHCs. The steric bulk of the NHC is most affected by changing the substituents on the heteroatom position.

1.1.3 Synthesis of *N*-Heterocyclic Carbenes

The large variety of NHCs currently in use is partially due to the wide variety of synthetic routes that have been developed. The most common synthetic method for obtaining symmetrical NHCs is the reaction of a primary amine with glyoxal and formaldehyde to give imidazolium salts; these salts can then be deprotonated by a strong base to form a free carbene (Scheme 1.6) that can generally be stored under inert atmosphere. Each of these synthetic steps, besides deprotonation, can be completed in air and give high yields of NHC.[17]

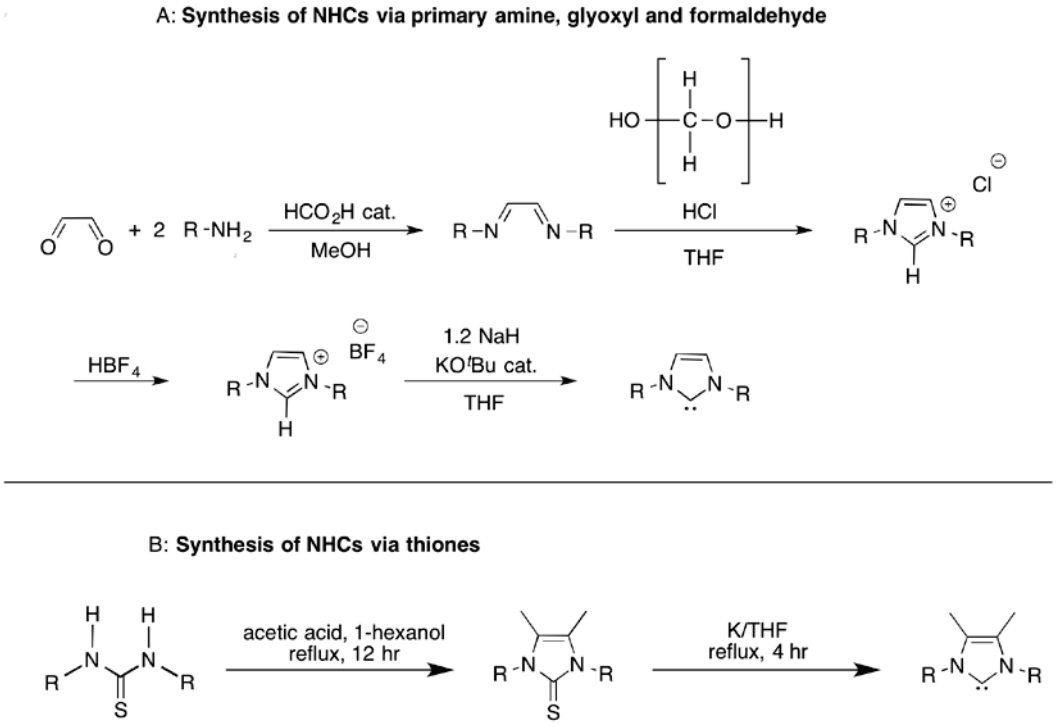

Scheme 1.6: Two commonly used synthetic routes for the formation of stable NHCs.

1.2 *N*-Heterocyclic Olefins

Similar to the development of NHCs, *N*-heterocyclic olefins (NHOs) (Scheme 1.7) have been known in the literature for many years.[18] In contrast to NHCs, NHOs remain an emerging class of ligand with only more recent sustained interest from the chemical community.[19–21] In NHOs, considerable electron density is placed at the terminal carbon atom within an exocyclic olefin residue, as shown by the resonance forms in Scheme 1.7; the resulting electron density at the terminal CH_2 group can be used to form a coordinative bond with a metal center. Due to the fact that many NHOs are derived from their *N*-heterocyclic carbene analogues, NHOs have similar tunable characteristics as previously discussed for NHCs. *N*-Heterocyclic olefins can be easily sterically and electronically tuned, making them promising candidates for use as ligands in catalysis. Due to the presence of a highly polarized terminal olefin group, the donor site in an NHO is of a softer nature than NHCs (according to the Hard-Soft Acid-Base Principle),[22] as the electron density is in an orbital of more p-character. This softer donor character may make the NHO a better donor than NHCs towards softer metals such as Ni(0) and Pd(0).[23]

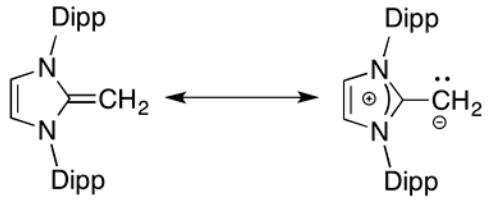

Scheme 1.7: Resonance structures of $[(HCNDipp)_2C{=}CH_2]$ (Dipp = 2,6-$^{i}Pr_2C_6H_3$), a commonly used NHO ligand. Upon coordination to a metal, the resonance form to the right is stabilized.

NHOs were first reported by Kuhn and coworkers in 1993[18] and the donating ability of these species was demonstrated by their coordination to electron deficient main group (BH_3) and transition metal ($Mo(CO)_5$) species. Our group has also explored the use of NHOs as Lewis bases in the stabilization of low oxidation state dihydrides such as GeH_2 and SnH_2.[21] This observation is of particular interest as more widely explored ligands, such as phosphines, were unable to form stable adducts with inorganic methylenes (EH_2; E = Si-Sn). More recently, NHOs have also been used in CO_2 sequestration[19] and to initiate the polymerization of polar methacrylate-based monomers.[20]

1.3. Bonding within Late Transition Metal Carbene Complexes

N-heterocyclic carbenes have been widely used as ligands in a variety of metal-carbene complexes. Specifically of interest in this Thesis is the coordination of carbenes to late transition metals (Group 8-12) as the resulting complexes can be active catalysts for important processes, such

as C-C or C-N bond formation.[12] Initially NHCs were thought to be mainly sigma-donating in nature with minimal to no π-backbonding occurring from the metal to the NHC ligand. However more recent work has determined that the degree of metal-to-carbon backbonding in an NHC-metal complex is not negligible.[24] In general, NHCs form polar M-C interactions with over 75 % of bonding electron density residing on the carbene carbon. In addition, about 15-20 % of the overall bond strength is due to the presence of the abovementioned C_{NHC}-M π-backbonding, which can be viewed as being mainly due to a M(d) to C-N π* interaction (Scheme 1.8).[14]

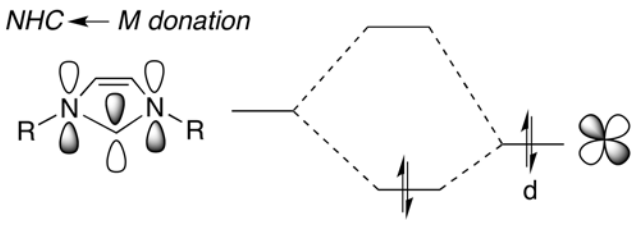

Scheme 1.8: A general diagram of the π-backbonding interaction between a metal and an NHC π-backbonding accounts for around 15-20 % of the M-C bond strength.

When one examines bond energies, transition metal (d-block) elements tend to follow different trends from the main group (p-block) elements. Specifically, the bond strength between a ligand and metal generally increases down a transition metal group whereas in the p-block the bond strength usually decreases down a group due to increased d-orbital overlap within M-L bonds.[25] This trend makes second row metals

attractive metal centers for transition metal catalysts. Second and 3rd row metals are often more rare, costly and toxic than the 1st row metals, so there is a real push to explore new catalysis systems based on Earth abundant metals such as iron, nickel and copper. Further down those groups, rhodium, iridium and palladium are some of the most rare metals in the Earth's crust but are used in some of the most ubiquitous transition metal based catalysts.[26]

The number of known NHC-transition metal complexes is vast.[27] One of the most important carbene-containing complexes developed in the past 20 years is Grubbs' second-generation olefin metathesis catalyst.[28] The phosphine-based first generation of the catalyst $[(Cy_3P)_2RuCl_2(CHPh)]$ is very active and tolerant to both electron donating and withdrawing functional groups, however the increased activity of the NHC second generation that makes this catalyst a useful tool for synthetic chemists seeking to activate more chemically robust olefins for metathesis (Scheme 1.9). This increase in activity is due to the enhanced donor strength of NHCs relative to phosphines, which enables dissociation of the PCy_3 ligand trans to the SIMes donor in Grubbs' 2nd generation catalyst to occur more easily, leading to the formation of the catalytically active 14 electron complex $[(SIMes)RuCl_2(CHPh)$.

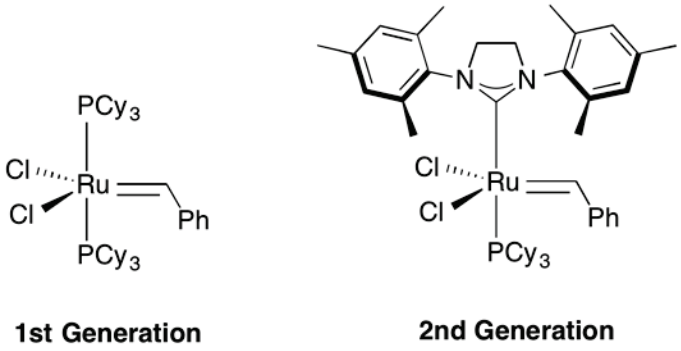

1st Generation **2nd Generation**

Scheme 1.9: Grubbs' 1st and 2nd generation catalyst

1.4. Suzuki-Miyaura Cross-Coupling

1.4.1 Background

NHC-transition metal complexes have been used as catalysts in cross-coupling reactions. Cross-coupling is an important reaction that uses a metal catalyst to form carbon-carbon and carbon-heteroatom bonds (Scheme 1.10). Specifically here I will focus on Suzuki-Miyaura cross-coupling. Akira Suzuki and coworkers first developed the system in 1979 based on the phosphine-palladium catalyst $[Pd(PPh_3)_4]$.[29] Due to the non-toxic nature of arylboronic acids $ArB(OH)_2$ often used in Suzuki-Miyaura coupling, this has become an important method to prepare value added pharmaceuticals throughout industry and has also been explored in great detail by academia. As a reflection of the importance of Suzuki-Miyaura cross-coupling, Akira Suzuki shared the 2010 Nobel Prize in Chemistry with Richard F. Heck and Ei-ichi Negishi for their work in the field of palladium-catalyzed cross-couplings for organic synthesis.[29,30]

At the most basic level, the Suzuki-Miyaura reaction involves the coupling of an organoboron species with an aryl halide, using a palladium-based catalyst in the presence of a base (Scheme 1.10). This transformation is generally used to prepare $C(sp^2)$-$C(sp^2)$ bonds and is amenable to various substrates, with the formation of biaryl products being the most common.

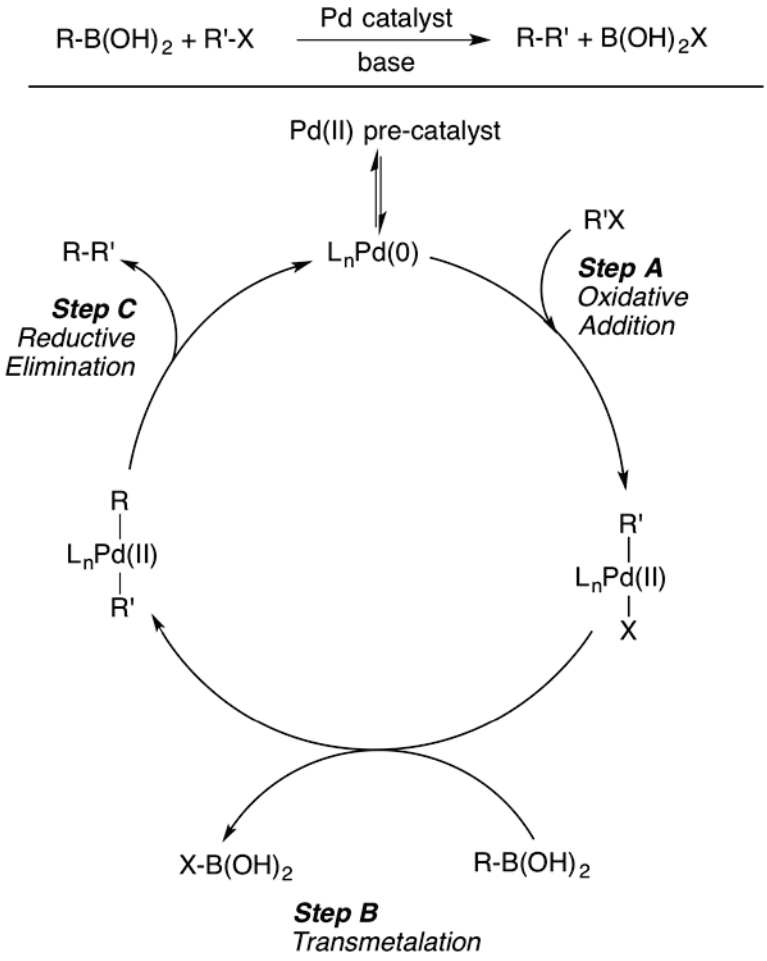

Scheme 1.10: The top reaction is a summary of the Suzuki-Miyaura cross-coupling reaction. Below is a proposed catalytic cycle with key transformations divided into three steps: A) Oxidative Addition (often the rate determining step), B) Transmetalation, and C) Reductive Elimination.

1.4.2 Mechanistic Insights

The catalytic cycle associated with Suzuki-Miyaura coupling has been widely studied, but is still not completely understood. The mechanism and kinetic rates depend heavily on the substrates in use and the nature of the catalyst and base. Here I will discuss a general mechanism for the cycle and how this mechanism is influenced by various factors.

The first step (Step A in Scheme 1.10) in the Suzuki-Miyaura catalytic cycle is the oxidative addition of an aryl halide (ArX; X = Cl, Br or I) to a low-coordinate, electron rich Pd(0) species. This reaction is usually the rate-determining step for most standard Suzuki-Miyaura couplings. The rate of this step is affected by three main factors; the first factor is the nature of the aryl halide, also the steric hindrance of both the aryl halide and boronic acid, the last factor is the activity of the catalyst. The nature of the aryl halide is influenced by steric effects and electronics.[12] The bond dissociation enthalpies (BDE) for the aryl halides increase as the halide becomes lighter (F > Cl > Br > I). Therefore it is more difficult to oxidatively add Ar-Cl than it is to add Ar-Br (Ar = aryl group), for example. Aryl chlorides have been targeted by industry as desirable substrates since they are less expensive and consequently more available than aryl bromides or iodides; however the high C-Cl BDEs often slow the reaction rate to unacceptable levels or even prevent oxidation addition from occurring.[14] In addition to the effects of the halide, the bulkier the aryl group is, the more difficult the oxidative

addition step becomes. The formation of $C(sp^3)$-$C(sp^3)$ and $C(sp^3)$-$C(sp^2)$ bonds are also difficult as a side reaction, β-hydride elimination, can occur after the oxidative addition step. β-Hydride elimination can quickly occur in the palladium-alkyl group formed, leading to the liberation of an alkene and formation of a metal hydride, which counteracts productive C-C bond formation.[31] The oxidative addition step can also be aided or hindered by the substituents on the aryl halide. Electron-withdrawing groups remove electron density from the carbon-halide bond, making the C-X bond more reactive by lowering the energy of the C-X σ* orbital. On the other side of the coin, electron-donating groups can make the oxidative addition step more difficult. Therefore on ongoing major theme of Suzuki-Miyaura cross-coupling research focuses on finding improved catalysts and reaction conditions that enable the coupling of difficult substrates, such as aryl chlorides, under mild conditions.

The rate of this first oxidative addition step is increased by the presence of a bulky spectator ligand on the palladium (0) species. This is not necessarily intuitive as it could be easy to think that a bulky spectator ligand would prevent the aryl halide from coordinating to the palladium center, and this may be true to some extent. However, the bulky spectator ligand also greatly increases the rate of generation of the reactive low-coordinate palladium (0) intermediate that reacts with the aryl halide (after ligand dissociation). In addition many large ancillary ligands, such as the

biarylphosphines developed by Buchwald (Scheme 1.11) help stabilize Pd(0) sites via additional arene-metal interactions.[12]

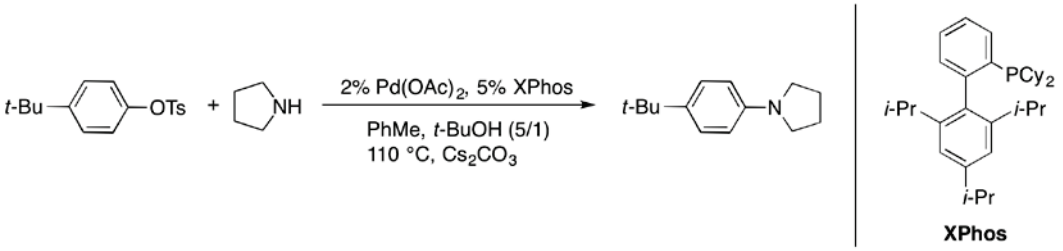

Scheme 1.11: An example of a biarylphosphine ligand, XPhos, as a ligand for carbon-nitrogen bond formation catalysis.[32]

The nature of the next step in the cycle, transmetalation (Scheme 1.10; Step B), is currently still under debate.[33] The role of the base in the transmetalation step has been investigated and two likely routes have been proposed as seen in Scheme 1.12. Pathway A proceeds via a four-coordinate borate that is generated in situ by the base (for simplicity this base is shown as hydroxide in the Scheme). Pathway B occurs via first an oxo-palladium which then coordinates with the boronic acid to form a boronate. Both pathways are viable routes, and the paths may differ depending on conditions of the reaction. Pathway B has been proposed to be the correct pathway for reactions under aqueous conditions, but the pathway is unclear in organic solvent. The presence of water can also cause protodeboronation, the replacement of the boron with a proton, preventing any coupling from occurring.

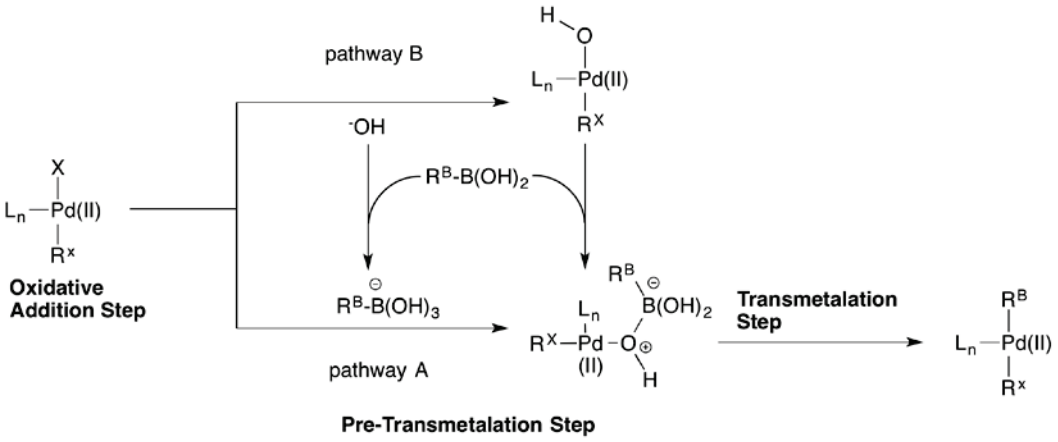

Scheme 1.12: Both pathways A and B result in the same palladium intermediate; in pathway A the base forms a borate. Pathway B the base forms both a borate and an oxo-palladium species.

The final step in the cycle is the reductive elimination of the two organic moieties attached to palladium (Scheme 1.10; Step C). This results in the formation of the coupled product, R-R′, and the regeneration of the active catalyst. This step is also aided by the presence of a bulky spectator ligand(s) on the palladium center, allowing for the regeneration of the Pd(0) active catalyst. The reductive elimination of the product relieves the extreme steric congestion around the palladium center, while bulky ligands provide a means of forcing the two eliminating groups to be in close proximity to each other (a requisite for C-C bond formation).[12]

1.4.3 Catalysis Design

As is true for nearly all types of catalysis, the current direction for Suzuki-Miyaura cross-coupling is towards milder conditions, lower catalytic loadings, and the use of less expensive and non-toxic substrates and catalysts. Most of these goals could be met with the design of new catalysts, and the pathway to an improved catalyst often follows an iterative process. Currently, the most active catalysts for Suzuki-Miyaura cross-coupling are based on the second row element, palladium, as the metal forms stronger M-L and M-X/R bonds than its lighter nickel congener, enabling stable intermediates to be formed, while these bonds are still weaker than for platinum, allowing important bond breaking processes like reductive elimination to occur on a catalytically competent rate.

Herrmann and his team developed one of the first carbene-supported palladium pre-catalysts for Suzuki-Miyaura coupling in 2002.[34] The pre-catalyst contained Arduengo's first NHC as a ligand [$Pd(IAd)_2$] (IAd = 1,3-di(adamantyl)imidazol-2-ylidene) and was remarkably active, achieving a turnover frequency (TOF) of 573 [(mol product)(mol Pd)$^{-1}$ h^{-1}] for the coupling of tolylchloride and phenylboronic acid. This was the highest TOF for a room temperature aryl chloride coupling at the time of publication; in this instance the base used for activation was CsF while the solvent was 1,4-dioxane (Table 1.1).

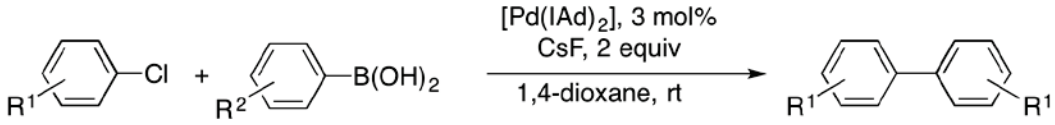

R^1	R^2	Time	Conversion %
4-CH_3	H	20 min	97
4-OCH_3	H	6 hrs	>99
4-CF_3	H	6 hrs	>99
4-$COCCH_3$	3-OCH_3	24 hrs	95

Table 1.1: Herrmann's early work with [$Pd(IAd)_2$] (IAd = [$(HCNAd)_2C$:]; Ad = adamantyl) as a catalyst for cross-coupling.

1.4.4 Ligand Design and the Pre-catalyst Concept

The requirements for an active Suzuki-Miyaura catalyst can be gleaned from the mechanism presented in Scheme 1.10 and the discussion in the previous section. Specifically, the catalyst should have a sterically encumbered spectator ligand (or ligands) to enable low-coordinate environments to form for the oxidative addition of substrates, while also aiding the reductive elimination step at the end of the cycle. However if the ligand is too bulky then access to the L_xPdRX intermediate by the coupling partner (*i.e.* the arylboronate) during transmetalation could be suppressed. Also, the ligand should be able to form reasonably stable M-L

interactions, especially to Pd(0) centers, thereby preventing metal loss and catalyst deactivation. One could enhance the M-L interaction by promoting Pd-L π-backbonding or by using a soft donor ligand (perhaps an NHO) that maximizes metal-ligand orbital overlap. It is important to note that if too much electron density is removed from the palladium (0) center via π-backbonding then oxidative addition becomes more challenging and the catalyst rate will get slower.

Given the high reactivity of many Pd(0) species, a common procedure is to use a Pd(II) pre-catalyst that is reduced *in situ* to yield an active Pd(0) catalyst. This leads to the development of a class of pre-catalysts containing ligands that are easily removed, leaving behind a very active palladium(0) species. The two classes of pre-catalysts that will be the focus of this introduction are the Pd-PEPPSI (Scheme 1.13) and (L)Pd(η^3-R-allyl)Cl (L = ligand) complexes.

The palladium-PEPPSI family of pre-catalyst were developed by Organ and coworkers in 2006.[35] PEPPSI is an acronym for Pyridine Enhanced Pre-catalyst Preparation Stabilization and Initiation. The PEPPSI system is widely used throughout industry and academia. PEPPSI-IPr is even available for purchase at chemical suppliers by the kilogram (for those with over $50k to spend).[36]

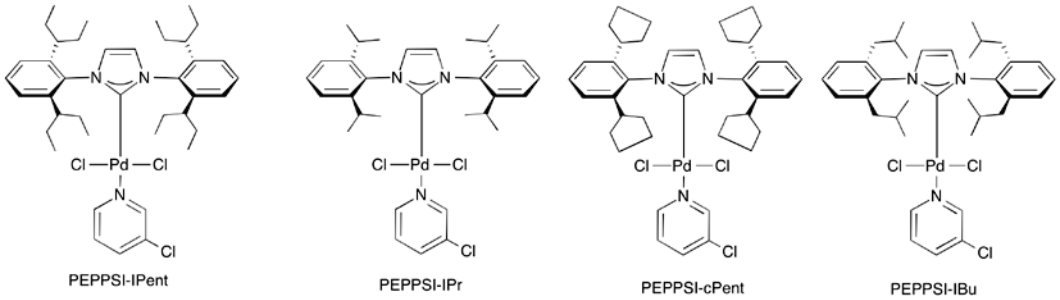

Scheme 1.13: Various Pd-PEPPSI catalysts synthesized by Organ and coworkers. This series was used to test the effects of ligand flexibility and overall steric bulk.

The utilization of 3-chloropyridine as the throwaway ligand in the PEPPSI pre-catalyst is a large part of the system's success. Just as the name suggests, the 3-chloropyridine ligand stabilizes the Pd(II) center so most PEPPSI complexes are air- and moisture-stable for long periods of time. Also, due to the lability of the ligand in solution the initiation step is enhanced. The pre-catalyst will easily lose the pyridine ligand, making the activation step faster and easier than previously published systems such as the Herrmann system discussed previously.[37]

Organ and coworkers' work with the PEPPSI pre-catalysts also gives insight into the design of a catalyst. A series of PEPPSI complexes were synthesized with varying steric bulk from the NHC around the palladium center, and key trends could be observed. For example, it was determined that increased, flexible bulk around the palladium center led to the most highly active pre-catalysts for Suzuki-Miyaura cross-coupling. This is evident in the percent conversions achieved for the coupling of 2,6-dimethylphenylboronic acid and 1-bromo-2-methoxynaphthalene (Table 1.2). The most successful pre-catalyst in Organ's original work was the

PEPPSI-IPent system. IPent is an NHC with bulky and very flexible 2,6-diisopropylphenyl substituents on the *N*-positions of the carbene ligand. Next, to verify the importance of the flexibility of the steric bulk, the activity of the PEPPSI-IPent pre-catalyst was compared with the PEPPSI-cPent complex. The steric bulk of cPent is similar in size to the bulk of IPent, however the cPent substituents are cyclized, making the bulk more restricted than the flexible IPent substituents. The PEPPSI-IPent system achieves a conversion more than 10 times faster than with PEPPSI-cPent.[37]

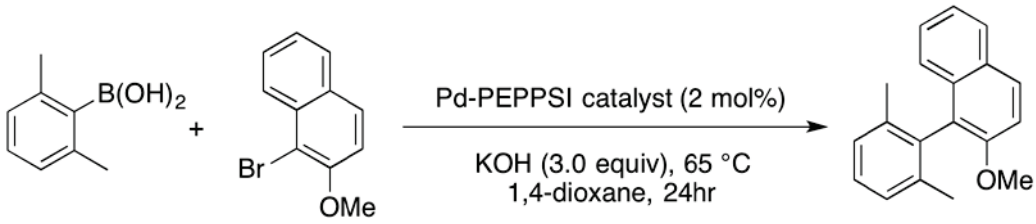

Pd-PEPPSI Catalyst	Percent Conversion (%)
PEPPSI-IPr	41
PEPPSI-IPent	91
PEPPSI-IBu	4
PEPPSI-cPent	9

Table 1.2: The percent conversion for this example reaction highlights the importance of flexible steric bulk in the NHC ligand in various PEPPSI pre-catalysts.

A catalyst group of related activity as the PEPPSI complexes was developed by Nolan and coworkers in 2005.[38] Nolan's catalyst, (NHC)Pd(allyl)Cl, utilizes an η^3-allyl sacrificial ligand that can be easily removed. Nolan has proposed two routes for the activation/reduction of the (NHC)Pd(allyl)Cl pre-catalyst. In one pathway (Scheme 1.14; Step 2A), chloride-alkoxide exchange is followed by a formal reductive elimination of the allylether $^{t}BuOCH_2CH{=}CH_2$ (Step 3A). In the second proposed route (Step 2B, Scheme 1.14), the $O^{t}Bu$ base directly attacks an allyl moiety leading to halide elimination and reduction at Pd. In each route, a low-coordinate NHC-Pd(0) catalyst is liberated.

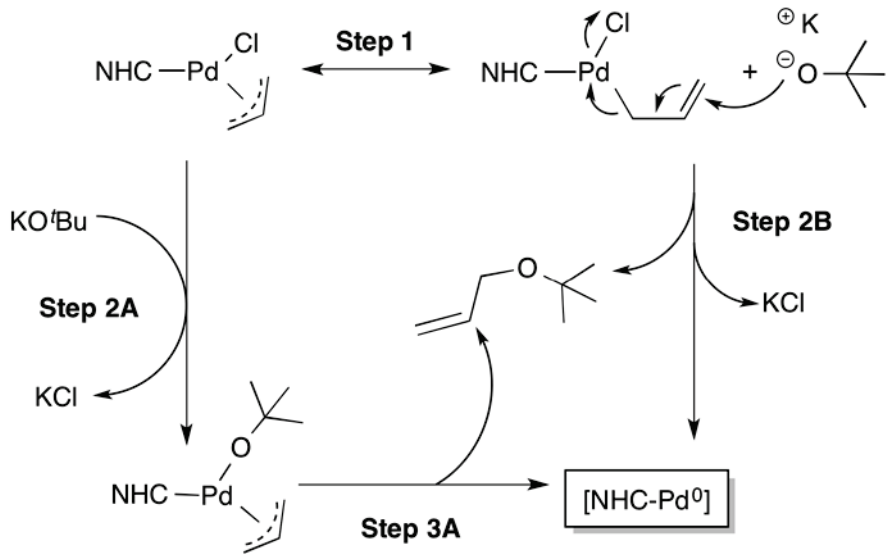

Scheme 1.14: Nolan's proposed mechanism of the activation of NHC-supported Pd(II) pre-catalyst.

The Nolan group also synthesized and studied a series of modified (NHC)Pd(R-allyl)Cl systems. The presence of an unsubstituted allyl ligand led to a more stable pre-catalyst, while placement of an alkyl or aryl group on the allyl ligand increased the steric bulk around the palladium center and decreases the back-bonding from the metal to the olefin, making the pre-catalyst less stable to reductive elimination. The most common and successful (NHC)Pd(R-allyl)Cl system is (IPr)PdCl(cinnamyl) (cinnamyl = 1-phenylallyl; IPr = $[(HCNDipp)_2C:]$).[38–40] (IPr)PdCl(cinnamyl) has been used to couple bulky aryl chlorides with sterically encumbered arylboronic acids at room temperature with catalytic loadings as low at 0.05 mol %.

1.5. Summary of Thesis Content

This thesis is comprised of two research chapters, wherein the work was completed over the course of 24 months between August 2013 and November 2015.

Chapter 2 explores the synthesis and the characteristics of *N*-heterocyclic olefins. An improved synthesis of NHOs is presented, which involves the installation of a terminal CH_2 group through the reaction of an *N*-heterocyclic carbene with an excess of $ClCH_2SiMe_3$. In addition to the improved general synthesis of NHOs, Chapter 2 provides an evaluation of NHO donor strength by examining IR and NMR data for various NHO-$Rh(CO)_2Cl$ complexes.

Chapter 3 focuses on the use of NHOs as ligands in transition metal-mediated catalysis. To begin, some preliminary coordination chemistry with late row metals such as gold and palladium is presented, and their structural and spectroscopic characteristic compared with known NHC analogues. Lastly the use of NHO-supported Pd(II) pre-catalysts for Suzuki-Miyaura cross-coupling is reported.

References

(1) Arduengo, A. J.; Harlow, R. L.; Kline, M. *J. Am. Chem. Soc.* **1991**, *113*, 361.

(2) Tschugajeff, L.; Skanawy-Grigorjewa, M.; Posnjak, A.; Skanawy-Grigorjewa, M. Z. *Anorg. Allg. Chem.* **1925**, *148*, 37.

(3) Rouschias, G.; Shaw, B. L. *J. Chem. Soc., Dalton Trans.* **1970**, 183.

(4) Burke, A.; Balch, A. L.; Enemark, J. H. *J. Am. Chem. Soc.* **1970**, *92*, 2555.

(5) Butler, W. M.; Enemark, J. H.; Parks, J.; Balch, A. L. *Inorg. Chem*. **1973**, *12*, 451.

(6) Fischer, E. O.; Maasböl, A. *Angew. Chem. Int. Ed. Engl.* **1964**, *3*, 580.

(7) Schrock, R. R. *J. Am. Chem. Soc*. **1974**, *96*, 6796.

(8) Igau, A.; Grutzmacher, H.; Baceiredo, A.; Bertrand, G. *J. Am. Chem. Soc*. **1988**, *110*, 6463.

(9) Wanzlick, H. W.; Jahnke, U. *Chem. Ber*. **1968**, *101*, 3753.

(10) Wanzlick, H. W.; Schikora, E. *Angew. Chem. Int. Ed. Engl.* **1960**, *72*, 494.

(11) Wanzlick, H. W. *Angew. Chem. Int. Ed. Engl*. **1962**, *1*, 75.

(12) Hartwig, J. F. Organotransition Metal Chemistry; *University Science Books*, **2010**.

(13) Díez-González, S. N-Heterocyclic Carbenes: From Laboratory Curiosities to Efficient Synthetic Tools; *Royal Society of Chemistry*, 2011.

(14) Fortman, G. C.; Nolan, S. P. *Chem. Soc. Rev.* **2011**, *40*, 5151.

(15) Dröge, T.; Glorius, F. *Angew. Chem. Int. Ed*. **2010**, *49*, 6940.

(16) Tolman, C. A. *Chem. Rev.* **1977**, *77*, 313.

(17) Bantreil, X.; Nolan, S. P. *Nat. Protoc.* **2011**, *6*, 69.

(18) Kuhn, N.; Bohnen, H.; Kreutzberg, J.; Bläser, D.; Boese, R. *Chem. Commun.* **1993**, 1136.

(19) Wang, Y.-B.; Wang, Y.-M.; Zhang, W.-Z.; Lu, X.-B. *J. Am. Chem. Soc.* **2013**, *135*, 11996.

(20) Jia, Y.-B.; Wang, Y.-B.; Ren, W.-M.; Xu, T.; Wang, J.; Lu, X.-B. *Macromolecules* **2014**, 47, 1966.

(21) Al-Rafia, S. M. I.; Malcolm, A. C.; Liew, S. K.; Ferguson, M. J.; McDonald, R.; Rivard, E. *Chem. Commun*. **2011**, *47*, 6987.

(22) Pearson, R. G. *J. Am. Chem. Soc*. **1963**, *85*, 3533.

(23) Fürstner, A.; Alcarazo, M.; Goddard, R.; Lehmann, C. W. *Angew. Chem. Int. Ed.* **2008**, *47*, 3210.

(24) Khramov, D. M.; Lynch, V. M.; Bielawski, C. W. *Organometallics* **2007**, *26*, 6042.

(25) Crabtree, R. H. The Organometallic Chemistry of the Transition Metals; *John Wiley & Sons Inc*., **2005**.

(26) Hanukoglu, I. List of Elements of the Periodic Table - Sorted by Abundance in Earth's crust http://www.science.co.il/PTelements.asp?s=Earth (accessed Aug 26, 2015).

(27) Nelson, D. J. *Eur. J. Inorg. Chem.* **2015**, 2012.

(28) Scholl, M.; Ding, S.; Lee, C. W.; Grubbs, R. H. *Org. Lett*. **1999**, *1*, 953.

(29) Suzuki, A. *Angew. Chem. Int. Ed.* **2011**, *50*, 6722.

(30) Negishi, E.-I. *Angew. Chem. Int. Ed.* **2011**, *50*, 6738.

(31) Cárdenas, D. J. *Angew. Chem. Int. Ed.* **2003**, *42*, 384.

(32) Huang, X; Anderson, K. W.; Zim, D.; Jiang, L.; Klapars, A.; Buchwald, S. L. *J. Am. Chem. Soc*. **2003**, *125*, 6653.

(33) Lennox, A. J. J.; Lloyd-Jones, G. C. *Angew. Chem. Int. Ed*. **2013**, *52*, 7362.

(34) Gstöttmayr, C. W. K.; Böhm, V. P. W.; Herdtweck, E.; Grosche, M.; Herrmann, W. A. *Angew. Chem. Int. Ed*. **2002**, *41*, 1363.

(35) O'Brien, C. J.; Kantchev, E. A. B.; Valente, C.; Hadei, N.; Chass, G. A.; Lough, A.; Hopkinson, A. C.; Organ, M. G. *Chem. Eur. J*. **2006**, *12*, 4743.

(36) PEPPSI-IPr Catalyst 98% http://www.sigmaaldrich.com/catalog/product/aldrich/669032?lang=en&region=CA (accessed Aug 26, 2015).

(37) Valente, C.; Calimsiz, S.; Hoi, K. H.; Mallik, D.; Sayah, M.; Organ, M. G. *Angew. Chem. Int. Ed***. 2012**, *51*, 3314.

(38) Marion, N.; Navarro, O.; Mei, J.; Stevens, E. D.; Scott, N. M.; Nolan, S. P. *J. Am. Chem. Soc.* **2006**, *128*, 4101.

(39) Marion, N.; Nolan, S. P. *Acc. Chem. Res.* **2008**, *41*, 1440.

(40) Díez-González, S.; Marion, N.; Nolan, S. P. *Chem. Rev.* **2009**, *109*, 3612.

Chapter Two: Improved Synthesis of *N*-heterocyclic Olefins and Evaluation of Their Donor Strength

2.1 Introduction

N-Heterocyclic olefins (NHOs) represent a relatively new and emerging carbon-based ligand class with donor characteristics that complement those found within their well-known *N*-heterocyclic carbene (NHC) counterparts. *N*-Heterocyclic olefins were first reported by Kuhn and coworkers in the early 1990s, and the initially reported NHOs, such as $ImMe_4CH_2$ ($[(MeCNMe)_2C{=}CH_2]$), were shown to be sufficiently nucleophilic to coordinate as neutral two-electron donors to both main group and transition metal-based species (*e.g.* BH_3, $W(CO)_5$, RhCl(1,5-cyclooctadiene)). From these initial studies it is expected that NHOs will exhibit similar coordination behavior as the widely explored phosphines and carbenes. However NHOs are anticipated to be softer donors when compared to NHCs as they possess highly polarized exocyclic C=C double bonds which places considerable electron density of high p-orbital character at the terminal/ligating carbon atoms;[1–5] as a result, NHOs might show affinity for low oxidation state Ni(0) and Pd(0) sites present during many catalytic processes.

These characteristics, along with a high inherent degree of structural tunability (attainable by either ring or methylene carbon substitution), could be utilized to advance both main group element and transition metal-based catalysis.[6]

The exploration of *N*-heterocyclic olefins as Lewis bases in our group began in 2011 with the synthesis of $IPrCH_2$ adducts of the low oxidation state dihydrides, GeH_2 and SnH_2 ($IPrCH_2$ = $[(HCNDipp)_2C{=}CH_2]$; Dipp = 2,6-$^{i}Pr_2C_6H_3$).[3] Notably, widely utilized phosphine donors failed to yield stable EH_2 complexes (E = Ge and Sn), thus illustrating a case where NHOs are superior ligands to common benchmark donors. Accordingly, our group[7–11] and others[12,13] have been actively preparing NHO complexes of electron deficient main group species, while the sequestration of CO_2[14] and the *N*-heterocyclic olefin-instigated polymerization of polar methacrylate-based monomers has been reported by the Lu group.[15]

In this chapter, a new efficient method to prepare sterically encumbered NHOs is described including preliminary coordination chemistry to form rhodium carbonyl complexes. The latter species were examined by spectroscopic, crystallographic and computational methods in order to ascertain the donating ability of *N*-heterocyclic olefins in relation to the known carbene ligand, IPr (IPr = $(HCNDipp)_2C$:).

2.2 Improved Synthesis of *N*-Heterocyclic Olefins

There are currently three known methods in the literature to prepare the most thoroughly studied NHO, $IPrCH_2$.[1–3,12] Each of these strategies, although successful, has its own considerable drawbacks. The first procedure listed in Scheme 2.1 (procedure A) was initially used by our own laboratory to prepare $IPrCH_2$ (**1**).[3] This one-pot method involves

mixing two equivalents of IPr with methyl iodide in toluene to install a terminal methylene, $=CH_2$, group at the carbenic carbon. In this process, one equivalent of IPr reacts with MeI to yield the imidazolium salt $[IPrCH_3]I$ *in situ*, which is then deprotonated by an additional equivalent of IPr to yield $IPrCH_2$ (**1**) in up to a 90 % yield.[3] However the final product contains variable amounts of residual IPr, which is difficult to separate from **1**. An alternative method to synthesize **1** was reported,[1,2,6] which leads to less IPr contamination in the final NHO product (Scheme 2.1; procedure B). In the first step, the strong Brønsted base, ^{n}BuLi, is used to deprotonate [IPrH]Cl to yield free IPr in solution, which is then alkylated by MeI to form [IPrMe]Cl. In the final step, more ^{n}BuLi is added to effect another deprotonation event leading to the formation of $IPrCH_2$ (**1**).[6] Despite the larger number of steps associated with procedure B, each transformation can be sequentially carried out in a single reaction flask. However this route yields $[Li(THF)_x]I$ as a by-product which has appreciable solubility in organic solvents (even in hexanes), which renders its separation from $IPrCH_2$ (**1**) by multiple filtrations difficult, resulting in low overall yields of pure **1**. Additionally, Robinson and coworkers reported a protocol (Scheme 2.1, procedure C) that involves backbone deprotonation of IPr using ^{n}BuLi in hexanes.[12] The intermediately formed Li-salt, [IPr]Li, can be methylated with MeI in toluene leading to the generation of $IPrCH_2$ via proton-transfer. This method gives pure $IPrCH_2$

(**1**) on a small scale, however, on a large scale product separation from LiI can still be problematic.

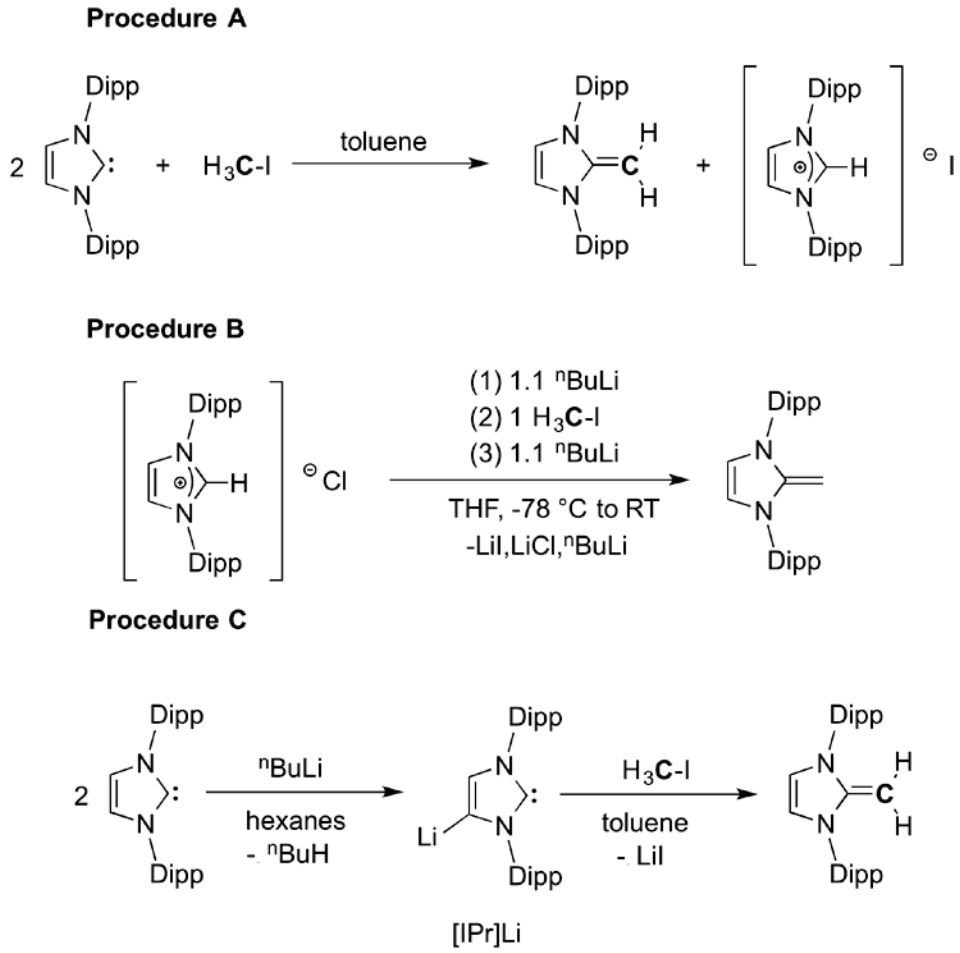

Scheme 2.1. Literature procedures for the preparation of $IPrCH_2$ (**1**) using an excess of IPr (procedure A), an exogenous base (procedure B) or via backbone-activated IPr (procedure C).

During the general explorations of the reactivity of **1** towards various electrophiles, I noticed that pure $IPrCH_2$ (**1**) could be prepared in a very efficient manner by combining IPr with an excess of $ClCH_2SiMe_3$

(*ca.* 4 equiv.) in toluene at ambient temperature (Scheme 2.1, procedure A). After the mixture is stirred for four days, a small amount of precipitate is formed that is easily separated by filtration, and removal of the volatiles from the filtrate yields **1** in good yield (71 %) as a spectroscopically pure solid (as determined by ^{1}H NMR spectroscopy). As shown in Scheme 2.2, this reaction produces $ClSiMe_3$ as a by-product and this transformation likely goes via the transient alkylsilyl imidazolium salt [IPr-CH_2-$SiMe_3$]Cl; it should also be mentioned that $ClSiMe_3$ does not react with IPr or IPrCH_2 at room temperature, thus simplifying the nature of the reaction profile in Scheme 3. This new synthesis is a large improvement over the protocols used to date and interestingly the same route can be used to prepare the related *N*-heterocyclic olefin, IMesCH_2 (IMes = [(HCNMes)$_2$C:], Mes = 2,4,6-$Me_3C_6H_2$; **2**). Complex **2** was synthesized by Dr. Christian Hering-Junghans. In this case, full conversion of IMes into IMesCH_2 is achieved in 12 hours with three equiv. of ClH_2CSiMe_3; the acceleration in reaction rate is likely due to the less hindered nature of the IMes nucleophile in relation to IPr. Unfortunately the backbone-methylated carbene ^{Me}IPr (^{Me}IPr = [(MeCNDipp)$_2$C:]), only reacts slowly with $ClCH_2SiMe_3$ at room temperature and formation of a high yield of ^{Me}IPrCH_2 (**3**) does not occur even after two weeks of stirring. Complex **3** was also synthesized by Dr. Christian Hering-Junghans. A possible explanation for the sluggish reactivity between ^{Me}IPr and $ClCH_2SiMe_3$, is that the backbone positioned Me groups in ^{Me}IPr push the flanking Dipp

groups forward, leading to greater steric crowding about the nucleophilic carbene donor center relative to in IPr.[16]

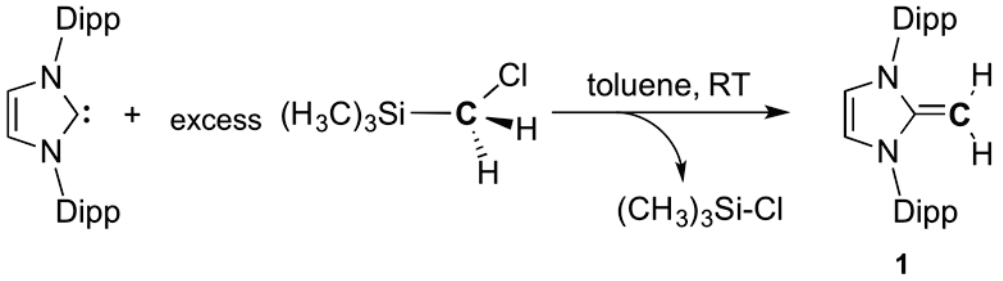

Scheme 2.2. Improved synthesis of $IPrCH_2$ using $ClCH_2SiMe_3$

2.3 Evaluation of *N*-Heterocyclic Olefin Donor Strengths

In addition to the synthesis of the abovementioned NHO-rhodium complexes, the known carbene-bound Rh(I) complex[17] IPr•$RhCl(CO)_2$ (**7**) was also prepared and determined its solid state structure was determined by single-crystal X-ray crystallography (Figure 2.2); this species will be a part of the comparative studies in the next section of this chapter.

As an initial starting point, the relative coordinating abilities of $IPrCH_2$ (**1**) and IPr were evaluated in a competition experiment. Specifically, a mixture containing a 1:1 mole ratio of $IPrCH_2$ (**1**) and IPr was combined with half a molar equivalent of $[Rh(\mu\text{-}Cl)(CO)_2]_2$ under the same reaction conditions discussed above (Scheme 2.3). After 12 hours it was determined by ^1H NMR spectroscopy that IPr binds preferentially to the rhodium center as the resulting ^1H NMR spectrum was consistent with the exclusive formation of IPr•$RhCl(CO)_2$ (**7**) and free $IPrCH_2$ (**1**). From

this experiment, it appears that IPr binds more strongly to the rhodium center, thereby preventing the coordination of $IPrCH_2$; related competition experiments have been run in our group using main group based Lewis acids, and consistently we see that IPr is a stronger donor than $IPrCH_2$.[9,11]

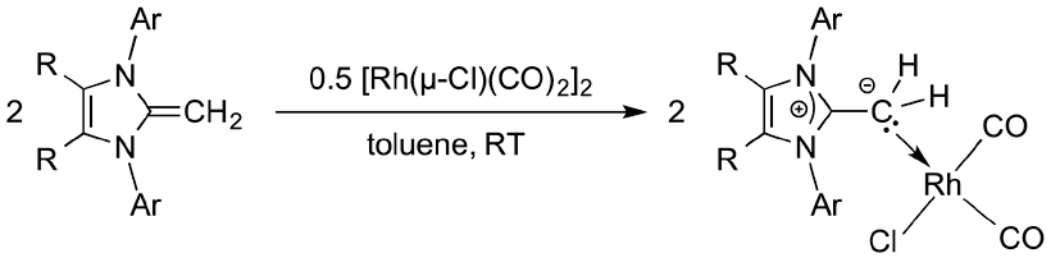

R = H, Ar = Dipp: $IPrCH_2$ (**1**) — $[IPrCH_2•RhCl(CO)_2]$ (**4**)
R = H, Ar = Mes: $IMesCH_2$ (**2**) — $[IMesCH_2•RhCl(CO)_2]$ (**5**)
R = Me, Ar = Dipp: $IPrMeCH_2$ (**3**) — $[IPrMeCH_2•RhCl(CO)_2]$ (**6**)

Scheme 2.3. Synthesis of the NHO•$RhCl(CO)_2$ complexes **4**-**6**.

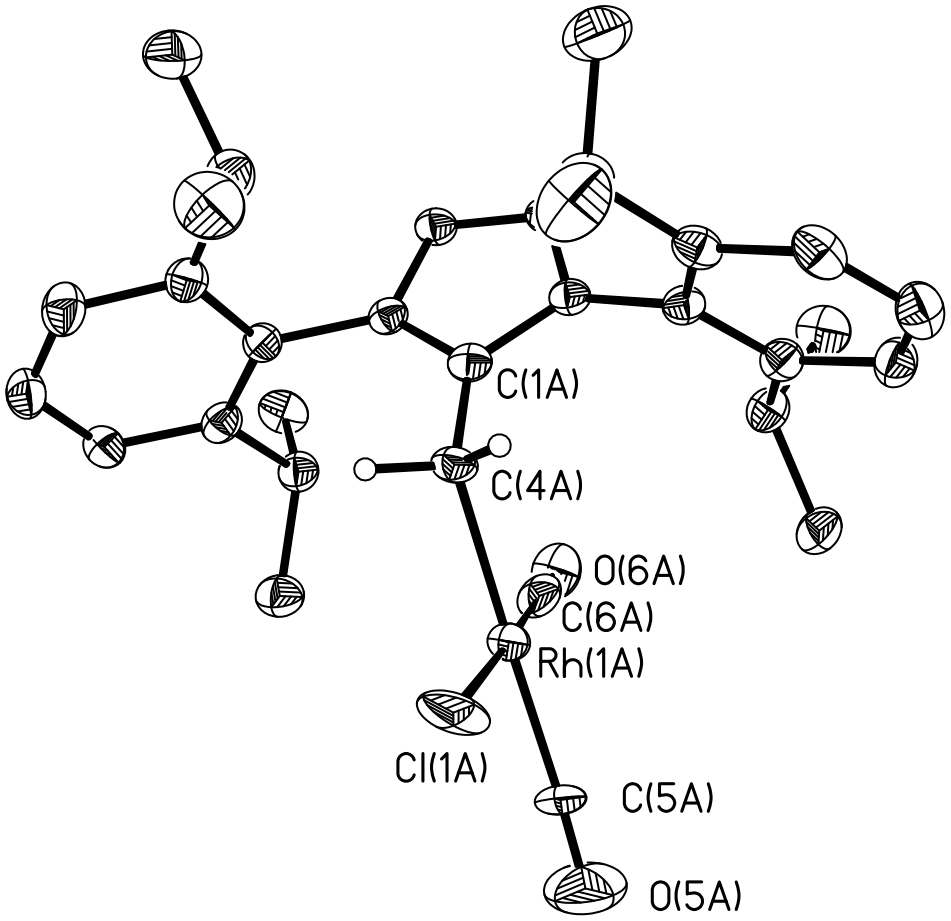

Figure 2.1. ORTEP drawing of the molecular structure of **4** (one of the independent molecules in the asymmetric unit). Ellipsoids are drawn at 30% probability, all hydrogen atoms (except on C4a) have been omitted for clarity. Selected bond lengths (Å) and angles (°): C1a−C41a 1.462(9), C4a−Rh 2.138(7), Rh−Cl1a 2.393(2), Rh−C5a 1.916(9), Rh−C6a 1.814(7) Å, C5a−O5a 1.080(12), C6a−O6a 1.147(10), C1a−C4a−Rh 120.1(4).

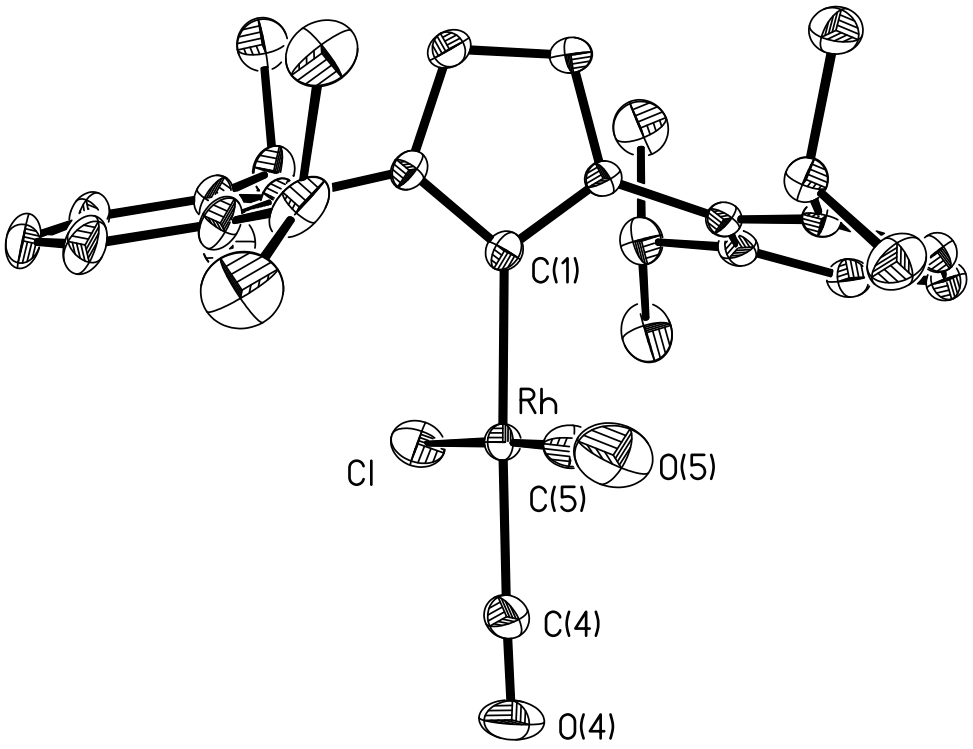

Figure 2.2. ORTEP drawing of the molecular structure of **7**. Ellipsoids are drawn at 30% probability, all hydrogen atoms have been omitted for clarity. Selected bond lengths (Å): C1−Rh 2.076(2), Rh−Cl1 2.3424(7), Rh−C4 1.900(3), Rh−C5 1.841(3), C4−O4 1.132(3), C5−O5 1.122(4) Å.

The molecular structures of compounds **4** and **7** enabled the Rh-C bond lengths involving the donor carbon atoms in the NHO and IPr-bound complexes to be compared. When the Rh-C distances are analyzed, one observes slightly elongated coordinative bonds within the NHO complexes **4** [2.138(7) Å] in relation to the carbene supported complex IPr•RhCl(CO)$_2$ (**7**) [2.076(2) Å]. For comparison, Rh-C bond lengths within structurally related square planar rhodium-carbene complexes fall in the range of 2.063 to 2.085 Å.[18–20] The small, yet statistically relevant, elongation in Rh-C bond length upon substituting an NHC by an NHO suggests that a stronger ligating interaction is present when *N*-heterocyclic carbenes are bound to Rh, in line with the abovementioned competition experiments. Rh−CO bond lengths in complex **4** are similar to the values found in the previously published NHC-Rh complexes.[18–20] In complex **4** the *cis* and *trans* Rh−CO bond lengths (*trans* Rh1-C5b 1.916(9), *cis* Rh1−C6b 1.814(7) Å) fall slightly outside the range of known NHC-Rh complexes [reported values: *trans* 1.897(2)-1.921(4) Å, *cis* 1.827(11)-1.871(4) Å]. In order to probe the bonding modes within these two carbon-based ligand classes, we also investigated the complexation of NHOs via spectroscopic and computational methods; some interesting effects were noted that are of possible general importance in guiding future explorations of NHO as ligands to support metal-mediated catalysis.

As mentioned above, various rhodium carbonyl complexes were prepared to gain insight into how ligands interact with metal centers (via

changes in the average ν(CO) IR stretching frequencies).[17] Previously, ν(CO) vibrational modes within tetrahedral L•Ni(CO)$_3$ complexes were used to evaluate ligand donating abilities, from which the Tolman Electronic Parameters (TEPs) could be obtained;[21] however the risks associated with handling nickel carbonyls makes the study of the analogous, less thermally labile, rhodium complexes much more attractive.[22]

The average $\nu_{av/rh}$(CO) IR stretching frequencies for complexes NHO•RhCl(CO)$_2$ (**4**-**6**) are listed in Table 2.1 and collectively they have significantly lower wavenumbers than in the NHC-capped complex IPr•RhCl(CO)$_2$ (**7**), which would initially suggest that, surprisingly (*vide supra*), NHOs are stronger donors than IPr. Using the previously published expression which converts $\nu_{av/rh}$(CO) values from L•RhCl(CO)$_2$ complexes into nickel-carbonyl derived TEP values (Table 2.1),[22] one again sees that the estimated TEP values for the *N*-heterocyclic olefins in this study (2024.6 to 2030.2 cm^{-1}) are lower than for IPr (2045.4 cm^{-1}) suggesting a much higher donor strength amongst NHOs.

Complex	$\nu_{av/Rh}$(CO) [cm^{-1}]	TEP (calc.)
4	2011	2029
5	2006	2025
6	2013	2030
7	2032	2045

Table 2.1. Carbonyl stretching frequencies $\nu_{av/Rh}$(CO) [cm^{-1}] and calculated TEP [cm^{-1}] (TEP = 0.8001×$\nu_{av/Rh}$(CO) + 420.0)

Given the apparently conflicting results from my IR data and the experimentally noted preferential binding of IPr to Rh over IPrCH_2, more comment is warranted on this subject here. Recently, questions have arisen about the validity of TEP values when structurally distinct ligands classes are compared (*e.g.* phosphines versus NHCs).[23] The model of a ligand transferring electron density onto a metal center, which would consequently transfer a portion of the electron density onto the carbonyl ligand has been used to rank a ligand's donating ability.[21] A complicating factor is that *N*-heterocyclic carbenes are strong σ-donors, as well as weak to moderate π-acceptors.[24] Therefore metal-to-carbene π-backbonding can reduce the overall electron density at a metal, which leads to an increase in the carbonyl stretching frequencies, giving the impression of a weaker

carbene-metal bond. These effects have been seen in previous studies of the electronic character of NHCs.[21] At this point, our understanding of metal-NHO interactions are somewhat nascent, however the IR data collected for the NHO•$RhCl(CO)_2$ series, when taken with the observed weaker coordinating abilities of these species relative to an NHC, suggests that little to no Rh-NHO π-backbonding is present, which would lead to lower than expected ν(CO)values (and lower associated TEP values) when compared to *N*-heterocyclic carbenes.

To further evaluate the carbene-metal bonding within an NHO-$RhCl(CO)_2$ complex, Dr. Christian Hering-Junghans completed DFT computational investigations on the model complex $ImMe_2CH_2$•$RhCl(CO)_2$ (**8**) and the related NHC analogue $ImMe_2$•$RhCl(CO)_2$ (**9**) at the BP86 DFT-level, with an DEF2-SVP[25,26] basis set and an ECP for Rh ($ImMe_2$ = $[(HCNMe)_2C:)]$.[27] Moreover, analytical calculation of the Hessian Matrix allowed the derivation of unscaled vibrational frequencies for complexes **4** and **5;** a similar approach has been reported by Tonner and Frenking for $RhCl(CO)_2$ complexes to obtain calculated TEP values for different donor systems.[28] The striking feature of the free NHO is the exocyclic π $C_{carbene}$=CH_2 double bond, which is polarized towards CH_2 (natural charge: *C*H_2 -0.72 e, $C_{carbene}$ 0.42 e), whereas the σ bond is unpolarized (determined by means of NBO analysis). Inspection of the Kohn-Sham orbitals shows a π-MO with a polarized π $C_{carbene}$=CH_2 bond as the HOMO of **1**, whereas the

π* is the high lying LUMO+9 (Figure 2.3). The optimized geometries of computational data for model compound $ImMe_2CH_2$•$RhCl(CO)_2$ agrees with the X-ray data (*e.g.* $d(C_{carbene}–CH_2)$ 1.45 Å, 1.460(11) Å in **4**). The average of symmetrical and asymmetrical CO stretching mode is given as $\nu_{Rh}(CO)$, as the coupling of both modes hampers the identification of the pure *trans*-CO mode (Table 2.2).

The $\nu_{Rh}(CO)$ mode for the $ImMe_2CH_2$•$RhCl(CO)_2$ (**8**) is 2017.8 cm^{-1}, which is considerably lower than the values determined for the analogous NHC complex $ImMe_2$•$RhCl(CO)_2$ (**9**) ($\nu_{Rh}(CO)$ = 2040.13 cm^{-1}). For **4** and **5** $\nu_{Rh}(CO)$ modes of 2010.5 and 2023.9 cm^{-1} were calculated. Using Frenking's linear regression[28] TEP_{Rh} values of 2017.3, 2034.9 and 2026.5 for **4**, **5** and $ImMe_2CH_2$•$RhCl(CO)_2$ were obtained. These values categorize NHOs as very strong (**4**, very strong donors TEP_{Rh} < 2026 cm^{-1}) to strong donors ($ImMe_2CH_2$•$RhCl(CO)_2$, **5**; 2027 < TEP_{Rh} < 2045 cm^{-1})[28].

Complex	ν_{Rh}(CO) [cm^{-1}]	TEP$_{Rh}$
4	2011	2017
5	2024	2035
8	2018	2027
9	2040	2056

Table 2.2. Calculated carbonyl stretching frequencies ν_{Rh}(CO) (cm^{-1}) and calculated TEP$_{Rh}$ (TEP$_{Rh}$ = 1.3080ν_{Rh}(CO) – 612.39).[22]

This finding is further underlined by inspection of the Kohn-Sham orbitals (MOs) of model complex **8** (Figure 2.3), which shows only small contributions of Rh d-orbital to NHO back-bonding in the HOMO-2 and HOMO-4, whereas the main σ-donation is displayed by HOMO-9 and the HOMO is a Rh-centered LP of dz^2-character. This is further supported by NBO analysis which gives small second order perturbation energies (E < 5 kcal/mol) for lone pair (Rh) to C−C π^* backbonding. Overall our computational studies are in line with the initial hypothesis that NHOs are good σ-donors, which is supported by rather low TEP$_{Rh}$ values computed for NHO-Rh complexes **4** and **5**.

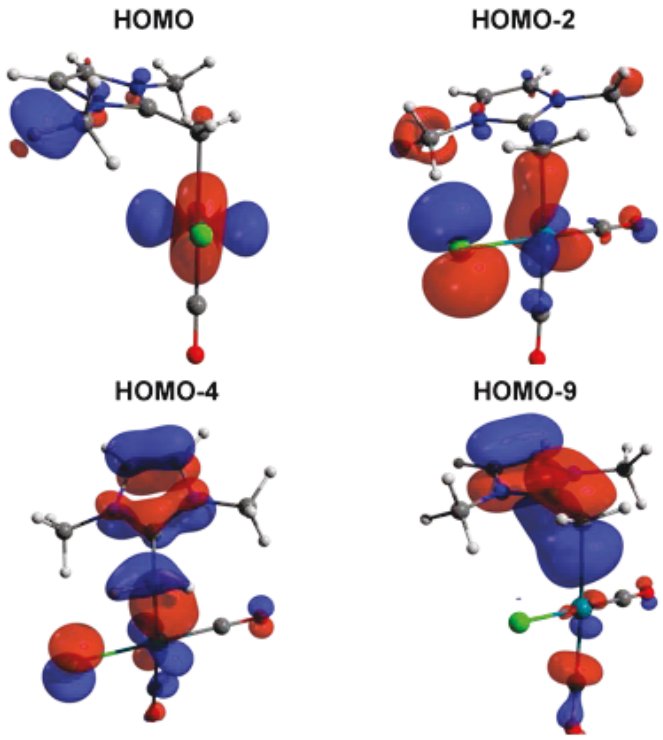

Figure 2.3. Selected MOs of $IMeCH_2$•$RhCl(CO)_2$ (**8**) (calculated on BP86/def2-SVP level of DFT).

Without the option of using the TEP values to directly compare the σ-donation abilities of NHCs and NHOs, additional insight into the bonding modes of the various carbene-rhodium complexes might be obtained from examining the ^{1}H and $^{13}C\{^{1}H\}$ NMR data of the corresponding L•$RhCl(CO)_2$ complexes. *J*-coupling constant values reflect the degree of s-electron density present within a σ-bond between two NMR active

nuclei.[23,29] For each of our Rh complexes discernable Rh-C coupling was observed between the exocyclic carbon donors of the *N*-heterocyclic olefin and the rhodium centers. HSQC and HMBC 2D NMR experiments were used to confirm the identity of the doublet $^{13}C\{^{1}H\}$ NMR resonance arising from CH_2-*Rh* coupling. The corresponding $^{1}J_{Rh\text{-}C}$ values associated with C_{NHO}-Rh couplings within compounds **4**-**6** are listed in Table 2.3 and all lie within the narrow range of 17.1 to 17.3 Hz. For comparison, the $^{1}J_{Rh\text{-}C}$ value for the NHC complex, IPr•RhCl(CO)$_2$ (**7**), is significantly larger [45.5 Hz]. This observation suggests that either stronger C-Rh covalent interaction exists within the NHC complex (**7**) leading to increased bonding electron density and a higher *J* value. However, one could also state that the lower $^{1}J_{Rh\text{-}C}$ values in the NHO complexes **4**-**6** stems from a decrease in s-orbital character within the coordinative Rh-C bond in comparison to in **7**; this observation is supported by the computational investigations discussed above.

Complex	δ [ppm]	$^{1}J_{RhC}$ [Hz]
4	12.8	17.1
5	9.2	17.3
6	16.1	17.1
7	180.2	45.4

Table 2.3. Chemical shifts and $J_{Rh\text{-}C}$ coupling constants for carbene-rhodium complexes.

2.4 Olefin-Backbone Activation Investigation

To further explore the possible lability of backbone C-H bonds in **1** (see Chapter 3) a deuterium labeling study was completed. The deuterium labeled analogue of **1** was synthesized via procedure B using methyliodide-d_3 (see Scheme 2.1) to form **1a** ((HCNDipp)$_2$C=CD$_2$). Complex **1a** was obtained in 23% yield and based on evidence from ^{1}H NMR spectroscopy, an NHO that was deuterated only at the terminal olefin appeared to be the product. The ^{1}H NMR spectra matched that of complex **1a**, excepting the missing CH_2 peak at 2.42 ppm. However upon further investigation by ^{2}H{^{1}H} NMR spectroscopy it was determined that some scrambling between the deuterated olefin and the protonated

backbone occurred. This conclusion was drawn due to the appearance of two peaks in the $^{2}H\{^{1}H\}$ NMR spectrum, a peak at 5.97 ppm occurred at the location of the backbone and a peak approximately twice the size of the backbone C-D peak occurred at xxx ppm, which was assigned to terminal CD_2 and likely some small amount of CDH group. I believe the scrambling was not observable in the ^{1}H NMR spectra as the level of scrambling was low. Heating of complex **1a** to 65 °C in C_6D_6 did not increase the scrambling levels. In addition, when **1a** and **1** are mixed in C_6D_6, no evidence of further scrambling occurs; thus it appears that the formation of backbone activated product in **1a** occurs during its synthesis and could be facilitated by side-products (such as the presence of LiI).

The following is a proposed general mechanism for the backbone activation and H/D scrambling process (Scheme 2.4): In step **A**, intermolecular deprotonation occurs to give a mesoionic carbene (MIC),[30] this intermediate then removes a deuterium atom from the terminal CHD_2 unit to reform a new NHO with a deuterium atom in the backbone position. MIC carbenes are known in the literature[30] and are also called abnormal carbenes (aNHCs) due to their lack of stable neutral canonical forms. MICs have been of great interest due to their very strong σ-donating ability in relation to standard NHCs.[31]

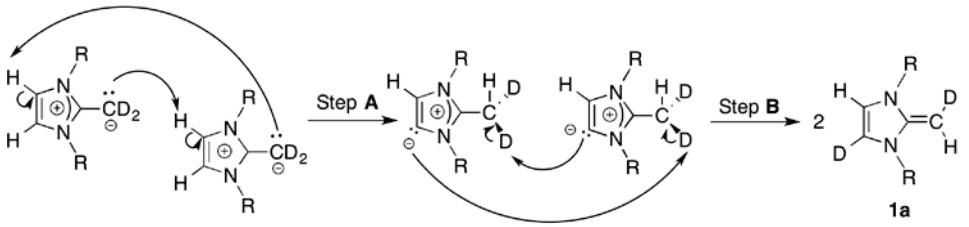

Scheme 2.4. A proposed mechanism to explain the scrambling of the olefin deuterium in complex **1a**.

2.5 Conclusion

In summary, an improved method for synthesizing $IPrCH_2$ via the transient alkylsilyl imidazolium salt [IPr-CH_2-$SiMe_3$]Cl was developed. The byproduct of the reaction is the volatile Me_3SiCl, which is easily removed from the product. In addition to developing the improved method for synthesizing **1**, the donor strengths of the NHOs were examined in relation to NHCs. The $IPrCH_2$•$Rh(CO)_2Cl$ complex provided insight into both the electron donating powers of **1** as well as the bonding mode of the ligand. In addition to the experiments, the bonding within NHOs were explored by computational models. The results of both the experimental and computational work suggest that NHOs are good σ-donors and very weak π-acceptors. The difference in bonding mode between NHOs and NHCs make NHOs particularly interesting. NHOs can not only be used as a new class of ligands, but the difference between them and NHCs can be used to gain further insight into the bonding characteristics of NHCs.

2.6 Experimental Section

All reactions were performed using standard Schlenk line techniques under an atmosphere of nitrogen or in an inert atmosphere glove box (Innovative Technology, Inc.). Solvents were dried using a Grubbs-type solvent purification system[32] manufactured by Innovative Technology, Inc., and stored under an atmosphere of nitrogen prior to use. Chloromethyltrimethylsilane, di-μ-chloro-tetracarbonyldirhodium(I), methyliodide, methyliodide-d_3, *n*-butyllithium (2.5 M solution in hexanes), and potassium tert-butoxide were purchased from Sigma-Aldrich and used as received. IPr, [IPrH]Cl[33] and [^{Me}IPrH]Cl[20] were prepared according to modified literature procedures. ^{1}H and ^{13}C{1H} NMR spectra were recorded on a 500 MHz Varian Inova instrument running VNMRJ 4 and referenced to the residual protonated solvent peak of known chemical shift. Elemental analyses were performed by the Analytical and Instrumentation Laboratory at the University of Alberta. Melting points were measured in sealed glass capillaries under nitrogen using a Mel-Temp melting point apparatus and are uncorrected. IR analyses were obtained on a ThermoScientific Nicolet FT100 FTIR spectrometer as a Nujol mull. UV/vis measurements were performed using a Varian Cary 300 Scan spectrophotometer.

Improved Synthesis of [(HCNDipp)$_2$C=CH$_2$] (1): To IPr (0.9265 g, 2.38 mmol) dissolved in 15 mL of THF was added $ClCH_2Si(CH_3)_3$ (1.1678 g, 9.52 mmol). After 72 hours of stirring a small amount of precipitate formed and the mixture was filtered. The volatiles were then removed from the filtrate under high vacuum to yield $IPrCH_2$ as a spectroscopically pure pale yellow solid (680 mg, 71 %). ^{1}H NMR, (498.1 MHz, C_6D_6): δ 1.22 (d, 12H, $^3J_{HH}$ = 6.9 Hz, CH(CH_3)$_2$), 1.36 (d, 12H, $^3J_{HH}$ = 6.9 Hz, CH(CH_3)$_2$), 2.42 (s, 2H, =CH_2), 3.35 (septet, 4H, $^3J_{HH}$ = 6.9 Hz, CH(CH$_3$)$_2$), 5.85 (s, 2H, N-CH-), 7.17 (d, 4H, $^3J_{HH}$ = 7.0 Hz, ArH), 7.22 (t, 2H, $^3J_{HH}$ = 7.0 Hz, ArH); ^{13}C{^{1}H} NMR (500 MHz, C_6D_6): δ 23.8 (CH(*C*H$_3$)$_2$), 24.3 (CH(*C*H$_3$)$_2$), 28.8 (*C*H(CH$_3$)$_2$), 44.3 (=*C*H$_2$), 114.6 (-N*C*H-), 124.5 (Ar*C*), 129.3 (Ar*C*), 134.9 (Ar*C*), 148.9 (Ar*C*), 152.5 (N-*C*-N).

Synthesis of [(MeCNDipp)$_2$C=CH$_2$] (2): [^{Me}IPrH]Cl (270 mg, 0.60 mmol) and KO^{t}Bu (160 mg, 1.43 mmol) were combined in THF (15 mL) and stirred at room temperature for 15 min to yield a yellow solution. Afterwards MeI (98 mg, 0.70 mmol) in THF (5 mL) was added and a yellow suspension formed immediately. The resulting mixture was further stirred overnight (12 h) and then filtered through a small pad of Celite, and the volatiles were then removed from the filtrate. The crude solids were extracted with hexanes (2 x 20 mL) and the extracts were filtered through Celite once more. The filtrate was concentrated to incipient crystallization and storage at −35 °C for 36 h resulted in the deposition of crystalline

blocks of **2** (210 mg, 86 %) that were suitable for X-ray crystallography. ^{1}H NMR (498.1 MHz, CD_2Cl_2): δ 1.22 (d, 12H, $^{3}J_{HH}$ = 7.0 Hz, CH(CH_3)$_2$), 1.42 (d, 12H, CH(CH_3)$_2$, $^{3}J_{HH}$ = 7.0 Hz), 1.58 (s, 6H, (NC(CH_3))$_2$), 2.33 (s, 2H, C=CH_2), 3.33 (septet, 4H, $^{3}J_{HH}$ = 7.0 Hz, CH(CH$_3$)$_2$), 6.75 (s, 2H, Ar-CH), 6.94-7.14 (m, 8H, o-Ar-CH), 7.17 (d, 4H, ArCH), 7.25 (t, 2H, ArCH); ^{13}C{^{1}H} NMR (75.46 MHz, CD_2Cl_2): δ 9.5 (NC(CH_3))$_2$), 24.0 (CH(*C*H$_3$)$_2$), 25.0 (CH(*C*H$_3$)$_2$), 28.8 (*C*H(CH$_3$)$_2$), 44.7 (C=*C*H$_2$), 115.8 (-N*C*(CH$_3$)-), 124.5 (Ar*C*), 129.2 (Ar*C*), 133.4 (Ar*C*), 149.6 (Ar*C*), 152.9 (N*C*N); Anal. Calc. % C, 83.67; H, 9.83; N, 6.50. Found C, 82.98; H, 9.90; N, 6.49.

Synthesis of [(MeCNMes)$_2$C=CH$_2$] (3): To a solution of IMes (333 mg, 1.09 mmol) in toluene (15 mL) a solution of ClCH$_2$SiMe$_3$ (540 mg, 4.40 mmol) in toluene (5 mL) was added at ambient temperature. The mixture became cloudy after 1 h and stirring was continued overnight (12 h). Afterwards the volatiles were removed *in vacuo* and the residue was extracted with toluene (20 mL) and filtered through a pad of Celite. Removal of the solvent from the filtrate and washing with hexanes (5 mL) resulted in the isolation of IMesCH$_2$ (110 mg, 32 %) as an off-white solid. ^{1}H NMR (498.12 MHz, C_6D_6): δ 2.11 (s, 6H, CH_3), 2.30 (s, 12H, CH_3), 2.56 (s, 2H, C=CH_2), 5.70 (s, 2H, NC*H*-), 6.79 (m, 4H, Ar-CH); ^{13}C{^{1}H} NMR (125.69 MHz, C_6D_6): δ 18.2 (-*C*H$_3$), 21.0 (-*C*H$_3$), 41.7 (C=*C*H$_2$), 113.1 (-N*C*H-), 129.6 (Ar*C*), 134.8 (Ar*C*), 137.6 (Ar*C*),

137.7 (Ar*C*), 148.6 (N*C*N); Anal. Calc. % C, 82.97; H, 8.23; N, 8.80. Found C, 82.42; H, 8.53; N, 8.52.

Synthesis of $IPrCH_2$•$RhCl(CO)_2$ (4): To $[Rh(CO)_2Cl]_2$ (42 mg, 0.11 mmol) in 5 mL of toluene was slowly added a solution of $IPrCH_2$ (87 mg, 0.22 mmol) in 5 mL of toluene. After combining the reagents, the resulting mixture was left undisturbed without stirring for 12 hours.[34] After this time period yellow crystals of $IPrCH_2$•$RhCl(CO)_2$, of suitable quality for X-ray crystallography, were formed which were separated from the mother liquor. The crystals were washed with 10 mL hexanes and dried under high vacuum to yield yellow needle-shaped crystals (53 mg, 82%). ^{1}H NMR (498.1 MHz, $CDCl_3$): δ 1.19 (d, 12H, $^3J_{HH}$ = 7.0 Hz, CH(CH_3)$_2$), 1.45 (d, 12H, $^3J_{HH}$ = 6.5 Hz, CH(CH_3)$_2$), 2.06 (d, 2H, $^2J_{HRh}$ = 1.5 Hz, H_2C-Rh), 2.38 (septet, 4H, $^3J_{HH}$ = 7.0, CH(CH$_3$)$_2$), 6.97 (s, 2H, N-CH-), 7.38 (d, 4H, $^3J_{HH}$ = 8.0 Hz, ArH), 7.38 (t, 2H, $^3J_{HH}$ = 6.9 Hz, ArH); ^{13}C{^{1}H} NMR (125.7 MHz, $CDCl_3$): δ 12.8 (d, $^1J_{CRh}$ = 17.1 Hz, -CH$_2$-Rh), 23.2 (CH(*C*H$_3$)$_2$), 26.0 (CH(*C*H$_3$)$_2$), 28.8 (*C*H(CH$_3$)$_2$), 120.7 (-N*C*H-), 125.3 (Ar*C*), 131.1 (Ar*C*), 131.3 (Ar*C*), 145.8 (Ar*C*), 166.7 (N-C-N), 183.7 (d, $^1J_{CRh}$ = 58.2 Hz, *C*O), 186.3 (d, $^1J_{CRh}$ = 77.6 Hz, *C*O); IR (Nujol, cm^{-1}): 1972 (νCO) and 2049 (νCO); Anal. Calc. % C, 60.36; H, 6.42; N, 4.69. Found C, 60.96; H, 6.45; N, 4.22; Mp (°C): 225-229; UV/vis (in CH_2Cl_2): λ_{max} = 228 nm, $\varepsilon = 1.13 \times 10^4$ L/(mol•cm).

Synthesis of IPr•RhCl(CO)$_2$ (7): This procedure is a variation on a previously published procedure.[6] To [Rh(CO)$_2$Cl]$_2$ (25 mg, 0.064 mmol) in 5 mL of toluene was slowly added a solution of IPr (50 mg, 0.12 mmol) in 5 mL of toluene. After combining the reagents, the resulting mixture was stirred for 12 hours. After this time a precipitate of IPrCH$_2$•RhCl(CO)$_2$ was formed and was separated from the mother liquor. The product was dried under high vacuum and X-ray quality crystals were subsequently obtained by cooling a solution of IPr•RhCl(CO)$_2$ in hexanes and dichloromethane at -35 °C. The resulting NMR was consistent with previously reported data for this product (27 mg, 73 %). ^{1}H NMR (500 MHz, $CDCl_3$): δ 1.28 (d, 12H, $^3J_{HH}$ = 7.0 Hz, CH(C*H*$_3$)$_2$), 1.39 (d, 12H, $^3J_{HH}$ = 6.5 Hz, CH(C*H*$_3$)$_2$), 2.90 (septet, 4H, $^3J_{HH}$ = 7.0, C*H*(CH$_3$)$_2$), 7.18 (s, 2H, N-C*H*-), 7.32 (d, 4H, $^3J_{HH}$ = 8.0 Hz, Ar*H*), 7.50 (t, 2H, $^3J_{HH}$ = 7.0 Hz, Ar*H*). ^{13}C{^{1}H} NMR (500 MHz, $CDCl_3$): δ 22.7 (CH(*C*H$_3$)$_2$), 26.4 (CH(*C*H$_3$)$_2$), 28.8 (*C*H(CH$_3$)$_2$), 124.1 (Ar*C*), 124.7 (-N*C*H-), 130.4 (Ar*C*), 135.0 (Ar*C*), 180.2 (d, $^1J_{CRh}$ = 45.5 Hz, N-*C*-N), 183.0 (d, $^1J_{CRh}$ = 73.5 Hz, *C*O), 184.7 (d, $^1J_{CRh}$ = 54.4 Hz, *C*O); IR (Nujol, cm^{-1}): 2073 (trans, νCO) and 1990 (cis, νCO).

Synthesis of ^{Me}IPrCH$_2$•RhCl(CO)$_2$ (6): 2 (51 mg, 0.12 mmol) in toluene (2 mL) was slowly added to a solution of [Rh(CO)$_2$Cl]$_2$ (23 mg, 0.06 mmol) in toluene (2 mL) and the yellow solution was placed in the freezer (−35 °C) without stirring. Standing overnight afforded [(^{Me}IPrCH$_2$)Rh(CO)$_2$Cl] as yellow crystalline solid (42 mg, 56 %). ^{1}H

NMR (300.13 MHz, CD_2Cl_2): δ 1.17 (d, 12H, $^3J_{HH}$ = 6.8 Hz, CH(CH_3)$_2$), 1.44 (d, 12H, $^3J_{HH}$ = 6.8 Hz, CH(CH_3)$_2$), 1.93 (s, 6H, (NC(CH_3))$_2$), 2.09 (d, 2H, $^1J_{CRh}$ = 2.9 Hz, C=CH_2), 2.66 (septet, 4H, $^3J_{HH}$= 6.8 Hz, CH(CH$_3$)$_2$), 7.35 (d, 4H, $^3J_{HH}$ = 7.9 Hz, ArCH), 7.53 (t, 2H, $^3J_{HH}$ = 7.0 Hz, ArCH); ^{13}C{^{1}H} NMR (125.69 MHz, CD_2Cl_2): δ 9.9 (NC(CH_3))$_2$), 16.1 (d, , $^1J_{CRh}$ = 17.1 Hz CH$_2$-Rh), 25.0 (CH(*C*H$_3$)$_2$), 25.3 (CH(*C*H$_3$)$_2$), 28.6 (*C*H(CH$_3$)$_2$), 124.3 (-N*C*(CH$_3$)-), 125.6 (Ar*C*), 129.4 (Ar*C*), 131.2 (Ar*C*), 146.4 (Ar*C*), 166.6 (N*C*N), 183.8 (d, $^1J_{CRh}$ = 58.2 Hz, *C*O), 187.4 (d, $^1J_{CRh}$ = 78.8 Hz, OC-Rh); Anal. Calc. % C, 61.49; H, 6.77; N, 4.48. Found C, 61.98; H, 6.76; N, 4.30; IR (Nujol, cm^{-1}): 2048 (trans, νCO), 1977 (cis, νCO).

Synthesis of IMesCH$_2$•RhCl(CO)$_2$ (5): IMesCH$_2$ (39 mg, 0.12 mmol) in toluene (2 mL) was slowly added to a solution of [Rh(CO)$_2$Cl]$_2$ (23 mg, 0.06 mmol) in toluene (2 mL) and the yellow solution was placed in the freezer (−35 °C) without stirring. Standing overnight afforded [(IMesCH$_2$)Rh(CO)$_2$Cl] as yellow crystalline solid (52 mg, 84 %). ^{1}H NMR (498.1 MHz, C_6D_6): δ 1.99 (d, 2H, $^1J_{CRh}$ = 2.8 Hz), C=C$H_2$2.23 (s, 12H, o-CH_3), 2.35 (*s*, 6H, p-CH_3), 6.88 (s, 2H, NC*H*=C*H*N), 7.04 (m, 4H, Ar-C*H*); ^{13}C{^{1}H} NMR (125.69 MHz, CD_2Cl_2): δ 9.2 (d, $^1J_{CRh}$ = 17.3 Hz, C-*C*H$_2$-Rh), 18.7 (o-*C*H$_3$)$_2$), 21.2 (m-*C*H$_3$)$_2$), 119.7 (-N*C*H-), 130.1, 131.6, 135.1, 140.4 (Ar*C*), 162.6 (N*C*N), 184.0 (d, $^1J_{CRh}$ = 57.7 Hz, -CO), 185.5 (d, $^1J_{CRh}$ = 77.6 Hz, -CO); Anal. Calc. % C, 56.21; H, 5.11; N, 5.46.

Found C, 56.05; H, 5.09; N, 5.31; IR (Nujol, cm^{-1}): 2049 (trans, νCO), 1961.5 (cis, νCO).

Competitive reaction of NHO and NHC with $[Rh(CO)_2Cl]_2$: To $[Rh(CO)_2Cl]_2$ (21 mg, 0.054 mmol) in 5 mL of toluene was added a solution of $IPrCH_2$ (43 mg, 0.11 mmol)in 5 ml of toluene and a solution of IPr (42 mg, 0.11 mmol) in 5 mL. After combining the reagents the resulting mixture was stirred for 12 hours. After this time period the product was dried under high vacuum. The resulting NMR was consistent with the formation of IPr•$RhCl(CO)_2$.

Synthesis of $IPrCD_2$ (1a): To a white slurry of 1,3-bis- (2,6-diisopropylphenyl)-imidazolium chloride, [IPrH]Cl (1.95 g, 3.42 mmol), in 20 mL of THF at -78 °C was added n-BuLi (2.4 mL, 3.83 mmol, 2.5 M solution in hexanes). The resulting yellow transparent solution was stirred for 20 min at room temperature. MeI-d_3 (0.239 mL, 3.84 mmol) was then added at -78 °C to yield a white precipitate. The resulting deuterated 2-methyl-imidazolium salt, $[IPrCD_3]I$ was then deprotonated *in situ* with n-BuLi (2.4 mL, 3.83 mmol, 2.5 M solution in hexanes) at -78 °C to obtain a pale yellow solution. The resulting solution was stirred at ambient temperature for 20 min, and afterwards the volatiles were removed to give a yellow solid. This solid residue was extracted with hexanes (20 mL) and filtered through Celite to yield yellow filtrate from which the product was isolated as a pale yellow solid upon removal of the volatiles, afforded

$IPrCD_2$ (29% yield, 0.39 g). ^1H NMR (498.1 MHz, C_6D_6): δ 1.22 (d, 12H, $^3J_{HH}$ = 6.9 Hz, $CH(CH_3)_2$), 1.36 (d, 12H, $^3J_{HH}$ = 6.9 Hz, $CH(CH_3)_2$), 3.35 (septet, 4H, $^3J_{HH}$ = 6.9 Hz, $CH(CH_3)_2$), 5.85 (s, 2H, N-C*H*-), 7.17 (d, 4H, $^3J_{HH}$ = 7.0 Hz, Ar*H*), 7.22 (t, 2H, $^3J_{HH}$ = 7.0 Hz, Ar*H*); $^{13}C\{^1H\}$ NMR (498.1 MHz, C_6D_6): δ 23.8 ($CH(CH_3)_2$), 24.3 ($CH(CH_3)_2$), 28.8 ($CH(CH_3)_2$), 44.3 ($=CH_2$), 114.6 (-N*C*H-), 124.5 (Ar*C*), 129.3 (Ar*C*), 134.9 (Ar*C*), 148.9 (Ar*C*), 152.5 (N-*C*-N). $^2H\{H\}$ NMR (498.1 MHz, C_6H_6): δ 2.42 (s, 2D, $=CD_2$), 5.87 (s, 1D, N-C*D*-).

Reaction of $IPrCD_2$ and $IPrCH_2$: $IPrCD_2$ (15 mg, 0.037 mmol) and $IPrCH_2$ (15 mg, 0.037 mmol) were dissolved in hexanes. Stirred for one hour at room temperature. Volatiles were removed by high vacuum. No reaction was observed.

2.7 Crystallographic Table

Table 2.5. Crystallographic Data for Compounds **4** and **7**.

	4	**7**
empirical formula	$C_{30}H_{42}ClN_2O_2Rh$	$C_{29}H_{36}ClN_2O_2Rh$
formula weight	643.05	582.96
crystal dimensions (mm)	0.30 × 0.16 × 0.09	0.20 × 0.16 × 0.13
crystal system	orthorhombic	monoclinic
space group	*Pca*21 (No. 29)	*P*21/*n* (an alternate setting of *P*21/*c* [No. 14])
unit cell		
a (Å)	19.8348 (4)	10.6168 (4)
b (Å)	19.8369 (4)	15.2645 (6)
c (Å)	16.9345 (3)	18.1611 (7)
β (°)		97.2005 (17)
V (Å^3)	6663.1 (2)	2920.0 (2)
Z	8	4
ρ calcd (g cm-3)	1.282	1.326
μ (mm-1)	5.107	5.771
temperature (°C)	–100	–100
2 θ_{max} (°)	140.06	148.28
total data	42851	5941
unique data (R_{int})	12314 (0.0228)	5941
observed data a [I>2σ(I)]	11909	5633
parameters	700	354
R_1 [I>2σ(I)][a]	0.0473	0.0266
wR_2 [all data][a]	0.1565	0.0762
difference map Δρ (e Å^{-3})	1.798 /–0.885	0.346 / –0.700

$^{f}R_1 = \Sigma||F_o| - |F_c||/\Sigma|F_o|$; $wR_2 = [\Sigma w(F_o^2 - F_c^2)^2/\Sigma w(F_o^4)]^{1/2}$

2.8 References

(1) Kuhn, N.; Bohnen, H.; Kreutzberg, J.; Blaeser, D.; Boese, R. J. Chem. Soc., Chem. Commun. 14 (1993) 1136

(2) Kronig, S.; Jones, P. G.; Tamm, M. *Eur. J. Inorg. Chem.* **2013**, 2301.

(3) Ibrahim Al-Rafia, S. M.; Malcolm, A. C.; Liew, S. K.; Ferguson, M. J.; McDonald, R.; Rivard, E. *Chem. Commun.* **2011**, *47*, 6987.

(4) Knappke, C. E. I.; Anthony J. Arduengo, I.; Jiao, H.; Neudörfl, J.-M.; von Wangelin, A. J. *Synthesis* **2011**, 3784.

(5) Fürstner, A.; Alcarazo, M.; Goddard, R.; Lehmann, C. W. *Angew. Int. Ed.* **2008**, *47*, 3210.

(6) Dumrath, A.; Wu, X. -F.; Neumann, H.; Spannenberg, A.; Jackstell, R.; Beller, M. *Angew. Int. Ed.* **2010**, *49*, 8988.

(7) Rivard, E. *Dalton Trans.* **2014**, *43*, 8577.

(8) Al-Rafia, S. M. I.; Ferguson, M. J.; Rivard, E. *Inorg. Chem.* **2011**, *50*, 10543.

(9) Malcolm, A. C.; Sabourin, K. J.; McDonald, R.; Ferguson, M. J.; Rivard, E. *Inorg. Chem.* **2012**, *51*, 12905.

(10) Al-Rafia, S. M. I.; Momeni, M. R.; McDonald, R.; Ferguson, M. J.; Brown, A.; Rivard, E. *Angew. Chem. Int. Ed.* . **2013**, 52, 6390.

(11) Berger, C. J.; He, G.; Merten, C.; McDonald, R.; Ferguson, M. J.; Rivard, E. *Inorg. Chem.* **2014**, *53*, 1475.

(12) Wang, Y.; Abraham, M. Y.; Gilliard, R. J.; Sexton, D. R.; Wei, P.;

Robinson, G. H. *Organometallics* **2013**, *32*, 6639.

(13) Ghadwal, R. S.; Reichmann, S. O.; Engelhardt, F.; Andrada, D. M.; Frenking, G. *Chem. Commun.* **2013**, *49*, 9440.

(14) Wang, Y. -B.; Wang, Y. -M.; Zhang, W. -Z.; Lu, X. -B. *J. Am. Chem. Soc.* **2013**, *135*, 11996.

(15) Jia, Y. -B.; Wang, Y. -B.; Ren, W. -M.; Xu, T.; Wang, J.; Lu, X. -B. *Macromolecules* **2014**, *47*, 1966.

(16) Ahmed, M.; Buch, C.; Routaboul, L.; Jackstell, R.; Klein, H.; Spannenberg, A.; Beller, M. *Chem. Eur. J.* **2007**, *13*, 1594.

(17) Sun, H.; Yu, X. -Y.; Marcazzan, P.; Patrick, B. O.; James, B. R. *Can. J. Chem.* **2009**, *87*, 1248.

(18) Chaplin, A. B. *Organometallics* **2014**, *33*, 3069.

(19) Tennyson, A. G.; Lynch, V. M.; Bielawski, C. W. *J. Am. Chem. Soc.* **2010**, *132*, 9420.

(20) Urbina-Blanco, C. A.; Bantreil, X.; Clavier, H.; Slawin, A. M. Z.; Nolan, S. P. *Beilstein J. Org. Chem.* **2010**, *6*, 1120.

(21) Dorta, R.; Stevens, E. D.; Scott, N. M.; Costabile, C.; Cavallo, L.; Hoff, C. D.; Nolan, S. P. *J. Am. Chem. Soc.* **2005**, *127*, 2485.

(22) Dröge, T.; Glorius, F. *Angew. Chem. Int. Ed.* **2010**, *49*, 6940.

(23) Ciancaleoni, G.; Scafuri, N.; Bistoni, G.; Macchioni, A.; Tarantelli, F.; Zuccaccia, D.; Belpassi, L. *Inorg. Chem.* **2014**, *53*, 9907.

(24) Khramov, D. M.; Lynch, V. M.; Bielawski, C. W. *Organometallics* **2007**, *26*, 6042.

(25) Weigend, F. *Phys. Chem. Chem. Phys.* **2006**, *8*, 1057.

(26) Weigend, F.; Ahlrichs, R. *Phys. Chem. Chem. Phys.* **2005**, *7*, 3297.

(27) Peterson, K. A.; Figgen, D.; Dolg, M.; Stoll, H. *J. Chem. Phys.* **2007**, *126*, 124101.

(28) Tonner, R.; Frenking, G. *Organometallics* **2009**, *28*, 3901.

(29) Vummaleti, S. V. C.; Nelson, D. J.; Poater, A.; Gómez-Suárez, A.; Cordes, D. B.; Slawin, A. M. Z.; Nolan, S. P.; Cavallo, L. *Chem. Sci.* **2015**, *6*, 1895.

(30) Gründemann, S.; Kovacevic, A.; Albrecht, M.; Faller, J. W.; Crabtree, R. H. *Chem. Commun.* **2001**, 2274.

(31) Bouffard, J.; Keitz, B. K.; Tonner, R.; Guisado-Barrios, G.; Frenking, G.; Grubbs, R. H.; Bertrand, G. *Organometallics* **2011**, *30*, 2617.

(32) Pangborn, A. B.; Giardello, M. A.; Grubbs, R. H.; Rosen, R. K.; Timmers, F. J. *Organometallics* **1996**, *15*, 1518.

(33) Bantreil, X.; Nolan, S. P. *Nat. Protoc.* **2011**, *6*, 69.

(34) Díez-González, S.; Marion, N.; Nolan, S. P. *Chem. Rev.* **2009**, *109*, 3612.

Chapter 3: NHO Gold and Palladium Complexes: Synthesis and Catalytic Activity.

3.1 Introduction

N-heterocyclic carbene (NHC) complexes of late transition metals play a large role in modern day synthetic chemistry due to their growing use as catalysts for many bond forming processes,[1–3] and in some cases, they facilitate the production of pharmaceutically relevant compounds.[4] As shown in the previous chapter, *N*-heterocyclic olefins (NHOs) have different bonding characteristics from NHCs that may allow for a new series of NHO-supported late transition metal complexes with potentially improved catalytic activities. In this Chapter a series of gold(I) and palladium(II) complexes containing the bulky donor $IPrCH_2$ ($IPrCH_2$ = $[(HCNDipp)_2C{=}CH_2$; Dipp = 2,6-$^{i}Pr_2C_6H_3$) are reported, along with preliminary comparative catalytic trials involving various new NHO and known IPr-based Pd(II) pre-catalysts. Specifically the investigation of carbon-carbon bond formation via Suzuki-Miyaura cross-coupling is described.

3.2 Gold-*N*-Heterocyclic Olefin Complexes

The importance of organometallic gold(I) complexes in catalysis and as pharmaceutically active molecules is on the rise. Specifically, NHC-gold complexes have proven to be successful homogenous catalysts for a variety of reactions, such as the hydration of alkynes;[5,6] in addition

their use as anti-cancer agents has been reported.[4,7–9] In general, *N*-heterocyclic carbene-gold complexes are straightforward to synthesize and there are two synthetic methods that are widely used: 1) direct coordination of a stable free carbene with a suitable Au(I) precursor; or 2) transmetalation involving a pre-formed metal-NHC complex (where M = Ag or Cu in Scheme 3.1).[10] It should also be mentioned that Alcarazo and coworkers were the first to synthesize a NHO-Au complex, however the reactivity of this molecular class has not been explored in detail.[11]

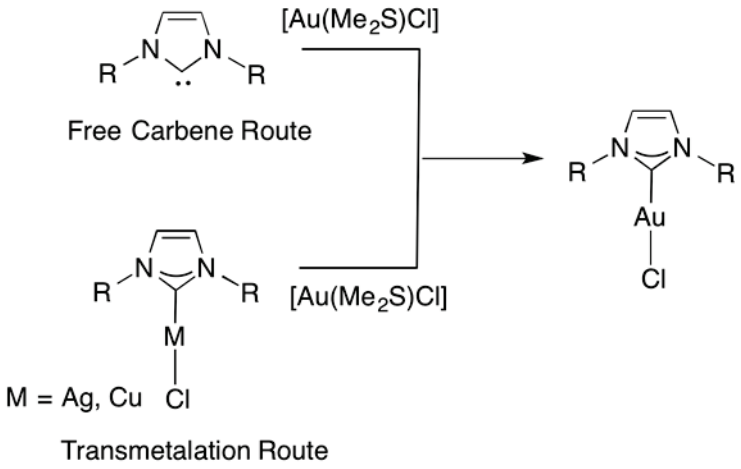

Scheme 3.1: Two general synthetic methods for preparing NHC-gold complexes.

Fortunately I was eventually able to develop a facile synthesis of NHO-gold(I) complexes after some initial troubleshooting. At first the reaction between $IPrCH_2$ and AuCl in a 1:1 ratio was explored, but instead of forming clean $IPrCH_2$•AuCl, a variety of unknown products were seen after analysis of the product mixtures by ^1H NMR spectroscopy. In addition, the reaction mixtures adopted deep pink colors, suggesting that

decomposition into Au(0) nanoparticles occurred.[6] As a result, the alternate Au(I) source, $(Me_2S)AuCl$, was examined, given that many stable NHC-Au complexes can be made using this reagent.[10] $(Me_2S)AuCl$ displayed much cleaner reactivity with $IPrCH_2$ and the number of NHO ligands bound to gold could be controlled by altering the stoichiometric ratio of $(Me_2S)AuCl$ to $IPrCH_2$ in THF. Specifically, $IPrCH_2$•AuCl (**2**) was obtained as a colorless solid in a 64 % yield, while the related linear Au(I) complex $[(IPrCH_2)_2Au]Cl$ (**3**) was isolated in a high yield of 94 % (Scheme 3.2). The overall procedure used to prepare **2** and **3** is very similar to the existing synthesis of IPr•AuCl.[10]

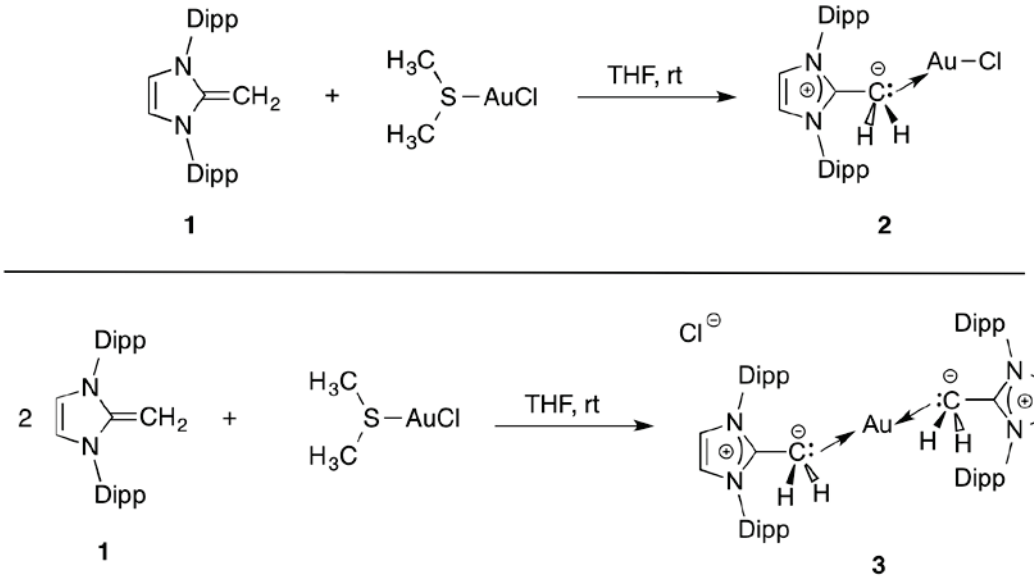

Scheme 3.2: Synthesis of complexes **2** and **3** using $(Me_2S)AuCl$ as a Au(I) source.

Both complexes **2** and **3** were characterized by ^1H and $^{13}C\{^1H\}$ NMR spectroscopy, elemental analysis and single-crystal X-ray

crystallography. The coordination of $IPrCH_2$ to a metal center can be confirmed by indicative NMR peak shifts. Particularly, the resonances associated with the olefinic backbone (C-H groups) of the central five-membered ring of IPr or $IPrCH_2$, and the resonances associated with the ligating carbon atoms are good markers. The general trend sees a downfield shift for both the backbone and olefin peak upon coordination.

	^{1}H backbone resonance (*ppm*)	^{1}H resonance of ligating CH_2 group (*ppm*)	^{13}C{^{1}H} backbone resonance (*ppm*)	^{13}C{^{1}H} resonance of ligating C atom (*ppm*)
(IPrCH$_2$)AuCl	6.95	2.09	125.3	5.2
[(IPrCH$_2$)$_2$Au]Cl	6.92	1.53	120.2	18.6
IPrAuCl[12]	7.15	N/A	124.3	175.5
[(IPr)$_2$Au](BF$_4$)	7.11	N/A	125.2	184.2

Table 3.1: A comparison of NMR data for complexes **2** and **3** to their known IPr analogues. All NMR spectra were recorded in $CDCl_3$.

As mentioned, the structures of $IPrCH_2$•AuCl (**2**) and $[(IPrCH_2)_2Au]Cl$ (**3**) were determined by X-ray crystallography. The results are shown in Figures 3.1 and 3.2. Insight into the relative Au-C bond strengths between the gold and the ligating carbon atoms can be derived from the bond lengths within the new NHO-Au complexes **2** and **3** and the previously published data for the IPr-Au complexes IPr•AuCl and $[(IPrCH_2)_2Au]BF_4$.[6] For both the mono- and di-substituted complexes, the IPr complexes have shorter C-Au bond lengths by *ca.* 0.07 to 0.10 Å in relation to the corresponding C-Au bonds in the NHO complexes (Table

3.2). This suggests that the NHC, IPr, is a stronger donor than the *N*-heterocyclic olefin $IPrCH_2$, and mirrors the overall trend in donating ability described in Chapter 2. The results from Chapter 2 suggests that NHOs in metal-carbene complexes participate in little to no backbonding with the metal center. For late transition metals that are electron rich like gold, this backbonding would serve to significantly strengthen the carbon-metal interaction. The results from Chapter 2 were further enforced by a simple competitive reaction between $IPrCH_2$ and IPr with $(Me_2S)AuCl$. When two equivalents of both $IPrCH_2$ and IPr were combined with a molar equivalent of $(Me_2S)AuCl$, it was noted by NMR that IPr coordinated preferentially to the gold center over $IPrCH_2$; a similar result was found in the reaction of a IPr/$IPrCH_2$ ligand mixture with $[Rh(CO)_2Cl]_2$ (Chapter 2).

A.

Complex	Gold-Carbon Bond Length (Å)	Gold-Chlorine Bond Length (Å)
IPr•AuCl	1.942(3)	2.2698(11)
($IPrCH_2$)•AuCl	2.050(3)	2.3043(8)

B.

Complex	Gold-Carbon Bond Length #1 (Å)	Gold-Carbon Bond Length #2 (Å)
$[(IPr)_2Au]BF_4$	2.024(7)	2.027(8)
$[(IPrCH_2)_2Au]$ Cl	2.094(4)	2.097(4)

Table 3.2: A comparison of bond lengths in complexes **2** and **3** to known IPr analogues.

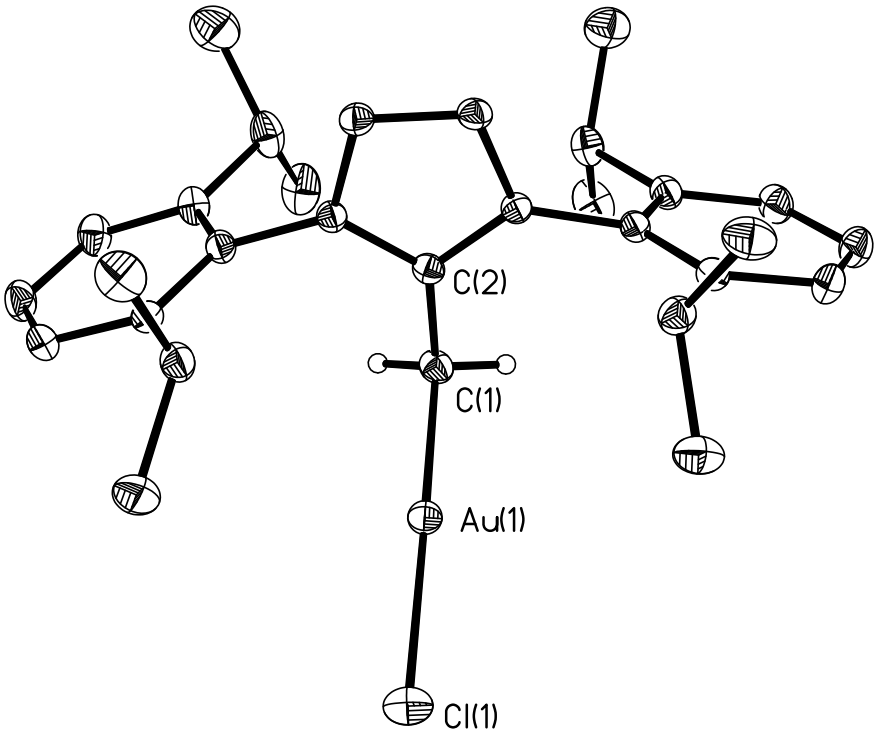

Figure 3.1 ORTEP of **2** with thermal ellipsoids drawn at a 30 % probability level; all hydrogen atoms except for C(1) have been omitted for clarity. Selected bond lengths (Å) and angles (°): C(1)-C(2) 1.451(3), C(1)−Au(1) 2.050(3), Cl(1)-Au(1) 2.3043(8); C(2)-C(1)-Au(1) 113.04(18), C(1)-Au(1)-Cl(1) 174.49(8).

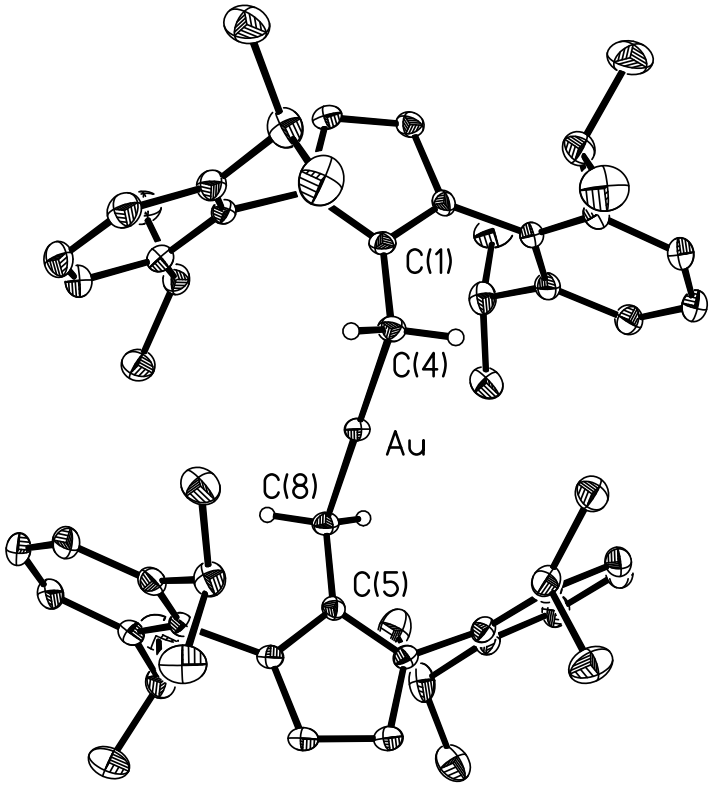

Figure 3.2 ORTEP of **3** with thermal ellipsoids drawn at a 30 % probability level; all hydrogen atoms except for C(4) and C(8) and the chloride counter ion have been omitted for clarity. Selected bond lengths (Å) and angles (°): C(1)-C(2) 1.452(6), C(5)-C(8) 1.442(6), C(1)−Au(1) 2.094(4), C(8)−Au(1) 2.097(4); C(2)-C(1)-Au(1) 109.6(3), C(5)-C(8)-Au(1) 109.1(3), C(1)-Au(1)-C(8) 179.72(18).

Examining the ORTEPs of complexes **2** and **3** reveals further differences from the original NHC-Au structures. Both **2** and **3** feature IPr units that are substantially bent away from the metal center. In complex **2** the C(2)-C(1)-Au angle linking the IPr unit to Au (via a methylene bridge) is 113.04(18)°, while narrower C-C-Au angles of 109.1(3) and 109.6(3)° are present in compound **3**. In The insertion of an extra CH_2 spacer and the abovementioned angled position of the IPr units in **3** leaves the gold center in this complex **3** significantly more sterically accessible than in $[(IPr)_2Au]BF_4$ where each carbene carbon of the IPr unit are approximately co-linear, to give a C-Au-C angle of 178.3(3)°. Nolan and coworkers tested $[(IPr)_2Au]BF_4$ as a catalyst for the hydration of alkynes and the transformation of propargylic acetates into enones. However this sterically hindered Au(I) complex showed no activity as the two IPr ligands likely hinder access to the gold center by the substrates investigated. Accordingly the less bulky NHO complex **3** may show interesting catalytic activity in this regard.

3.3 Palladium-*N*-Heterocyclic Olefin (NHO) Complexes

The importance of palladium-NHC complexes cannot be overstated. Palladium-NHC complexes are used throughout industry and academia for a large range of catalytic applications, such as the cross-coupling reactions pioneered by Heck, Negishi and Suzuki.[3,13,14] As a result, we were also interested in preparing potential palladium(II) pre-

catalysts containing the geometrically flexible, yet still sterically encumbered, ligand $IPrCH_2$.

The coordination of $IPrCH_2$ to palladium was initially challenging. In a similar fashion as noted for gold, the direct reaction of $IPrCH_2$ with $PdCl_2$ did not afford the desired product despite trying different solvent media (such as THF, DCM, and toluene) and temperatures ranging from room temperature to 130 °C. In order to improve the solubility of the Pd(II) source and hopefully yield cleaner reactivity, $IPrCH_2$ was combined with the known labile complex $Cl_2Pd(NCPh)_2$. When bis(benzonitrile)palladium(II) chloride was dissolved in toluene and an equimolar amount of $IPrCH_2$ was slowly added, a dark orange precipitate formed. After this product was isolated and recrystallized from CH_2Cl_2/hexanes at -35 °C, yellow crystals were obtained; however, when re-crystallizations (in CH_2Cl_2/hexanes) were conducted at room temperature, a mixture of red and yellow crystals formed. Interestingly, X-ray crystallography later identified the yellow crystals as the bis(NHO) complex *trans*-$[(IPrCH_2)_2PdCl_2]$ (**4**) (Scheme 3.3) while the red crystals were found to be the structural isomer *trans*-$[(a\text{-}IPrCH_2)_2PdCl_2]$ (**5**) whereby ligation transpired via an olefinic carbon atom; complexes with this type of ligation are termed "abnormal NHC" or a-NHC complexes in the literature.[17] Figures 3.3 and 3.4 contain the refined structures of compounds **4** and **5**, respectively. The co-existence of **4** and **5** in the re-crystallized sample suggests that the NHO-Pd complex **4** is in equilibrium

with its abnormally coordinated a-NHC counterpart **5** with preferential crystallization of the NHO complex **4** at lower temperatures. When the reaction between $IPrCH_2$ and $Cl_2Pd(NCPh)_2$ is conducted in toluene, only the formation of **4** is noted (at room temperature), however when crystallized at room temperate some complex **5** is formed in small amounts. Complex **5** can also be formed by gently heating a solution of initially pure **4** in $CDCl_3$ to 50 °C, with 12 % conversion noted after 2 hours. It is not possible to say if further heating would push the equilibrium further toward **5** as the complex is not tolerant to high heating about 70 °C.

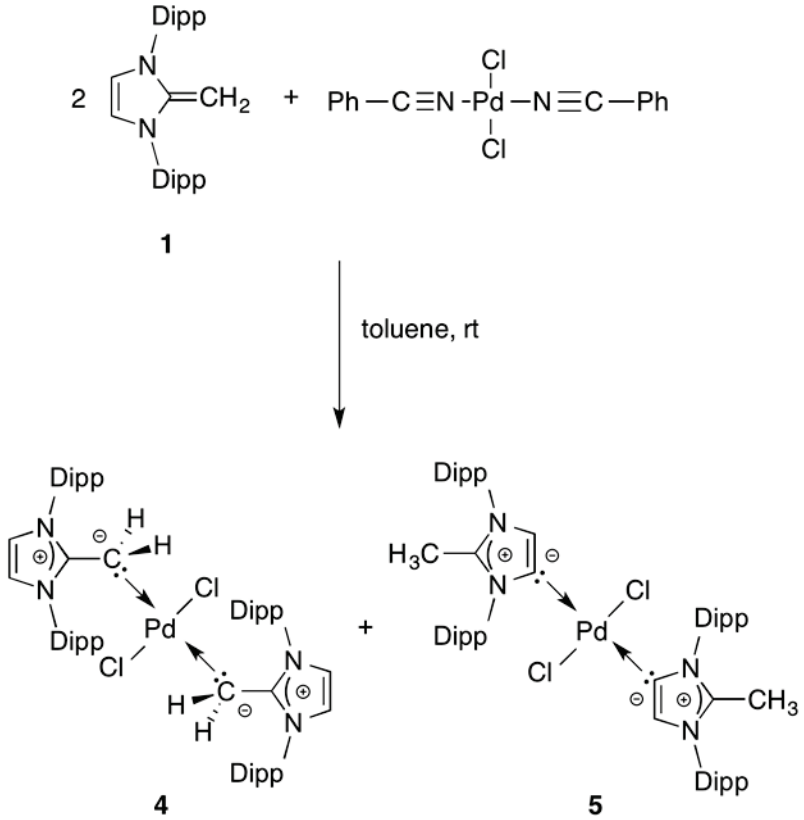

Scheme 3.3: The synthetic route to both the normally coordinated NHO complex **4** and the abnormally coordinated complex **5**.

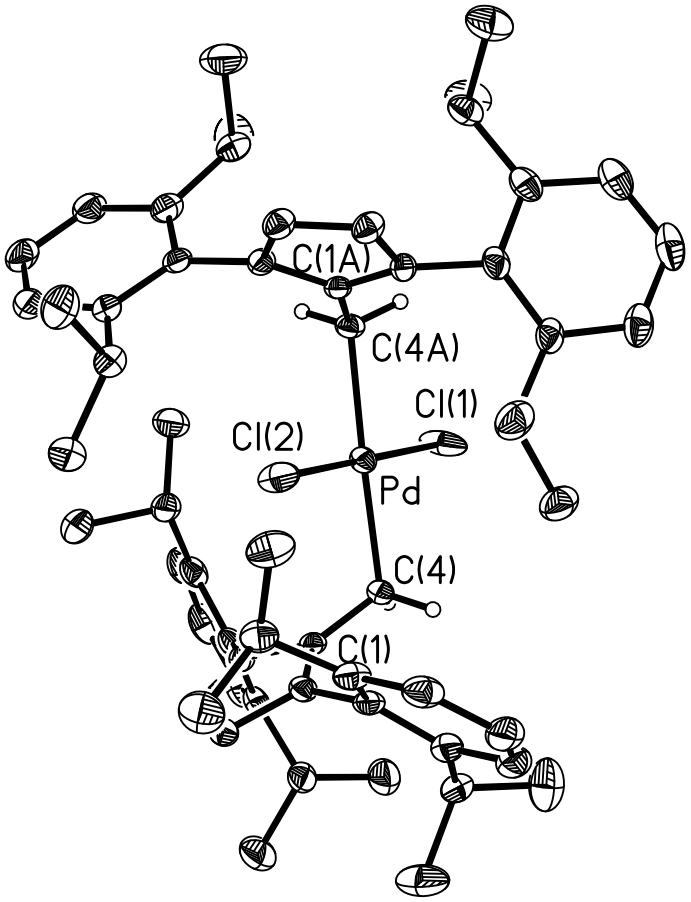

Figure 3.3: ORTEP of compound of **4**. Ellipsoids are drawn at a 30% level probability with all hydrogen atoms except C(4) and C(4a) have been omitted for clarity. Selected bond lengths (Å) and angles (°): C(4)−Pd 2.144(5), C(1)−C(4) 1.425(7); C(4)−Pd−C(4A) 176.7(3), C(1)−C(4)−Pd 91.65(14).

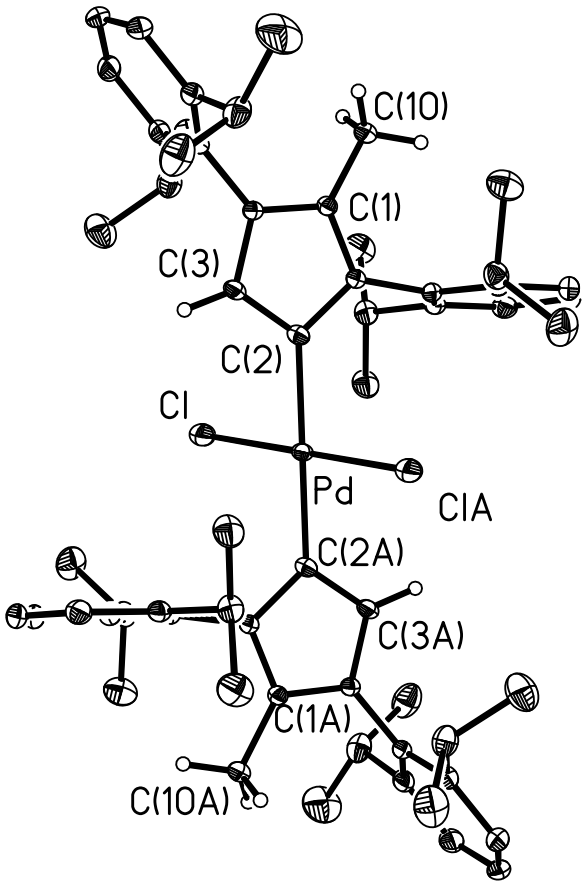

Figure 3.4. ORTEP of **5** with ellipsoids drawn at a 30 % probability level; all hydrogen atoms except for C(3), C(3A), C(10), C(10A) have been omitted for clarity. Selected bond lengths (Å) and angles (°): C(2)−Pd 2.0422(16), C(1)−C(10) 1.481(2); C(2)−Pd−C(2A) 180.00(13).

A similar overall NHO coordination geometry is seen in complex **4** as was seen in the Au(I) complex $[(IPrCH_2)_2Au]BF_4$ **3**, with trans ligation noted in both compounds. However in the Pd(II) complex **4**, the Pd-C-C angle formed by the $IPrCH_2$ ligand is quite narrow [91.62(14)°] suggesting that coordination is mediated by an orbital at C of high p-character. The NMR spectra of **4** and **5** match the trends mentioned for the gold NHO complexes **2** and **3**, where both the backbone and exocyclic CH_2 resonances shift downfield upon relative to in free $IPrCH_2$.

Work previously mentioned in Chapter 2 of this thesis may shed light on a mechanism for the abnormal coordination mode of $IPrCH_2$ shown in Scheme 3.6A. During an attempt to synthesize $IPrCD_2$ it was observed that the deuterium atoms on the terminal olefin scrambled with the protons at the backbone position during synthesis. I have proposed a mechanism for the scrambling of the protons, and this mechanism may also give insight into the formation of compound **5**. In the scrambling process a free aNHC exists (although very probably for a very short time) and is able to coordinate to the palladium center via the C4/5 carbon. (Scheme 3.4)

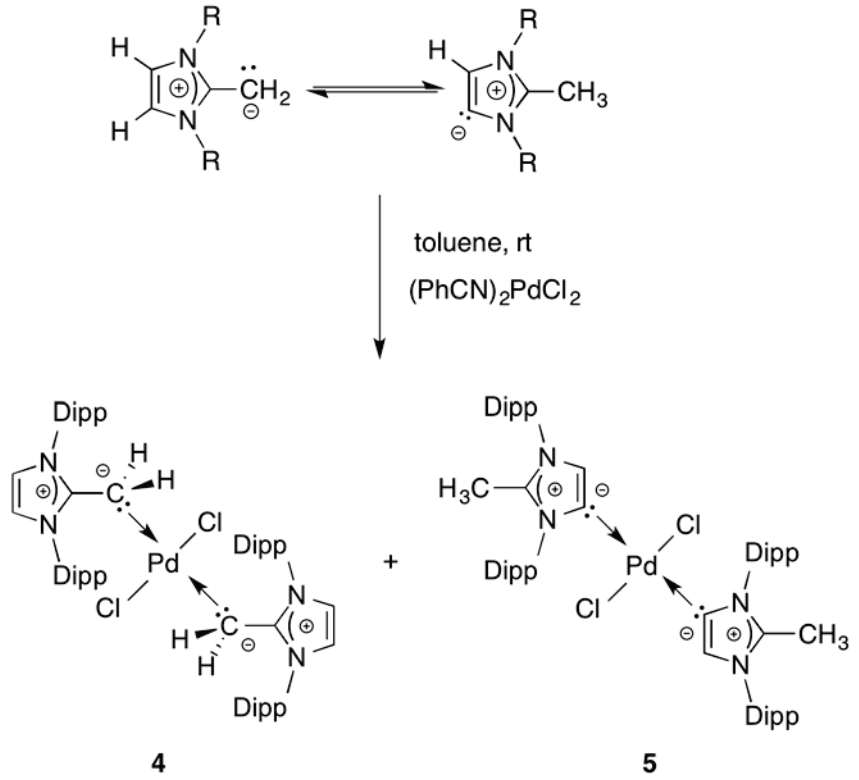

Scheme 3.4: Results from the deuterium study completed in Chapter 2 suggest that a free aNHC may exist in a solution of compound **1**. This free aNHC could very likely coordinate with the palladium center, forming complex **5**.

As stated, abnormal carbenes (a-NHC) ligate to metals and related electron deficient centers via the C4/5 positions (Scheme 3.4); in addition, these species are sometimes referred to as mesionic carbenes as they do not posses any resonance forms that are devoid of formal charges in their uncomplexed state. Crabtree and coworkers reported the first a-NHC complex in 2001 from the reaction of an alkyl pyridine-functionalized imidiazolium salt with $[H_5Ir(PPh_3)_2]$.[15,16] An alternative synthetic method to form aNHC ligands is by blocking the C2 position, thereby forcing coordination in an "abnormal" fashion. (Scheme 3.5)

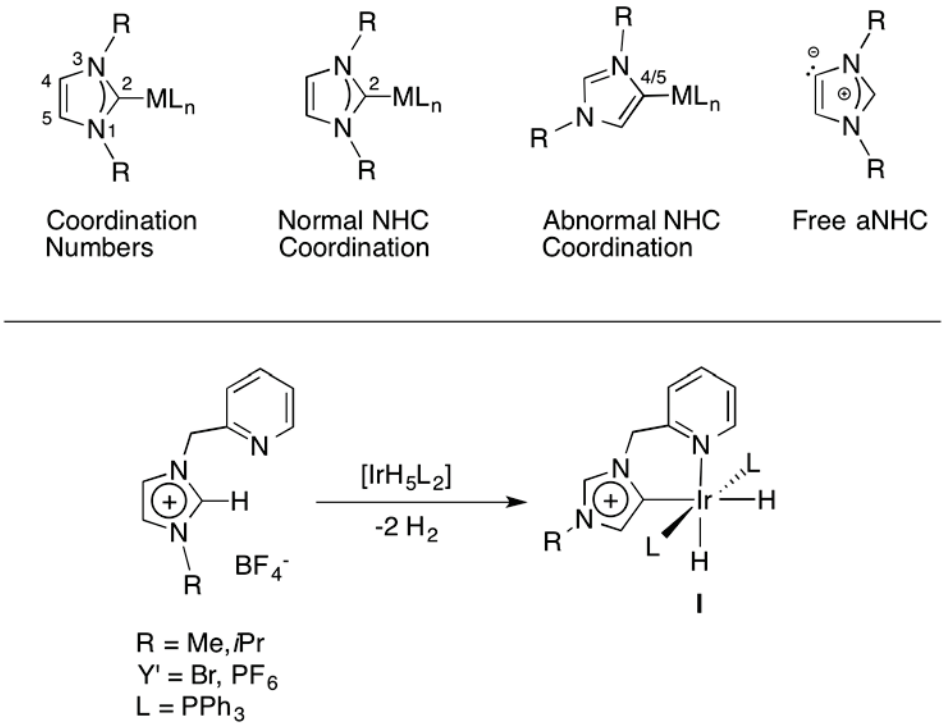

Scheme 3.5: Normally coordinated NHCs are coordinated via the 2 position, while abnormally coordinated NHCs are coordinated via the 4/5 positions (top). Crabtree's synthesis of the first a-NHC complex **I** (bottom).

Complexes **4** and **5** exist in equilibrium due to both steric and electronic factors. The steric bulk of $IPrCH_2$ may encourage abnormal coordination and also the increase donating ability of a-NHCs relative to what is expected in an NHO could drive a-NHC complexation via the formation of stronger C-Pd bonds (in the case of **5** vs. **4**). Interestingly Nolan and coworkers showed that IMes complexes (IMes = $[(HCNMes)_2C:]$; Mes = 2,4,6-$Me_3C_6H_2$) of $PdCl_2$ also exhibit both traditional and abnormal binding modes, depending on the type of base used to generate IMes *in situ* (from the imidiazolium salt [IMesH]Cl; Scheme 3.5).[19] The bis NHC complex *trans*-$[(IMes)_2PdCl_2]$ **6** is favored

when a weaker base such as Cs_2CO_3 is used to generate the carbene, while the presence of more strongly basic acetate ions promotes the formation of the abnormal NHC complex *trans*-[(a-IMes)$_2$PdCl$_2$] **7** (Scheme 3.6). Nolan tested the catalytic activity of complexes **6** and **7** and found that **7** is more catalytically active than **6** for a sample Suzuki cross-coupling reaction. This may be due to the expected stronger donor strength of the abnormal carbene compared to the normally coordinated carbene.[19]

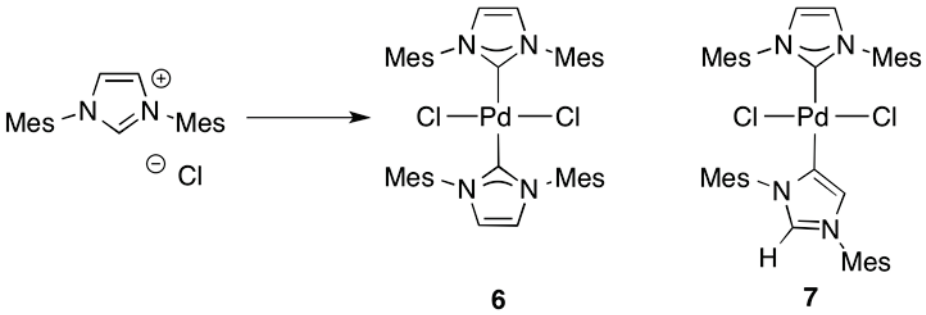

$Pd(OAc)_2$, Dioxane, 80 °C	<1 %	74 %
$PdCl_2$, Dioxane, Cs_2CO_3, 80 °C	68 %	<1 %

Scheme 3.6: Nolan's work on the formation of the NHC-Pd complex **6** and the base-dependent formation of the a-NHC-Pd complex **7**; isolated yields are given.

As previously discussed complex **4** is the major product formed when $IPrCH_2$ is combined with $Cl_2Pd(NCPh)_2$, while heating **4** in $CDCl_3$ affords a small quantity of the a-NHC complex **5**. Motivated by Nolan's observation that base-induced a-NHC formation is possible, I reacted the imidiazolium salt [$IPrCH_3$]I with $Pd(OAc)_2$; in this case, clean formation of the expected red colored a-NHC product *trans*-[(a-$IPrCH_3$)$_2$PdI$_2$] (**5b**) was noted. This observation clearly shows that the nature of the base

(anions) present in the reaction mixture has a strong influence over which coordination mode an NHO adopts, and such factors need to be kept in mind when performing catalysis with $IPrCH_2$ as a supporting ligand. Using Nolan's method, reacting two equiv. of the imidiazolium salt [IPrMe]Cl with palladium acetate afforded the complex *trans*-[(a-$IPrCH_2)_2PdCl_2$] (**5**) as a red solid. Using this method it is possible to isolate compound **5**.

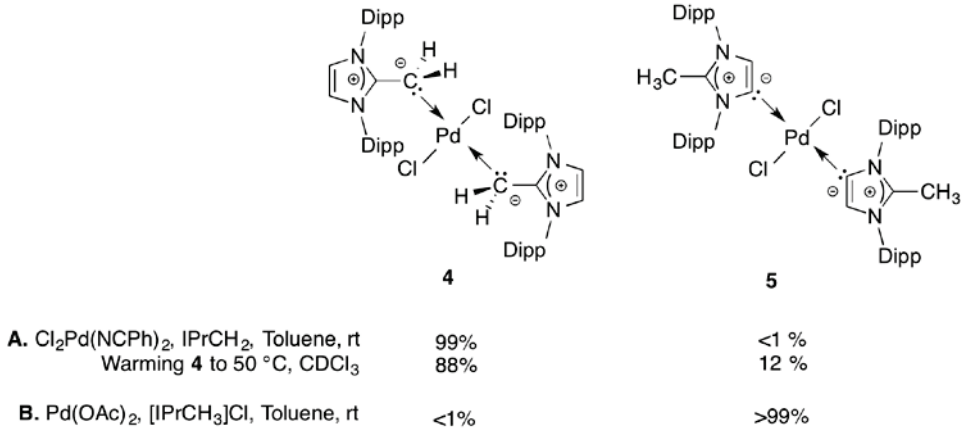

Scheme 3.7: The two routes to complexes **4** and **5**.

3.3.2 *N*-Heterocyclic Olefin Palladium Complexes Designed for Catalysis

In addition to the formation of the NHO and a-NHC complexes **4** and **5**, NHO analogues of common NHC-palladium pre-catalysts were also synthesized. Following the work of Organ and coworkers,[14] an NHO analogue of their PEPPSI systems *trans*-[(IPrCH$_2$)PdCl$_2$(3-chloropyridine)] **8** was prepared by reacting IPrCH$_2$ in neat 3-chloropyridine with PdCl$_2$ at 80 °C (Scheme 3.8). The molecular structure of **8** was confirmed by ^{1}H and ^{13}C{^{1}H} NMR spectroscopy, elemental analysis, as well as single-crystal X-ray diffraction.

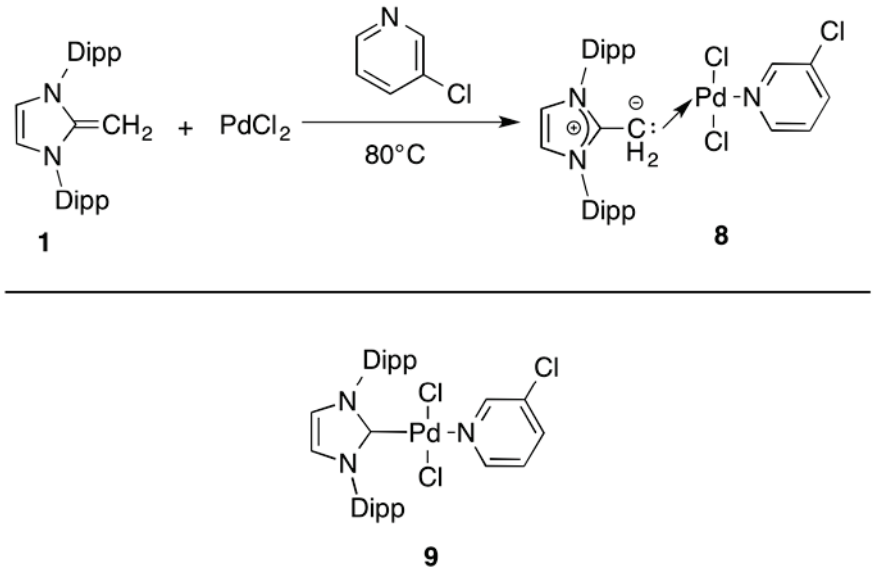

Scheme 3.8: Synthetic route to complex **8**, an NHO analogue of the well-known PEPPSI complex **9**.

The overall geometry about Pd in the NHO complex **8** matched that noted in Organ's NHC analogue [(IPr)PdCl$_2$(3-chloropyridine)] (**9**).[16]

However as was seen in the NHO-gold complexes, complex **8** had slightly longer bond M-C lengths than the corresponding distances in the IPr-PEPPSI complex **9** (Table 3.3). This further corroborates our proposal that $IPrCH_2$ is a weaker donor than IPr. The X-ray structure of **8** also allowed us to determine the distance from the C(1) carbon of the IPr unit to the palladium center (Figure 3.5) This distance can be used to show how far removed the steric bulk of the $IPrCH_2$ ligand is from the palladium center in relation to the NHC, IPr. When one examines this distance in complex **8**, a value of 2.953 Å is obtained, while in Organ's NHC complex, the Pd-C(1) bond length involving the IPr group is 1.969(3) Å.

Complex	Palladium-Carbon Bond Length (Å)	Palladium-Nitrogen Bond Length (Å)
8 ($IPrCH_2$-PEPPSI)	2.027(3)	2.145(3)
9 (IPr-PEPPSI)	1.969(3)	2.137(2)

Table 3.3: Selected bond lengths in complexes **8** and **9**.

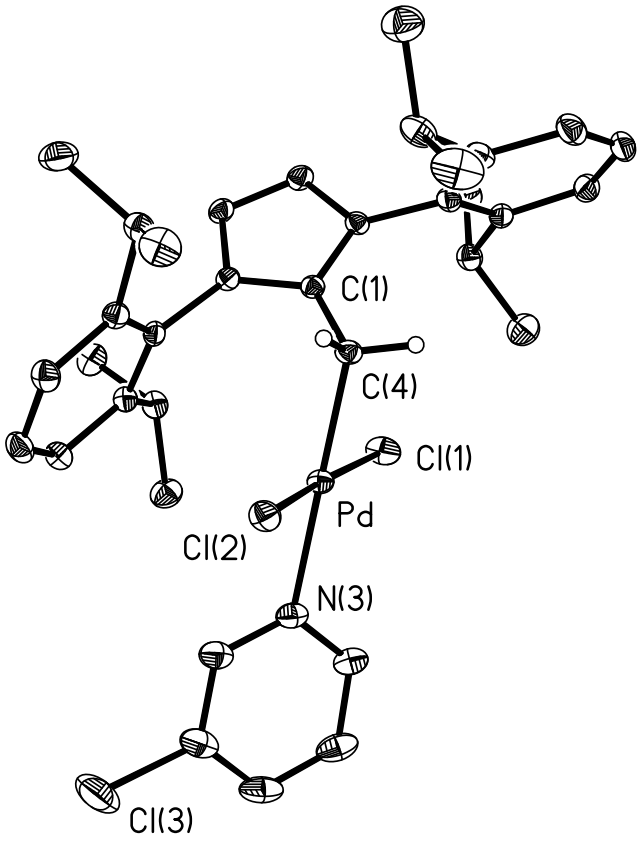

Figure 3.5: ORTEP of **8** with thermal ellipsoids drawn at a 30 % probability level; all hydrogen atoms except for C(4) have been omitted for clarity. Selected bond lengths (Å) and angles (°): C(4)−Pd 2.027(3), Pd−N(3) 2.145(3); C(4)−Pd−N(3) 179.21(12), C(1)−C(4)−Pd 114.4(2), Cl(1)-Pd-Cl(2) 174.20(3).

An *N*-heterocyclic olefin variant of Nolan's well-known IPr-PdCl(cinnamyl)[20] (cinnamyl = η^3-$H_2CCHCHPh$) pre-catalyst was also synthesized (Scheme 3.9). The synthesis of ($IPrCH_2$)PdCl(cinnamyl) **10** proceeded smoothly by the addition of two equiv. of $IPrCH_2$ to $[PdCl(cinnamyl)]_2$ in toluene. Large yellow crystals of **10** were subsequently obtained (from a CH_2Cl_2/hexanes solvent mixture) that enabled characterization of the material via X-ray crystallography (Figure 3.6). Interestingly, compound **10** yields broad resonances for the Me groups in the flanking Dipp substituents within the $IPrCH_2$; attempts to resolve these signals into the expected doublet resonance by heating to 60 °C led to decomposition of **10**. Notably, the related complex IPr•PdCl(cinnamyl) **11** yields two well-resolved doublet patterns for the Me environments, suggesting a more hindered environment around Pd in realtion to **10** and slow rotation of the Dipp groups on the NMR timescale.

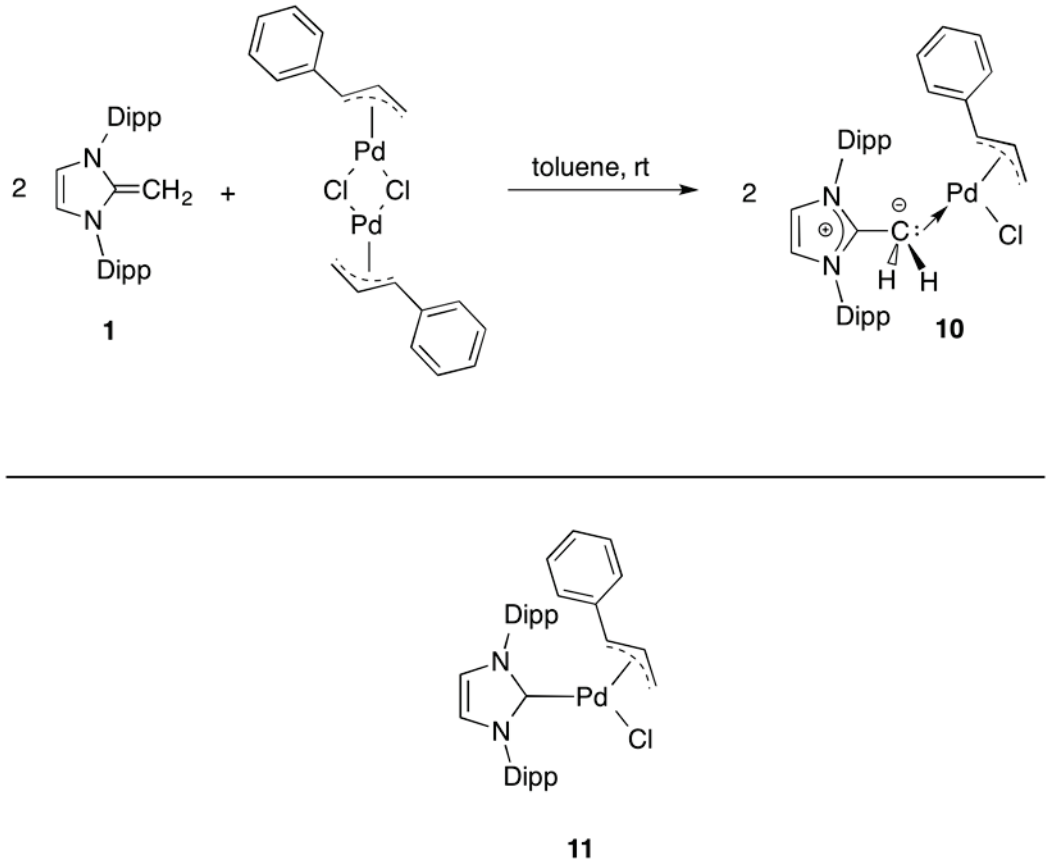

Scheme 3.9: Synthesis of complex **10**, the NHO analogue of Nolan's IPr•PdCl(cinnamyl) pre-catalyst (**11**).

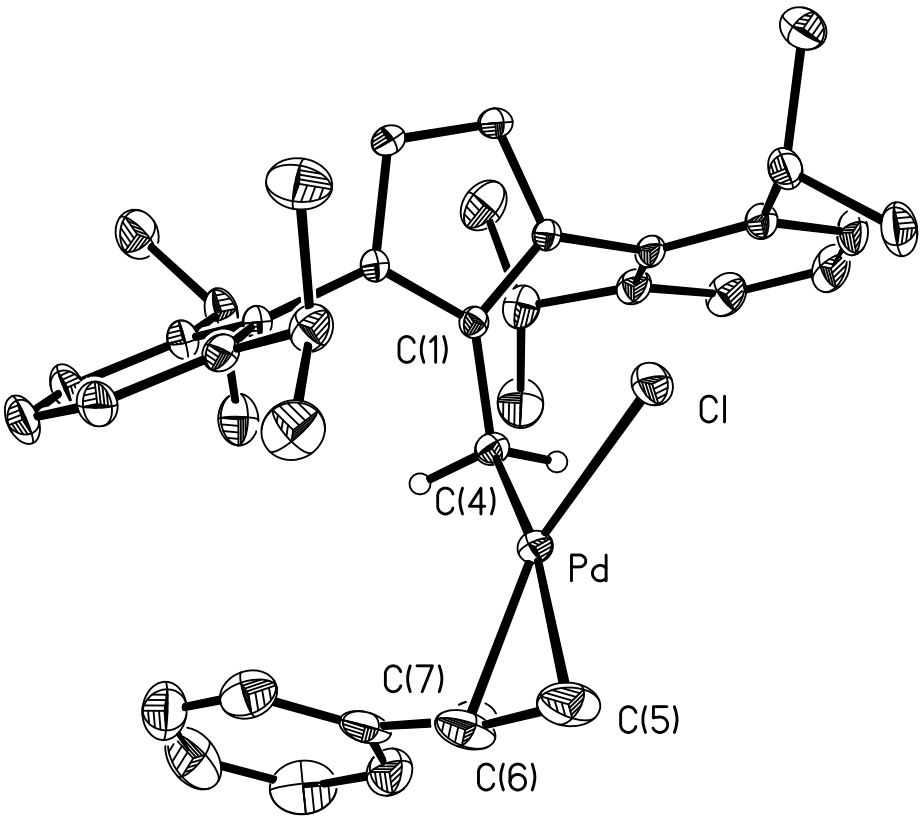

Figure 3.6: ORTEP of **10** with thermal ellipsoids drawn at a 30 % probability level; all hydrogen atoms except C(4) have been omitted for clarity. Selected bond lengths (Å) and angles (°): C(4)−Pd 2.134(3), Pd−C(5) 2.165(4), Pd−C(6) 2.118(3), Pd−C(7) 2.139(4); C(1)−C(4)−Pd 115.56(19), C(4)-Pd-C(5) 163.80(14), Cl-Pd-C(4) 99.57(8).

When one compares the metrical parameters of the cinnamyl/NHO complex **10** with its NHC counterpart **11**, a similar trend is noted in the M-C bond lengths involving the neutral carbon-based donors. For example, the C_{IPrCH2}-Pd distance [2.134(3) Å] in **10** is slightly longer than the C_{IPr}-Pd bond length of 2.041(9) Å in **11**. The adjacent Pd-C distances involving the Pd-cinnamyl group in **10** lie in a narrow range of 2.118(3) to 2.165(4) Å, while the bulkier nature of the IPr ligand in **11** causes more distortion in the cinnamyl binding mode, as evidenced by a wider range of Pd-C distances [2.084(10) to 2.281(9)].[23] Thus as with complex **8**, the steric bulk of the $IPrCH_2$ in complex **10** is further removed from the palladium center in relation to the NHC analogues.

3.4.1 *N*-Heterocyclic Olefin-Palladium Complexes as Catalysts

The NHO-Pd complexes **8** and **10** were designed with the end goal of promoting cross-coupling catalysis. Suzuki-Miyaura cross-coupling was chosen as the initial test reaction due to our group's prior use of this C-C bond forming reaction to prepare conjugated polymers.[21] Suzuki-Miyaura cross-coupling typically involve arylboronic acids ($ArB(OH)_2$) and aryl halides as substrates. This transformation is generally accomplished using Pd(II) pre-catalysts that are reduced in situ to catalytically active palladium (0) species. The main steps of the Suzuki-Miyaura cross-coupling cycle are oxidative addition, followed by a transmetalation step (nucleophilic attack of an aryl anion on a Pd-X bond;

X = halide, OH or OAc), and the final product is released through a reductive regenerates the Pd(0) catalyst (see Chapter 1 for more details). Designing a catalyst that performs well at each of these steps is a challenge. What might increase the rate of one step might decrease the rate of a different step, thus catalyst design represents a balancing act.

The oxidative addition of ArX species to Pd(0) centers is usually rate-limiting. The presence of a bulky ligand facilitates the formation of low-coordinate Pd(0) centers, which encourages a more rapid oxidation addition step with arylhalides (to form $L_xPdAr(X)$ species; L = ligand; X = halide). Also, a ligand with strong π-backbonding removes electron density from the electron rich palladium center, thereby slowing down oxidative addition of ArX. The transmetalation step relies on the presence of base to form a boronate $[ArB(OH)_2(Base)]^{-x}$ and the ability to access the reactive Pd-X bond, thus extremely bulky ligands or substrates could prevent the transfer of the aryl group from the boronic acid to the palladium center. It is this step that we envision a possible enhancement in rate when NHOs are used in place of NHCs as ligands.

The final step is the reductive elimination of the two aryl groups to form the final product. A bulky ligand once again aids in this step and when great steric strain exists around the palladium center, reductive elimination becomes more facile. *N*-heterocyclic olefins are generally weaker donors than NHCs, however the more polarizable nature of the carbon-based lone-pair used to form C-Pd interactions in NHO complexes

might enhance bonding to the soft Pd(0) centers formed during catalysis and prevent metal loss (catalyst decomposition). These differences from NHCs may make NHO ligands excellent ligands for palladium catalysts.

When comparing the activity of two catalysts it is necessary to compare them under the exact same reaction conditions. In this way, it should have been straightforward to compare the activities of the NHO complexes **4/5**, **8**, and **10** to their known NHC analogues using previously published conditions for catalysts. Initial tests showed catalytic activity for all NHO complexes, however as time progressed and more tests were completed, the conversion rates for complexes **4/5**, **8**, and **10** dropped to zero. Even more frustrating, the conversion rates for the known NHC complexes, **9** and **11** also dropped to zero. This at first suggested a procedural problem. A variety of the conditions were tried for complexes **8-11** in an attempt to solve the lack of conversion problem (in the test reaction between $PhB(OH)_2$ and 4-bromotoluene. This included varying the solvent from anhydrous 1,4-dioxane to tetrahydrofuran, and then to toluene, and finally *tert*-butyl alcohol (stored outside, not in a glovebox). No improvement was seen from one solvent to another. Another variable that was tested was the order in which the reagents were added to the reaction, specifically Organ recommended that the base was added directly to the boronic acid and allowed to stir for a short period of time.[14] However, upon consultation with other members of our Chemistry Department, the base was added last after all other reagents were

combined to prevent deactivating the boronic acid; again no improvement was seen. Besides order of addition of the base, both potassium tert-butoxide and cesium carbonate were tested as the base in the reaction; as before, no improvement was seen. All substrates were initially analyzed by ^{1}H NMR and some by GC, and the substrates were determined to be pure. The reactions were run with the isolated pre-catalysts as well as the pre-catalyst synthesized in situ; likewise different sources of palladium were tested, such as $PdCl_2$, $Pd(OAc)_2$ and $Cl_2Pd(NCPh)_2$, with no improvement. Different temperatures and time of reactions were tested, none showed any sign of improvement. A small sample of commercially available (IPr)$PdCl_2$(3-chloropyridine) catalyst was tested, and also showed little to no conversion. All of these experiments pointed towards the arylboronic acid being the source of the difficulties.

Boronic acids have proven to be difficult to work with in specific settings due to the fact that they exist in equilibrium with the cyclized boroxine and water (Scheme 3.10).[22] The boroxines are less reactive than boronic acid, particularly for Suzuki-Miyaura cross-coupling. As all cross-coupling reactions were set up in a glovebox, the anhydrous environment encouraged the dehydration of the arylboronic acids over time. To prevent the formation of boroxines in a cross-coupling reaction, water is frequently added to the solvent; however, when adding either an NHC or NHO to a palladium precursor, water is not tolerable. This explains the dropping conversion rates observed over the months of testing. The longer

the boronic acids were stored in the glovebox the less reactive they were becoming. In the end, the problem was easily rectified. The boronic acids were removed from the glove box, dissolved in water and then the water was removed just prior to catalyst trials. The resulting white powder was nearly pure boronic acid, with little to no boroxine present (< 99% according to NMR). The recrystallized boronic acid was then used successfully to test NHO complex-based catalysts as previously discussed.

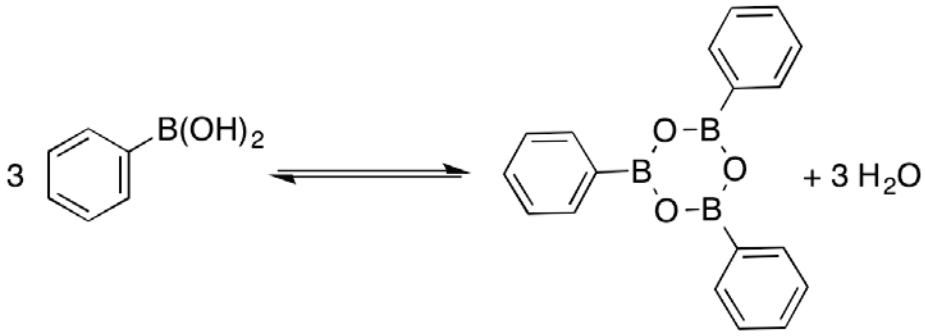

Scheme 3.10 The equilibrium between boronic acids and boroxines.

3.4.2 Results of Preliminary Catalytic Tests

A set of conditions was decided upon based on previously published work with complexes **9** and **11**.[13,14] Specifically, all reactions were conducted in 1,4-dioxane with a slight deficit of aryl halide (0.125 mmol) in relation to the arylboronic acid (0.150 mmol). The carbon-based ligand (either $IPrCH_2$ or IPr) or protonated pre-ligand was then combined with a *ca.* 5 mol. % loading of palladium source relative to the substrates. After the reaction was stirred for one minute, 0.375 mmol of potassium

tert-butoxide was added, followed by heating to 80 °C for 2 hours. After work-up the resulting products were analyzed by ^{1}H NMR spectroscopy. Each catalyst trial was completed in duplicate with the reported yields and conversions listed as an average of two runs. Yield percent is based on NMR yields using the internal standard, benzyl ether. The conversion percent was calculated by comparing the amount of product versus starting aryl halide as seen in the NMR spectra of the products.

The initial cross-coupling reactions were conducted using phenylboronic acid and *p*-bromotoluene as reactants (Table 3.4). These substrates were selected due to the lack of sterically demanding substituents and the ease with which the arylbromides tend to react in Suzuki-Miyaura coupling. As a result this substrate pair would quickly reveal if the NHO substituted complexes had any catalytic activity.

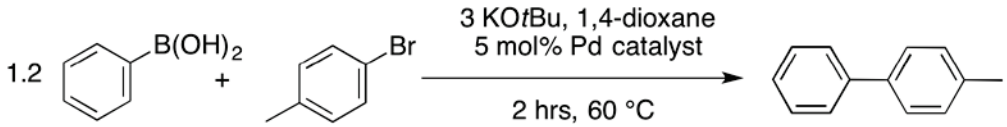

Entry	Ligand Added	Palladium Source	Yield (%)	Conversion (%)
1	2 equiv. $IPrCH_2$	$Cl_2Pd(NCPh)_2$	38	63
2	2 equiv. IPr	$Cl_2Pd(NCPh)_2$	38	38
3	---	complex **8**	10	17
4	---	complex **9**	15	16
5	1 equiv. $IPrCH_2$	$[Pd(cinnamyl)Cl]_2$	57	>99
6	1 equiv. IPr	$[Pd(cinnamyl)Cl]_2$	43	>99
7	2 equiv. $[IPrCH_3]I$	$Pd(OAc)_2$	34	57
8	1:1 equiv. IPr:$IPrCH_2$	$Cl_2Pd(NCPh)_2$	44	79

Table 3.4: Initial results from cross-coupling study. All yields and conversions were determined by NMR.

Table 3.4 shows that all the catalysts tested were successful at coupling the simple substrates to some degree; moreover comparative trials with IPr coordinated Pd catalysts were included. Of note, the $[IPrCH_3]I$ and $Pd(OAc)_2$ pre-catalyst combination is more likely to form an a-NHC-Pd complex (**5b**) (entry 1) whereas the $IPrCH_2$ and

$Cl_2Pd(NCPh)_2$ combination (entry 7) is more likely to form the NHO-Pd complex (**4**). Recalling the previous discussion about the synthesis of **4** and **5**, even at higher temperatures only a small percentage of the product mixture is **5** (around 12 % after 2 hours at 50 °C). When comparing the two pre-catalyst mixtures, similar product conversions were noted.

The most active NHO-based catalytic system is the *in situ* generated cinnamyl-palladium complex **10** (entry 5), with quantitative conversion of the starting materials to the desired product; based on these results, this system was selected for further testing.

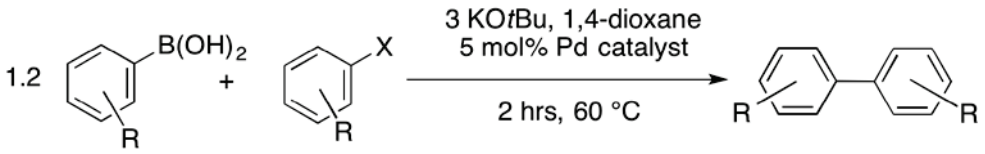

Boronic Acid	Aryl Halide	($IPrCH_2$) %Yield	($IPrCH_2$) % Conv.	(IPr) %Yield	(IPr) % Conv.
phenylboronic acid	4-bromotoluene	37.9	>99	42.6	>99
phenylboronic acid	4-chlorotoluene	39.5	>99	44.2	>99
mesitylboronic acid	2-bromomesitylene	9.5	28	21.2	54
mesitylboronic acid	2-chloro-1,3-dimethylbenzene	3.5	9	20.6	47

Table 3.5: Cross-coupling trials involving more hindered substrates using cinnamyl-palladium dimer as the palladium source (5 mol. % Pd) and addition of one equivalent of either $IPrCH_2$ or IPr . All yields were calculated by NMR.

To further test the activity of complex **10**, more difficult to couple arylchloride and sterically encumbered substrates were chosen (Table 3.5). Complex **10** performed equally well as complex **11** on both the 4-bromo and 4-chlorotoluene couplings with $PhB(OH)_2$, but fell behind complex **11** when the more bulky substrates, 2-bromomesitylene and 2-chloro-1,3-dimethylbenzene were tested.

3.4.3 Analysis of Preliminary Catalytic Tests

Overall the NHO catalysts performed well, but their activities lagged behind known benchmark NHC catalysts when more hindered or arylchloride substrates were investigated. To reveal the possible reasons for this, we will have to look again at the mechanism of Suzuki-Miyaura cross-coupling. The effect of the ligand on the catalyst is a balance between steric and electronic effects. Based on the results presented in Chapter 2 the interactions between a NHO and a metal are different when compared to that of *N*-heterocyclic carbenes as NHOs participate in minimal M-C π-backbonding. Such an interaction is likely important in stabilizing the reactive palladium (0) species formed in the cross-coupling cycle. In addition to the π-backbonding, overall $IPrCH_2$ is a weaker donor than IPr, thus a combination of these two factors could result in catalyst deactivation via metal extrusion during cross-coupling. This hypothesis is supported by the observation that the NHO catalyzed reactions turn black within the first 10-15 minutes, compared to the NHC catalyzed reactions which just darken slightly before the end of the experiment. The black color could be due to the presence of palladium metal and indicate deactivation of the catalyst.

The steric effects of the $IPrCH_2$-supported palladium complexes are easier to quantify and visualize. It has been proposed that bulky ligands stabilize the palladium (0) species, therby increasing the rate of oxidative addition and also aid in the last step, reductive elimination.

While NHOs and NHCs might appear to have a similar level of steric bulk they are not equal. This can be quantified when looking at the molecular structure of the complexes **8** and **10**. When the structures of these complexes are examined in relation to their NHC analogues it is seen that the bulk of the $IPrCH_2$ ligand is lifted away from the palladium center.

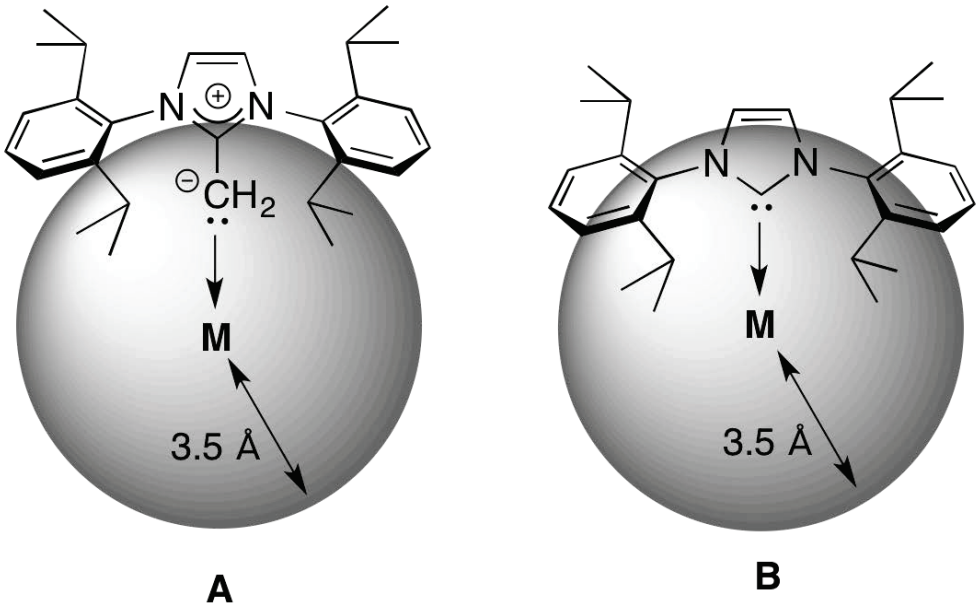

Figure 3.7: A qualitative comparison of the percent buried volume for $IPrCH_2$ (**A**) and IPr (**B**).

The steric bulk of a ligand on a transition metal is typically measured in percent buried volume.[23,24] Percent buried volume is defined as "the percent of the total volume of a sphere occupied by a ligand. The sphere has a defined radius and has the metal center at the core."[25] A common radius for the sphere is 3.5 ÅThis radius is selected as it generates a sphere around the metal center that matches well the volume

carved out by coordinating NHC ligands (such as IPr). In addition to a consistent radius, it is best to compare metal complexes that differ only by the replacement of a single ligand. Luckily for researchers an online tool titled Sambvca has been designed to calculate percent buried volume based on a .cif file of the molecular structure.[26] A comparison between IPr•AuCl and IPrCH_2•AuCl (**2**) shows that IPr covers 44.5% of the 3.5 Å sphere around gold, while complex **2** covers only 36%. An increase in percent buried volume generally leads to a marked improvement in catalytic activity.[27] The increased distance between the metal center and the steric bulk in the NHO based catalysts, as well as the flexibility of the steric bulk may explain why the NHO based catalysts tested in this work have lower conversion results than the NHC based catalysts.

3.5 Conclusions

The introduction of NHO ligands to catalysis represents a promising new research avenue. The complexes discussed in this chapter are similar to the well-explored NHC-transition metal complexes, but vary in key ways. This difference is perhaps best seen in the preliminary catalytic studies. NHO-palladium complexes perform as well as leading catalysts for Suzuki-Miyaura cross-coupling of reactive substrates, but not as well as known NHC-palladium complexes when more sterically hindered substrates are chosen. However, this is not cause for concern. In the large and varied world of catalytic cross-coupling the difference between NHOs and NHCs may be utilized for other applications. Future investigation into the application of NHO-transition metal complexes will be required to understand the power of an NHO.

3.6 Experimental Section

All reactions were performed using standard Schlenk line techniques under an atmosphere of nitrogen or in an inert atmosphere glove box (Innovative Technology, Inc.). Solvents were dried using a Grubbs-type solvent purification system[28] manufactured by Innovative Technology, Inc., and stored under an atmosphere of nitrogen prior to use. Anhydrous 1,4-dioxane, bis(benzonitrile)palladium(II) chloride, palladium(II) acetate, palladium(II) chloride, gold(I) chloride, chloro(dimethylsulfide)gold(I), cinnamylchloride, 3-chloropyridine, cesium carbonate and potassium tert-butoxide were purchased from Sigma-Aldrich and used as received. IPr,[29] $IPrCH_2$,[30] and $[IPrCH_3]I$[37] were prepared according to literature procedures while the palladium(cinnamyl)chloride dimer[31] was prepared via a modified literature procedure. ^1H and $^{13}C\{^1H\}$ NMR spectra were recorded on a 700 MHz, 500 MHz or 400 MHz Varian Inova instrument running VNMRJ 4 and referenced to the residual protonated solvent peak of known chemical shift. Elemental analyses were performed by the Analytical and Instrumentation Laboratory at the University of Alberta.

Synthesis of $IPrCH_2AuCl$ (2)

To a mixture of $(Me_2S)AuCl$ (25 mg, 0.085 mmol) and $IPrCH_2$ (34 mg, 0.085 mmol) was added 2 mL of THF. After stirring for 3 hrs. a purple solution was seen over white precipitate. The supernatant was decanted away and the remaning white precipitate was washed with 5 mL of THF. The product was then extracted from the precipitate with 3 mL of CH_2Cl_2. The extract was filtered through a small pad of Celite, and the volatiles were removed from the filtrate under vacuum to yield **2** as a colorless solid (33 mg, 61 %). ^{1}H NMR (500 MHz, $CDCl_3$): δ 1.20 (d, 12H, $^3J_{HH}$ = 7.0 Hz, CH(CH_3)$_2$), 1.45 (d, 12H, $^3J_{HH}$ = 7.0 Hz, CH(CH_3)$_2$), 2.11 (s, 2H, H_2C-Au), 2.70 (septet, 4H, $^3J_{HH}$ = 7.0 Hz, CH(CH$_3$)$_2$), 6.97 (s, 2H, N-CH-), 7.37 (d, 4H, $^3J_{HH}$ = 7.5 Hz, ArH), 7.54 (t, 2H, $^3J_{HH}$ = 7.5 Hz, ArH). ^{13}C{^{1}H} NMR (500 MHz, $CDCl_3$): δ 5.0 (Au-CH$_2$), 23.3 (CH(CH$_3$)$_2$), 25.5 (CH(CH$_3$)$_2$), 29.2 (CH(CH$_3$)$_2$), 120.2 (-NCH-), 125.1 (ArC), 130.5 (ArC), 131.4 (ArC), 146.0 (ArC) and 161.5 (N-C-N). Anal. Calc. % C, 52.96; H, 6.03; N, 4.41. Found C, 51.57; H, 6.25; N, 4.40. Melting Point: 201 °C (decomposition). See Figure 3.7 for NMR spectra of compound **2**.

Synthesis of $[(IPrCH_2)_2Au]Cl$ (3)

To a mixture of $(Me_2S)AuCl$ (25 mg, 0.085 mmol) and $IPrCH_2$ (68 mg, 0.17 mmol) was added 2 mL of THF. After stirring for 3 hrs. a pale brown solution was seen over a white precipitate. The supernatant was decanted away and the remaining white precipitate was washed with 5 mL of THF.

The product was extracted with 3 mL of CH_2Cl_2 and the solution was filtered through a small pad of Celite. The volatiles were then removed from the filtrate under vacuum to yield **3** as a colorless solid (81 mg, 81 %). ^{1}H NMR (500 MHz, C_6D_6): δ 0.89 (d, 24H $^3J_{HH}$ = 7.0 Hz, CH(CH_3)$_2$), 1.08 (d, 24H, $^3J_{HH}$ = 7.0 Hz, CH(CH_3)$_2$), 1.53 (s, 4H, H_2C-Au), 2.45 (septet, 8H, $^3J_{HH}$ = 7.0 Hz, CH(CH$_3$)$_2$), 6.92 (s, 4H, N-CH-), 7.22 (d, 8H, $^3J_{HH}$ = 7.5 Hz, ArH), 7.54 (t, 4H, $^3J_{HH}$ = 7.5 Hz, ArH). ^{13}C{^{1}H} NMR (500 MHz, $CDCl_3$): δ 18.6 (Au-CH$_2$), 22.6 (CH(CH_3)$_2$), 25.5 (CH(CH_3)$_2$), 29.1 (CH(CH$_3$)$_2$), 120.2 (-NCH-), 125.1 (ArC), 130.7 (ArC), 131.3 (ArC), 146.0 (ArC) and 161.8 (N-C-N). Anal. Calc. % C, 64.82; H, 7.32; N, 5.40. Found C, 64.60; H,7.43; N, 5.32.

Competitive Reaction between (Me_2S)AuCl and a 1:1 mixture of IPr and IPrCH$_2$

To a mixture of (Me_2S)AuCl (25 mg, 0.085 mmol), IPrCH$_2$ (68 mg, 0.17 mmol) and IPr (66 mg, 0.17 mmol) was added 3 mL of THF. After stirring for 3 hrs. a pale brown solution was seen over a white precipitate. The supernatant was decanted away and the remaining white precipitate was washed with 5 mL of THF. The product was extracted with 3 mL of CH_2Cl_2 and the solution was filtered through a small pad of Celite. The volatiles were then removed from the filtrate under vacuum to yield a colorless solid. The resulting ^{1}H NMR spectrum of the products in C_6D_6 indicates the presence of IPr•AuCl and free IPrCH$_2$.

Synthesis of *trans*-($IPrCH_2$)$_2PdCl_2$ (4)

To a solution of $Cl_2Pd(NCPh)_2$ (168 mg, 0.44 mmol) in 10 mL of toluene was added a solution of $IPrCH_2$ (175 mg, 0.43 mmol) in 5 mL of toluene. The resulting mixture was stirred overnight to give an orange precipitate. The supernatant was decanted and the precipitate was washed with 20 mL toluene and then dried under vacuum.[32] The product was extracted from the precipitate with 10 mL CH_2Cl_2 and filtered. The product was precipitated by adding 15 mL of hexanes. The solution was decanted leaving **4** as an orange solid (226 mg, 72 % yield) that was dried under vacuum. Crystals that were suitable for X-ray crystallography were obtained by dissolving **4** in a minimal amount of CH_2Cl_2, followed by layering of the solution with hexanes and cooling for -35 °C for 48 hours. ^{1}H NMR (500 MHz, C_6D_6): δ 1.09 (d, 24H, $^3J_{HH}$ = 7.0 Hz, CH(C*H*$_3$)$_2$), 1.48 (d, 24H, $^3J_{HH}$ = 6.5 Hz, CH(C*H*$_3$)$_2$), 2.55 (s, 4H, H_2C-Pd), 2.90 (septet, 8H, $^3J_{HH}$ = 6.5 Hz, C*H*(CH$_3$)$_2$), 6.33 (s, 4H, N-C*H*-), 7.12 (d, 8H, $^3J_{HH}$ = 7.5 Hz, Ar*H*), 7.31 (t, 4H, $^3J_{HH}$ = 7.5 Hz, Ar*H*). ^{13}C{^{1}H} NMR (500 MHz, $CDCl_3$): δ 23.1 (CH(*C*H$_3$)$_2$), 26.4 (CH(*C*H$_3$)$_2$), 28.9 (*C*H(CH$_3$)$_2$), 68.0 (Pd-*C*H$_2$), 121.7 (-N*C*H-), 124.9 (Ar*C*), 131.0 (Ar*C*), 131.4 (Ar*C*), 145.7 (Ar*C*) and 161.9 (N-*C*-N). Melting Point: 226 °C (decomposition). UV/vis (in THF): λ_{max} = 399 nm, ε = 1.12 x 10^3 L/(mol•cm). See Figure 3.8 for NMR spectra of compound **4**.

Synthesis of (a-IPrCH$_3$)$_2$PdCl$_2$ (5)

Complex **4** (20 mg, 0.02 mmol) was dissolved in 1 mL of $CDCl_3$ and heated at 50 °C for two hours to produce a red-orange solution. An ^{1}H NMR spectrum was immediately taken afterward, showing 12 % percent of **4** converted to **5**; collection of an informative $^{13}C\{^1H\}$ NMR spectrum was not possible due to the low solubility of the Pd complexes. X-ray quality crystals of **5** (red blocks) were obtained by dissolving **4** in minimal amount of CH_2Cl_2, followed by adding a layer of hexanes on top, and then storing the vial at room temperature for 48 hours. This procedure affords a mixture of both **4** and **5** that can be manually separated due to their different colors. Complex **5** was synthesized in very low yield. (Yield 12%, by NMR, 2.3 mg) Data for **5**: ^{1}H NMR (500 MHz, C_6D_6): δ 1.17 (d, 24H, $^3J_{HH}$ = 6.5 Hz, CH(C*H*$_3$)$_2$), 1.36 (d, 24H, $^3J_{HH}$ = 7.0 Hz, CH(C*H*$_3$)$_2$), 2.07 (s, 6H, *H*$_3$C-), 2.40 (septet, 8H, $^3J_{HH}$ = 6.5 Hz, C*H*(CH$_3$)$_2$), 7.38 (d, 8H, $^3J_{HH}$ = 7.5 Hz, Ar*H*), 7.60 (t, 4H, $^3J_{HH}$ = 7.5 Hz, Ar*H*), 8.41 (s, 2H, N-C*H*-). $^{13}C\{^1H\}$ NMR (700 MHz, $CDCl_3$): δ 23.3 (CH(*C*H$_3$)$_2$), 24.5 (CH(*C*H$_3$)$_2$), 29.1 (*C*H(CH$_3$)$_2$), 31.5 (Pd-*C*H$_2$), 124.7 (-N*C*H-), 125.3 (Ar*C*), 129.427 (*C*-Pd) 132.4 (Ar*C*), 133.0 (Ar*C*), 144.6 (Ar*C*) and 144.9 (N-*C*-N).

Alternative Synthesis of (a-IPrCH$_3$)$_2$PdCl$_2$ (5)

To a 5 mL solution of [IPrCH$_3$]Cl (215 mg, 0.50 mmol) in 5 mL of THF was added Pd(OAc)$_2$ (53 mg, 0.24 mmol). The reaction mixture was stirred overnight at 65 °C to give a red solution with a small amount of light colored precipitate. The precipitate was removed via filtration. The volatiles were then removed under vacuum and the resulting red solid was re-dissolved in 1 mL of CH_2Cl_2 and 15 mL of hexanes added. The mixture sat at room temperature for 4 hours. The resulting precipitate was separated from the supernatant and dried to give **5** as a red solid (20mg, 8.5 % Yield). NMR data matched the data reported above.

Synthesis of (IPrCH$_2$)Pd(3-chloropyridyl)Cl (8)

To IPrCH$_2$ (203 mg, 0.51 mmol) in 2 mL of 3-chloropyridine was added $PdCl_2$ (88.5 mg, 0.50 mmol). The resulting mixture was stirred overnight at 80 °C to yield a dark orange solution. The solution was diluted with 10 mL of CH_2Cl_2 and filtered through a small pad of silica gel. The volatiles were removed from the filtrate under vacuum, and the resulting orange solid was dissolved in 1 mL of CH_2Cl_2 and 15 mL of hexanes was added. The resulting precipitate was separated from the soluble fraction and then dried to give pure **8** as a yellow solid (106 mg, 31 %). ^{1}H NMR (700 MHz, C_6D_6): δ 1.15 (d, 12H, $^3J_{HH}$ = 6.3 Hz, CH(C*H*$_3$)$_2$), 1.41 (d, 12H, $^3J_{HH}$ = 7.0 Hz, CH(C*H*$_3$)$_2$), 2.62 (s, 2H, H$_2$C-Pd), 2.94 (septet, 4H, $^3J_{HH}$ = 7.0 Hz, C*H*(CH$_3$)$_2$), 7.08 (s, 2H, N-C*H*-, overlapping with m, 1H, Ar*H*), 7.39 (d, 4H, $^3J_{HH}$ = 7.7 Hz, Ar*H*), 7.57 (m, 2H, Ar*H*

overlapping with m, 1H, Ar*H*), 8.62 (d, 1H, $^3J_{HH}$ = 5.6 Hz, Ar*H*), 8.70 (d, 1 H, $^3J_{HH}$ = 2.1 Hz, Ar*H*). $^{13}C\{^1H\}$ NMR (500 MHz, $CDCl_3$): δ 22.9 ($CH(CH_3)_2$), 26.4 ($CH(CH_3)_2$), 29.2 ($CH(CH_3)_2$), 53.5 (Pd-CH_2), 121.8 (-N*C*H-), 124.2, 125.0, 125.4, 131.4, 131.8, 136.7, 146.9, 149.5, 150.6 (Ar*C*) and 164.4 (N-*C*-N). UV-vis (in THF): λ_{max} = 375 nm, $\varepsilon = 1.42 \times 10^3$ L/(mol•cm). Melting Point: 143 °C (decomposition).

Alternate synthesis of (IPr)Pd(3-chloropyridyl)Cl (9)

To a solution of [IPrH]Cl (213 mg, 0.51 mmol) in 2 mL of 3-chloropyridine was added $PdCl_2$ (88.5 mg, 0.50 mmol) and K_2CO_3 (345.5 mg, 2.5 mmol). The resulting mixture was stirred overnight at 80 °C to yield a yellow-green solution. The solution was cooled to room temperature and then diluted with 10 mL of CH_2Cl_2 and filtered through a small pad of silica gel. The volatiles were removed from the filtrate under vacuum and the resulting yellow-green solid was dissolved in *ca.* 1 mL of CH_2Cl_2. 15 mL of hexanes was then added leading to the precipitation of **9** as a yellow-green solid. The insoluble product was then separated from the supernatant and dried (281 mg, 80 %). NMR spectra matched those previously reported.[33]

Synthesis of (IPrCH$_2$)Pd(cinnamyl)Cl (10)

To a solution of $[Pd(cinnamyl)Cl]_2$ (100 mg, 0.19 mmol) in 10 mL of toluene was added a solution of $IPrCH_2$ (171 mg, 0.43 mmol) in 5 mL of

toluene. The resulting mixture was stirred overnight to give a yellow slurry. The supernatant was decanted away and the resulting precipitate was washed with 10 mL of toluene and then dried under vacuum. The precipitate was then dissolved in *ca.* 2 mL of CH_2Cl_2 (*ca.* 2 mL) and 2 mL of hexanes was layered on top of the solution. After 24 hrs. large yellow crystals of **10** formed (218 mg, 87 %) that were suitable for X-ray crystallography. ^{1}H NMR (500 MHz, C_6D_6): δ 1.22 (d, 12H, $^3J_{HH}$ = 6.5 Hz, CH(CH_3)$_2$), 1.34 (d, 12H, $^3J_{HH}$ = 7.0 Hz, CH(CH_3)$_2$), 2.31 (s, 2H, CH(CH_3)$_2$), 3.02 (d, 2H, η^3-CH_2-CH-CH-), 3.67 (d, 2H, η^3-CH_2-CH-CH-), 5.03 (m, 2H, η^3-CH_2-CH-CH-), 6.34 (s, 2H, N-C*H*-), 6.90-6.84 (m, Ar*H*), 7.12-7.13 (m, Ar*H*), 7.18-7.22 (m, Ar*H*). Anal. Calc. % C, 67.16; H, 7.16; N, 4.23. Found C, 68.05; H, 7.51; N, 4.49. Melting Point: 172 °C (decomposition). UV-vis (in THF): λ_{max} = 369 nm, ε = 2.60 x 10^4 L/(mol•cm).

Modified synthesis of (IPr)Pd(cinnamyl)Cl (11)

To [Pd(cinnamyl)Cl]$_2$ (100 mg, 0.19 mmol) in 10 mL of toluene was added a solution of IPr (167 mg, 0.43 mmol) in 5 mL of toluene. The resulting mixture was stirred overnight to give a yellow slurry. The supernatant was decanted and the precipitate was washed with 10 mL of toluene and then dried under vacuum. The precipitate was then dissolved in *ca.* 2 mL of CH_2Cl_2 and 2 mL of hexanes was layered on top of the solution. After 24 hrs. large yellow crystals of **11** formed (69 mg, 56 %); NMR data matched previously published data.[20]

General Procedure for Suzuki-Miyaura Cross Coupling Trials

A vial was charged with boronic acid (0.150 mmol) and 1 mL of 1,4-dioxane. The solution was stirred to dissolve the boronic acid and the aryl halide (0.125 mmol). For the catalysts formed *in situ*, a palladium source (5 mol. %) and ligand were added. The only pre-catalysts that were added in pure form where the PEPPSI systems **8** and **9** (also 5 mol. % loadings). The contents of the vial were then stirred, yielding a yellow-orange solution. Potassium *tert*-butoxide (0.325 mmol) in 1 mL of 1,4-dioxane was then added and the resulting solution was left to stir at 60 °C for 2 hours. Afterwards, the solution was cooled to room temperature and diluted with 2 mL of chloroform, and then washed with 4 mL of water; the organic fraction was then filtered through a small pad of silica gel and the volatiles were removed under vacuum. Product conversions were then estimated by comparing the NMR spectra with known data in the literature.

The following compounds were synthesized and their identities confirmed by NMR spectroscopy in $CDCl_3$.

4-Phenyltoluene:[34] ^{1}H NMR: 2.39 (s, 3H, C*H*$_3$), 7.24 (d, 2H, $^3J_{HH}$ = 3.0, Ar-*H*), 7.33-7.30 (t, 1H, $^3J_{HH}$ = 3.0, Ar-*H*), 7.43-7.41 (t, 2H, $^3J_{HH}$ = 2.0, Ar-*H*), 7.49 (d, 2H, $^3J_{HH}$ = 6.0 Ar-*H*), 7.58, 7.57 (d, 2H, $^3J_{HH}$ = 3.0 Ar-*H*)

2,2',4,6,6'-Pentamethylbiphenyl: ^{1}H NMR: 1.86 (s, 6H, CH_3), 1.90 (s, 6H, CH_3), 2.32 (s, 3H, CH_3), 6.94 (s, 2H, Ar*H*), 7.18-7.09 (m, 3H, Ar*H*).[35]

Bismesitylene: ^{1}H NMR: 1.86 (s, 12 H, CH_3), 2.23 (s, 6H, CH_3), 6.93 (s, 4H, Ar*H*).[36]

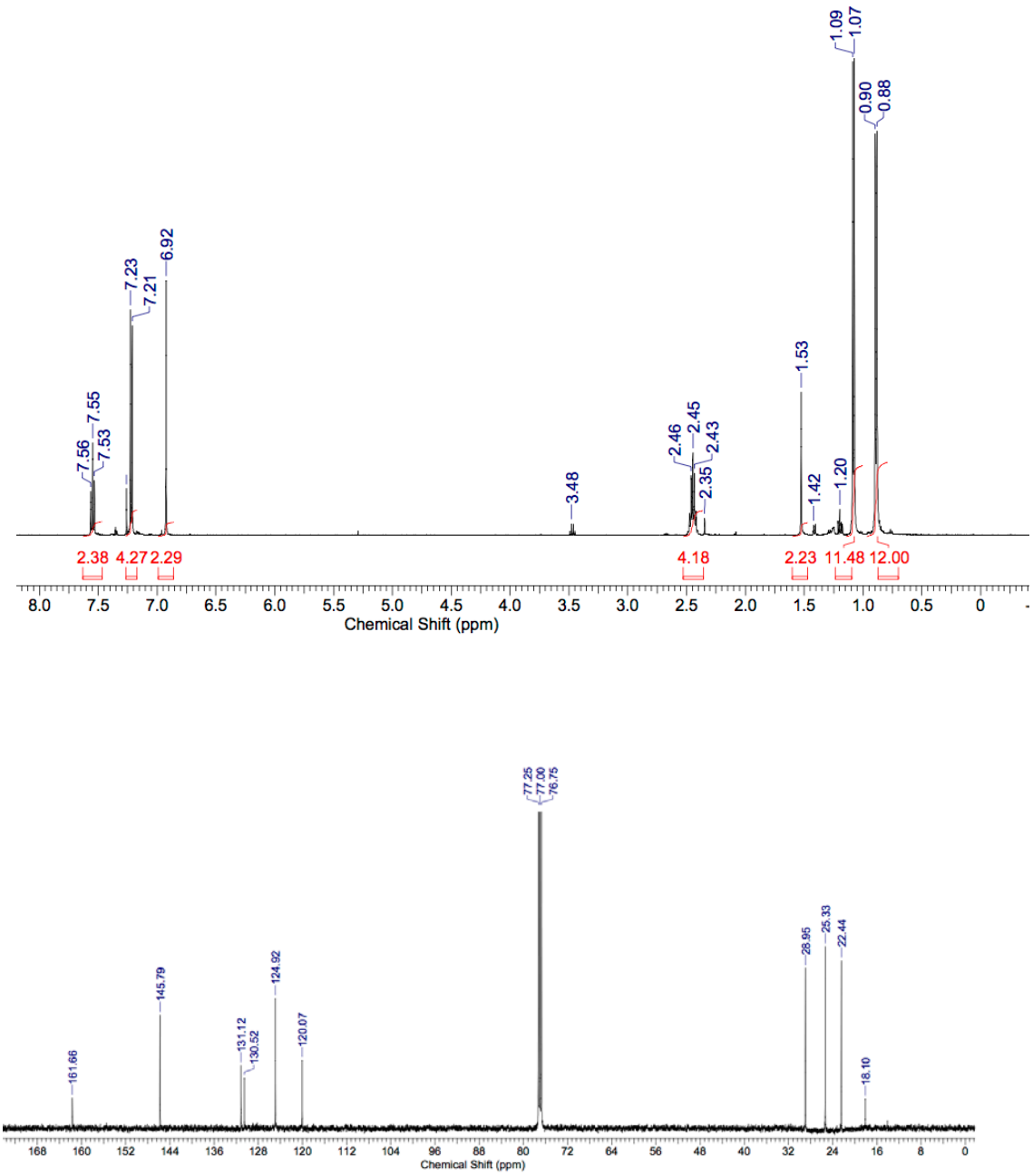

Figure 3.8: ^{1}H NMR and $^{13}C\{^{1}H\}$ NMR spectra for compound **2** in $CDCl_3$.

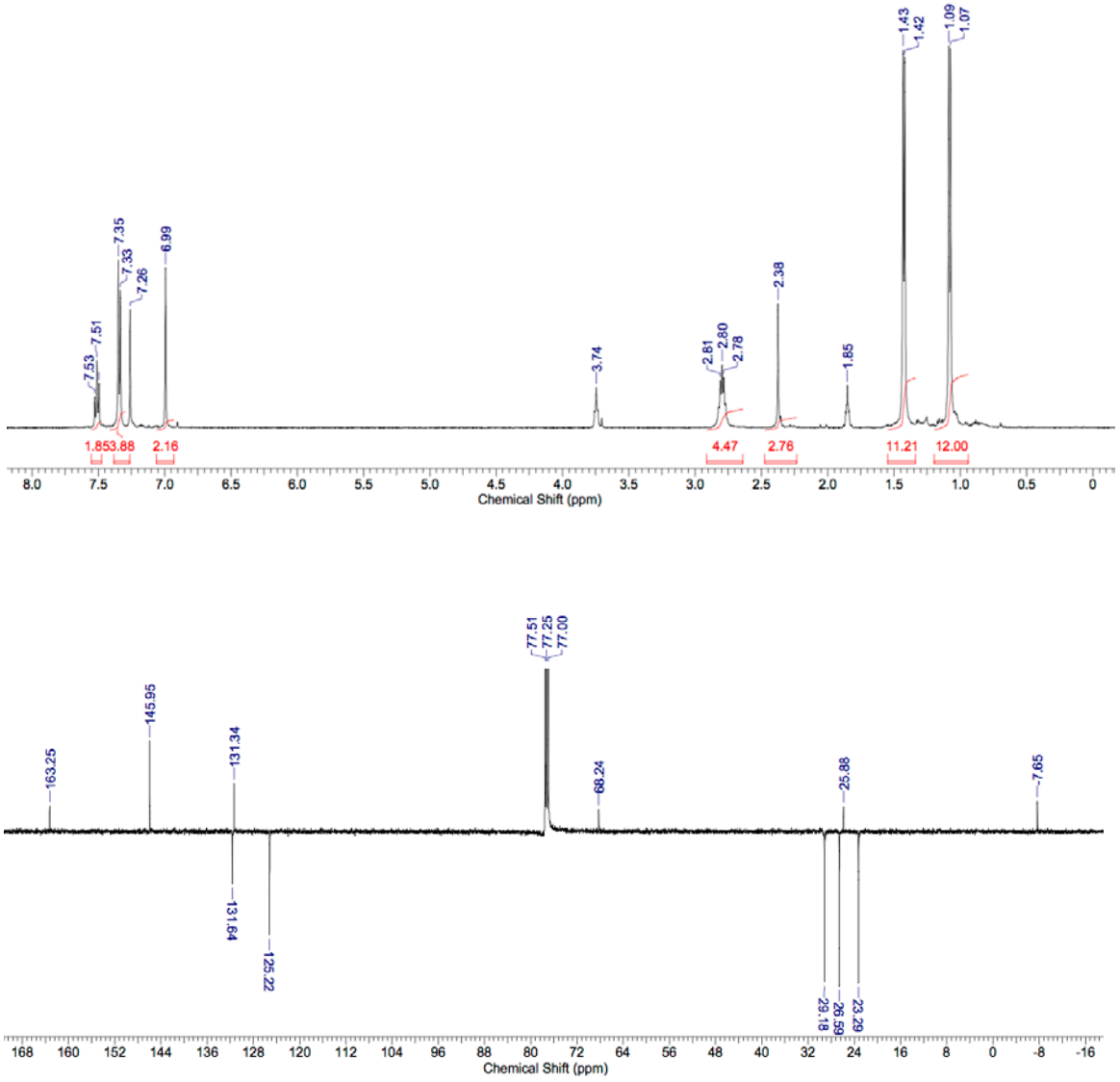

Figure 3.9: ^{1}H NMR and $^{13}C\{^{1}H\}$ (APT) NMR spectra for compound **4** in $CDCl_3$.

3.7 X-ray Crystallographic Data

Table 3.7 Crystallographic data for compounds **2** and **3**.

	2	**3**
empirical formula	$C_{28}H_{38}AuClN_2$	$C_{63}H_{91}AuCl_9N_4$
formula weight	628.97	1420.41
crystal dimensions (mm)	0.23 × 0.17 × 0.14	0.45 × 0.27 × 0.24
crystal system	monoclinc	monoclinic
space group	$P2_1/n$	$P2_1/n$
unit cell		
a (Å)	11.3789 (4)	12.5775(6)
b (Å)	13.7126(5)	21.3986(10)
c (Å)	17.4226(6)	25.9972(12)
β (°)	92.1870(10)	90.031(6)
V (Å^3)	2716.54(17)	6996.9(6)
Z	4	4
ρ calcd (g cm^{-3})	1.538	1.348
μ (mm^{-1})	5.53	2.485
temperature (°C)	–80	–100
2 θ_{max} (°)	27.498	56.54
total data	50419	64683
unique data (R_{int})	6233 (0.0372)	17191 (0.0246)
observed data a [I>2σ(I)]	5414	13977
parameters	183	686
R_1 [I>2σ(I)]	0.0272	0.0486
wR_2 [all data][a]	0.0480	0.1275
difference map Δρ (e Å^{-3})	1.517 /–0.545	2.497 / –1.558

[a] $R1 = ||Fo| - |Fc||/|Fo|$; $wR2 = [w(Fo^2 - Fc^2)^2/w(Fo^4)]^{1/2}$.

Table 3.8 Crystallographic data for compounds **4** and **5**.

	4	**5**
empirical formula	$C_{60}H_{86}Cl_2N_4OPd$	$C_{56}H_{76}Cl_{1.67}I_{0.33}N_4Pd$
formula weight	1056.62	1012.68
crystal dimensions (mm)	0.45 × 0.27 × 0.24	0.32 × 0.22 × 0.03
crystal system	orthorhombic	monoclinc
space group	*Pbcn*	$P2_1/n$
unit cell		
a (Å)	12.4423(7)	10.7812(4)
b (Å)	26.5010(14)	21.4456(8)
c (Å)	17.8243(10)	12.4922(5)
β (°)		113.2499(4)
V (Å^3)	5877.3 (6)	2653.76(18)
Z	4	2
ρ calcd (g cm^{-3})	1.194	1.267
μ (mm^{-1})	3.684	0.664
temperature (°C)	–100	–100
2 θ_{max} (°)	148.83	54.93
total data	38355	23100
unique data (R_{int})	5935 (0.0463)	6061 (0.0292)
observed data a [I>2σ(I)]	5196	5157
parameters	5935	6061
R_1 [I>2σ(I)]	0.0788	0.0285
wR_2 [all data]	0.1950	0.0723
difference map Δρ (e Å^{-3})	1.634 / –0.821	0.420 /–0.328

$^f R1 = ||Fo| - |Fc||/|Fo|$; $wR2 = [w(Fo^2 - Fc^2)^2/w(Fo^4)]^{1/2}$

Table 3.9 Crystallographic data for compounds **8** and **10**

	8	**10**
empirical formula	$C_{34}H_{44}Cl_5N_3Pd$	$C_{37}H_{47}ClN_2Pd$
formula weight	778.37	661.61
crystal dimensions (mm)	0.26 × 0.13 × 0.05	0.19 × 0.13 × 0.06
crystal system	monoclinic	orthorhombic
space group	*I2/a*	$P2_12_12_1$
unit cell		
a (Å)	23.7782(8)	14.2612(4)
b (Å)	13.4816(5)	14.6370(4)
c (Å)	24.4070(8)	16.2443(5)
β (°)	109.8466(5)	
V (Å^3)	7359.4(4)	3390.85(17)
Z	8	4
ρ calcd (g cm^{-3})	1.405	1.296
μ (mm^{-1})	0.894	5.325
temperature (°C)	–100	–100
2 θ_{max} (°)	55.10	144.71
total data	32668	23620
unique data (R_{int})	8576 (0.0503)	6683 (0.0320)
observed data a [I>2σ(I)]	6518	6534
parameters	8467	6683
R_1 [I>2σ(I)]	0.0441	0.0235
wR_2 [all data]	0.1274	0.0632
difference map Δρ (e Å^{-3})	0.838 /–0.879	0.985 / –0.560
Flack param.		0.001(3)

$^f R1 = ||Fo| - |Fc||/|Fo|$; $wR2 = [w(Fo^2 - Fc^2)^2/w(Fo^4)]^{1/2}$

3.8 References

(1) Ackermann, L.; Kaspar, L. T.; Gschrei, C. J. *Chem. Commun.* **2004**, 2824.

(2) Marion, N.; Nolan, S. P. *Acc. Chem. Res.* **2008**, *41*, 1440.

(3) Gstöttmayr, C. W. K.; Böhm, V. P. W.; Herdtweck, E.; Grosche, M.; Herrmann, W. A. *Angew. Chem. Int. Ed.* **2002**, *41*, 1363.

(4) Aher, S. B.; Muskawar, P. N.; Thenmozhi, K.; Bhagat, P. R. *Eur. J. Med. Chem.* **2014**, *81*, 408.

(5) Nolan, S. P. *Acc. Chem. Res.* **2011**, *44*, 91.

(6) Gaillard, S.; Bosson, J.; Ramón, R. S.; Nun, P.; Slawin, A. M. Z.; Nolan, S. *P. Chem Eur. J.* **2010**, *16*, 13729.

(7) Barnard, P. J.; Baker, M. V.; Berners-Price, S. J.; Day, D. A. *J. Inorg. Biochem.* **2004**, *98*, 1642.

(8) Hickey, J. L.; Ruhayel, R. A.; Barnard, P. J.; Baker, M. V.; Berners-Price, S. J.; Filipovska, A. *J. Am. Chem. Soc.* **2008**, *130*, 12570.

(9) Nandy, A.; Dey, S. K.; Das, S.; Munda, R. N.; Dinda, J.; Saha, K. D. *Mol. Cancer* **2014**, *13*, 57-71.

(10) Collado, A.; Gómez-Suárez, A.; Martin, A. R.; Slawin, A. M. Z.; Nolan, S. P. *Chem. Commun.* **2013**, *49*, 5541.

(11) Fürstner, A.; Alcarazo, M.; Goddard, R.; Lehmann, C. W. *Angew. Chem. Int. Ed.* **2008**, *47*, 3210.

(12) Liu, S.-T.; Lee, C.-I.; Fu, C.-F.; Chen, C.-H.; Liu, Y.-H.; Elsevier, C. J.; Peng, S.-M.; Chen, J.-T. *Organometallics* **2009**, *28*, 6957.

(13) Chartoire, A.; Nolan, S. P. In New Trends in Cross-Coupling; Colacot, T., Ed.; *RSC Catalysis Series*; Royal Society of Chemistry: Cambridge, **2014**; pp 139–227.

(14) Valente, C.; Calimsiz, S.; Hoi, K. H.; Mallik, D.; Sayah, M.; Organ, M. G. *Angew. Chem. Int. Ed.* **2012**, *51*, 3314.

(15) Gründemann, S.; Kovacevic, A.; Albrecht, M.; Faller, J. W.; Crabtree, R. H. *Chem. Commun.* **2001**, 2274.

(16) Gründemann, S.; Kovacevic, A.; Albrecht, M.; Faller, J. W.; Crabtree, R. H. *J. Am. Chem. Soc.* **2002**, *124*, 10473.

(17) Sini, G.; Eisenstein, O.; Crabtree, R. H. *Inorg. Chem.* **2002**, *41*, 602.

(18) Eguillor, B.; Esteruelas, M. A.; Oliván, M.; Puerta, M. *Organometallics* **2008**, *27*, 445.

(19) Lebel, H.; Janes, M.K.; Charette, A.B.; Nolan, S. P. *J. Am. Chem. Soc.* **2004**, *126*, 5046.

(20) Viciu, M.S.; Germaneau, R.F.; Nolan, S. P. *Org. Lett*. **2002**,*4*, 4053.

(21) He, G.; Kang, L.; Torres Delgado, W.; Shynkaruk, O.; Ferguson, M. J.; McDonald, R.; Rivard, E. *J. Am. Chem. Soc.* **2013**, *135*, 5360.

(22) Hall, D. G., *Boronic Acids: Preparation and Applications in Organic Synthesis, Medicine and Materials (Volume 1 and 2), Second Edition* - Wiley Online Library; Wiley-VCH Verlag GmbH & Co., **2011**.

(23) Viciu, M.S.; Navarro, O.; Germaneau, R.F.; Kelly, III, R.A.; Sommer, W.; Marion, N.; Stevens, E.D.; Cavallo, L.; Nolan, S. P. *Organometallics* **2004**, *23*, 1629.

(24) Dröge, T.; Glorius, F. *Angew. Chem. Int. Ed*. **2010**, *49*, 6940.

(25) Clavier, H.; Nolan, S. P. *Chem. Commun*. **2010**, *46*, 841.

(26) Poater, A.; Cosenza, B.; Correa, A.; Giudice, S.; Ragone, F.; Scarano, V.; Cavallo, L. *Eur. J. Inorg. Chem*. **2009**, 1759-1766.

(27) Wu, L.; Drinkel, E.; Gaggia, F.; Capolicchio, S.; Linden, A.; Falivene, L.; Cavallo, L.; Dorta, R. *Chem. Eur. J*. **2011**, *17*, 12886.

(28) Pangborn, A. B.; Giardello, M. A.; Grubbs, R. H.; Rosen, R. K.; Timmers, F. J. *Organometallics* **1996**, *15*, 1518.

(29) Bantreil, X.; Nolan, S. P. *Nat. Protoc*. **2011**, *6*, 69.

(30) Powers, K.; Hering-Junghans, C.; McDonald, R.; Ferguson, M. J.; Rivard, E. *Polyhedron*. DOI: 10.1016/j.poly.2015.07.070.

(31) Marion, N.; Navarro, O.; Mei, J.; Stevens, E. D.; Scott, N. M.; Nolan, S. P. *J. Am. Chem. Soc.* **2006**, *128*, 4101.

(32) Prasad, B. A. B.; Gilbertson, S. R. *Org. Lett*. **2009**, *11*, 3710.

(33) O'Brien, C. J.; Kantchev, E. A. B.; Valente, C.; Hadei, N.; Chass, G. A.; Lough, A.; Hopkinson, A. C.; Organ, M. G. *Chem. Eur. J*. **2006**, *12*, 4743.

(34) Bandari, R.; Höche, T.; Prager, A.; Dirnberger, K.; Buchmeiser, M. R. *Chem. Eur. J*. **2010**, *16*, 4650.

(35) Ackermann, L.; Potukuchi, H. K.; Althammer, A.; Born, R.; Mayer, P. *Org. Lett*. **2010**, *12*, 1004.

(36) Cahiez, G.; Chaboche, C.; Mahuteau-Betzer, F.; Ahr, M. *Org. Lett.* **2005**, *7*, 1943.

(37) Al-Rafia, S. M. I.; Ferguson, M. J.; Rivard, E.; *Inorg. Chem*. **2011**, *50*, 10543.

Chapter 4: Summary and Future Work

4.1 Summary

An improved synthesis of the *N*-heterocyclic olefin $IPrCH_2$ was developed and the bonding characteristics of this carbon-based ligand were explored via the preparation of the Rh(I) complex $IPrCH_2$•$Rh(CO)_2Cl$. By analyzing the IR stretching frequencies of the carbonyl groups it was determined that NHOs were good σ-donors, but likely participate in very little π-backbonding with metal centers (an observation supported by computational studies). The coordination activity of NHOs was further explored with gold and palladium centers and the palladium complexes were tested as pre-catalysts for Suzuki cross-coupling reactions. As described in Chapter 3, the newly prepared NHO-palladium complexes showed similar activities as known pre-catalysts based on NHCs for the coupling of reactive arylbromides and unhindered arylboronic acids. However, the NHC-palladium pre-catalysts were more active than their NHO counterparts when it came to instigating the coupling of arylchlorides with more hindered arylbornic acids. One possible reason for the lower conversions with NHO-complexes, is faster catalyst decomposition, as evidence by the formation of black reaction mixtures during the catalysis trials.

4.2 Future Work for NHO-Gold Complexes

The NHO-gold complexes were synthesized and characterized, but their reactivity within the context of catalysis not tested. Gold-NHC complexes have been used as catalysts for a variety of reactions, such as the cycloisomerization and hydration of alkynes. As a result, it would be interesting if the Au(I)-NHO complexes $IPrCH_2$•AuCl and $[(IPrCH_2)_2Au]Cl$ would be viable catalysts for the abovementioned transformation, as the $IPrCH_2$ gives a more sterically accessible Au(I) center in relation to the known IPr-Au(I) species.[1]

Another possible route of exploration is the use of NHO-gold complexes for anti-cancer applications. The field is relatively new, but growing. An important characteristic of anti-cancer agents is their lipophilicity.[2] The NHO-Au complexes may have different characteristics for inter-cell transport.

4.3 Future Work for NHO-Palladium Complexes

The initial catalytic tests showed that NHO-palladium complexes are catalytically active. However, the well-known NHC-palladium complexes proved to be more active in general. The NHO-palladium complexes may have greater activity under different conditions, for different types of substrates and for different types of catalytic cycles. A detailed optimization study of the Suzuki cross-coupling cycle catalyzed by the NHO-Pd complexes discussed in Chapter 3 should be undertaken.

This would include testing different solvents, temperatures, stoichiometric ratio of reagents, and sources of base. Also, an investigation into the stability of the studied NHO-Pd complexes should be completed. This could be accomplished by running NMR scale cross-coupling reactions that are monitored by ^{1}H NMR. If evidence of decomposition of the catalyst is seen, the reason for instability may be determinable.

In addition to palladium catalyzed reactions, further research into other NHO complexes may yield good results. The shortcomings of NHOs that were found with the palladium complexes, little steric strain and a lack of π-backbonding, may be benefits for early transition metal complexes. Metal centers that might be of interest include titanium, zirconium and vanadium. Early metal-NHC complexes have been studied as catalysts for the polymerization of small molecules such as ethane. The lack of π-backbonding may not be a hindrance for these less electron rich centers. Also the metal centers are smaller than the later transition metals, so the removed steric bulk of the NHO ligand may be an advantage.

References

(1) Gaillard, S.; Bosson, J.; Ramón, R. S.; Nun, P.; Slawin, A. M. Z.; Nolan, S. P. *Chem. Eur. J.* **2010**, *16*, 13729.

(2) Hickey, J. L.; Ruhayel, R. A.; Barnard, P. J.; Baker, M. V.; Berners-Price, S. J.; Filipovska, A. *J. Am. Chem. Soc.* **2008**, *130*, 12570.

(3) Díez-González, S. N-Heterocyclic Carbenes: From Laboratory Curiosities to Efficient Synthetic Tools; *Royal Society of Chemistry*, 2011.

Complete Bibliography

Chapter One

(1) Arduengo, A. J.; Harlow, R. L.; Kline, M. *J. Am. Chem. Soc.* **1991**, *113*, 361.

(2) Tschugajeff, L.; Skanawy-Grigorjewa, M.; Posnjak, A.; Skanawy-Grigorjewa, M. Z. *Anorg. Allg. Chem.* **1925**, *148*, 37.

(3) Rouschias, G.; Shaw, B. L. *J. Chem. Soc., Dalton Trans.* **1970**, 183.

(4) Burke, A.; Balch, A. L.; Enemark, J. H. *J. Am. Chem. Soc.* **1970**, *92*, 2555.

(5) Butler, W. M.; Enemark, J. H.; Parks, J.; Balch, A. L. *Inorg. Chem*. **1973**, *12*, 451.

(6) Fischer, E. O.; Maasböl, A. *Angew. Chem. Int. Ed. Engl.* **1964**, *3*, 580.

(7) Schrock, R. R. *J. Am. Chem. Soc*. **1974**, *96*, 6796.

(8) Igau, A.; Grutzmacher, H.; Baceiredo, A.; Bertrand, G. *J. Am. Chem. Soc*. **1988**, *110*, 6463.

(9) Wanzlick, H. W.; Jahnke, U. *Chem. Ber*. **1968**, *101*, 3753.

(10) Wanzlick, H. W.; Schikora, E. *Angew. Chem. Int. Ed. Engl.* **1960**, *72*, 494.

(11) Wanzlick, H. W. *Angew. Chem. Int. Ed. Engl*. **1962**, *1*, 75.

(12) Hartwig, J. F. Organotransition Metal Chemistry; *University Science Books*, **2010**.

(13) Díez-González, S. N-Heterocyclic Carbenes: From Laboratory

Curiosities to Efficient Synthetic Tools; *Royal Society of Chemistry*, 2011.

(14) Fortman, G. C.; Nolan, S. P. *Chem. Soc. Rev.* **2011**, *40*, 5151.

(15) Dröge, T.; Glorius, F. *Angew. Chem. Int. Ed*. **2010**, *49*, 6940.

(16) Tolman, C. A. *Chem. Rev.* **1977**, *77*, 313.

(17) Bantreil, X.; Nolan, S. P. *Nat. Protoc.* **2011**, *6*, 69.

(18) Kuhn, N.; Bohnen, H.; Kreutzberg, J.; Bläser, D.; Boese, R. *Chem. Commun.* **1993**, 1136.

(19) Wang, Y.-B.; Wang, Y.-M.; Zhang, W.-Z.; Lu, X.-B. *J. Am. Chem. Soc.* **2013**, *135*, 11996.

(20) Jia, Y.-B.; Wang, Y.-B.; Ren, W.-M.; Xu, T.; Wang, J.; Lu, X.-B. *Macromolecules* **2014**, 47, 1966.

(21) Al-Rafia, S. M. I.; Malcolm, A. C.; Liew, S. K.; Ferguson, M. J.; McDonald, R.; Rivard, E. *Chem. Commun*. **2011**, *47*, 6987.

(22) Pearson, R. G. *J. Am. Chem. Soc*. **1963**, *85*, 3533.

(23) Fürstner, A.; Alcarazo, M.; Goddard, R.; Lehmann, C. W. *Angew. Chem. Int. Ed.* **2008**, *47*, 3210.

(24) Khramov, D. M.; Lynch, V. M.; Bielawski, C. W. *Organometallics* **2007**, *26*, 6042.

(25) Crabtree, R. H. The Organometallic Chemistry of the Transition Metals; *John Wiley & Sons Inc*., **2005**.

(26) Hanukoglu, I. List of Elements of the Periodic Table - Sorted by Abundance in Earth's crust

http://www.science.co.il/PTelements.asp?s=Earth (accessed Aug 26, 2015).

(27) Nelson, D. J. *Eur. J. Inorg. Chem.* **2015**, 2012.

(28) Scholl, M.; Ding, S.; Lee, C. W.; Grubbs, R. H. *Org. Lett*. **1999**, *1*, 953.

(29) Suzuki, A. *Angew. Chem. Int. Ed.* **2011**, *50*, 6722.

(30) Negishi, E.-I. *Angew. Chem. Int. Ed.* **2011**, *50*, 6738.

(31) Cárdenas, D. J. *Angew. Chem. Int. Ed.* **2003**, *42*, 384.

(32) Huang, X; Anderson, K. W.; Zim, D.; Jiang, L.; Klapars, A.; Buchwald, S. L. *J. Am. Chem. Soc*. **2003**, *125*, 6653.

(33) Lennox, A. J. J.; Lloyd-Jones, G. C. *Angew. Chem. Int. Ed*. **2013**, *52*, 7362.

(34) Gstöttmayr, C. W. K.; Böhm, V. P. W.; Herdtweck, E.; Grosche, M.; Herrmann, W. A. *Angew. Chem. Int. Ed*. **2002**, *41*, 1363.

(35) O'Brien, C. J.; Kantchev, E. A. B.; Valente, C.; Hadei, N.; Chass, G. A.; Lough, A.; Hopkinson, A. C.; Organ, M. G. *Chem. Eur. J*. **2006**, *12*, 4743.

(36) PEPPSI-IPr Catalyst 98% http://www.sigmaaldrich.com/catalog/product/aldrich/669032?lang=en&region=CA (accessed Aug 26, 2015).

(37) Valente, C.; Calimsiz, S.; Hoi, K. H.; Mallik, D.; Sayah, M.; Organ, M. G. *Angew. Chem. Int. Ed***. 2012**, *51*, 3314.

(38) Marion, N.; Navarro, O.; Mei, J.; Stevens, E. D.; Scott, N. M.;

Nolan, S. P. *J. Am. Chem. Soc.* **2006**, *128*, 4101.

(39) Marion, N.; Nolan, S. P. *Acc. Chem. Res.* **2008**, *41*, 1440.

(40) Díez-González, S.; Marion, N.; Nolan, S. P. *Chem. Rev.* **2009**, *109*, 3612.

Chapter Two

(1) Kuhn, N.; Bohnen, H.; Kreutzberg, J.; Blaeser, D.; Boese, R. J. Chem. Soc., Chem. Commun. 14 (1993) 1136

(2) Kronig, S.; Jones, P. G.; Tamm, M. *Eur. J. Inorg. Chem.* **2013**, 2301.

(3) Ibrahim Al-Rafia, S. M.; Malcolm, A. C.; Liew, S. K.; Ferguson, M. J.; McDonald, R.; Rivard, E. *Chem. Commun.* **2011**, *47*, 6987.

(4) Knappke, C. E. I.; Anthony J. Arduengo, I.; Jiao, H.; Neudörfl, J.-M.; von Wangelin, A. J. *Synthesis* **2011**, 3784.

(5) Fürstner, A.; Alcarazo, M.; Goddard, R.; Lehmann, C. W. *Angew. Int. Ed.* **2008**, *47*, 3210.

(6) Dumrath, A.; Wu, X. -F.; Neumann, H.; Spannenberg, A.; Jackstell, R.; Beller, M. *Angew. Int. Ed.* **2010**, *49*, 8988.

(7) Rivard, E. *Dalton Trans.* **2014**, *43*, 8577.

(8) Al-Rafia, S. M. I.; Ferguson, M. J.; Rivard, E. *Inorg. Chem.* **2011**, *50*, 10543.

(9) Malcolm, A. C.; Sabourin, K. J.; McDonald, R.; Ferguson, M. J.; Rivard, E. *Inorg. Chem.* **2012**, *51*, 12905.

(10) Al-Rafia, S. M. I.; Momeni, M. R.; McDonald, R.; Ferguson, M. J.; Brown, A.; Rivard, E. *Angew. Chem. Int. Ed.* . **2013**, 52, 6390.

(11) Berger, C. J.; He, G.; Merten, C.; McDonald, R.; Ferguson, M. J.; Rivard, E. *Inorg. Chem.* **2014**, *53*, 1475.

(12) Wang, Y.; Abraham, M. Y.; Gilliard, R. J.; Sexton, D. R.; Wei, P.; Robinson, G. H. *Organometallics* **2013**, *32*, 6639.

(13) Ghadwal, R. S.; Reichmann, S. O.; Engelhardt, F.; Andrada, D. M.; Frenking, G. *Chem. Commun.* **2013**, *49*, 9440.

(14) Wang, Y. -B.; Wang, Y. -M.; Zhang, W. -Z.; Lu, X. -B. *J. Am. Chem. Soc.* **2013**, *135*, 11996.

(15) Jia, Y. -B.; Wang, Y. -B.; Ren, W. -M.; Xu, T.; Wang, J.; Lu, X. -B. *Macromolecules* **2014**, *47*, 1966.

(16) Ahmed, M.; Buch, C.; Routaboul, L.; Jackstell, R.; Klein, H.; Spannenberg, A.; Beller, M. *Chem. Eur. J.* **2007**, *13*, 1594.

(17) Sun, H.; Yu, X. -Y.; Marcazzan, P.; Patrick, B. O.; James, B. R. *Can. J. Chem.* **2009**, *87*, 1248.

(18) Chaplin, A. B. *Organometallics* **2014**, *33*, 3069.

(19) Tennyson, A. G.; Lynch, V. M.; Bielawski, C. W. *J. Am. Chem. Soc.* **2010**, *132*, 9420.

(20) Urbina-Blanco, C. A.; Bantreil, X.; Clavier, H.; Slawin, A. M. Z.; Nolan, S. P. *Beilstein J. Org. Chem.* **2010**, *6*, 1120.

(21) Dorta, R.; Stevens, E. D.; Scott, N. M.; Costabile, C.; Cavallo, L.; Hoff, C. D.; Nolan, S. P. *J. Am. Chem. Soc.* **2005**, *127*, 2485.

(22) Dröge, T.; Glorius, F. *Angew. Chem. Int. Ed.* **2010**, *49*, 6940.

(23) Ciancaleoni, G.; Scafuri, N.; Bistoni, G.; Macchioni, A.; Tarantelli, F.; Zuccaccia, D.; Belpassi, L. *Inorg. Chem.* **2014**, *53*, 9907.

(24) Khramov, D. M.; Lynch, V. M.; Bielawski, C. W. *Organometallics* **2007**, *26*, 6042.

(25) Weigend, F. *Phys. Chem. Chem. Phys.* **2006**, *8*, 1057.

(26) Weigend, F.; Ahlrichs, R. *Phys. Chem. Chem. Phys.* **2005**, *7*, 3297.

(27) Peterson, K. A.; Figgen, D.; Dolg, M.; Stoll, H. *J. Chem. Phys.* **2007**, *126*, 124101.

(28) Tonner, R.; Frenking, G. *Organometallics* **2009**, *28*, 3901.

(29) Vummaleti, S. V. C.; Nelson, D. J.; Poater, A.; Gómez-Suárez, A.; Cordes, D. B.; Slawin, A. M. Z.; Nolan, S. P.; Cavallo, L. *Chem. Sci.* **2015**, *6*, 1895.

(30) Gründemann, S.; Kovacevic, A.; Albrecht, M.; Faller, J. W.; Crabtree, R. H. *Chem. Commun.* **2001**, 2274.

(31) Bouffard, J.; Keitz, B. K.; Tonner, R.; Guisado-Barrios, G.; Frenking, G.; Grubbs, R. H.; Bertrand, G. *Organometallics* **2011**, *30*, 2617.

(32) Pangborn, A. B.; Giardello, M. A.; Grubbs, R. H.; Rosen, R. K.; Timmers, F. J. *Organometallics* **1996**, *15*, 1518.

(33) Bantreil, X.; Nolan, S. P. *Nat. Protoc.* **2011**, *6*, 69.

(34) Díez-González, S.; Marion, N.; Nolan, S. P. *Chem. Rev.* **2009**, *109*, 3612.

Chapter Three

(1) Ackermann, L.; Kaspar, L. T.; Gschrei, C. J. *Chem. Commun.* **2004**, 2824.

(2) Marion, N.; Nolan, S. P. *Acc. Chem. Res.* **2008**, *41*, 1440.

(3) Gstöttmayr, C. W. K.; Böhm, V. P. W.; Herdtweck, E.; Grosche, M.; Herrmann, W. A. *Angew. Chem. Int. Ed.* **2002**, *41*, 1363.

(4) Aher, S. B.; Muskawar, P. N.; Thenmozhi, K.; Bhagat, P. R. *Eur. J. Med. Chem.* **2014**, *81*, 408.

(5) Nolan, S. P. *Acc. Chem. Res.* **2011**, *44*, 91.

(6) Gaillard, S.; Bosson, J.; Ramón, R. S.; Nun, P.; Slawin, A. M. Z.; Nolan, S. *P. Chem Eur. J.* **2010**, *16*, 13729.

(7) Barnard, P. J.; Baker, M. V.; Berners-Price, S. J.; Day, D. A. *J. Inorg. Biochem.* **2004**, *98*, 1642.

(8) Hickey, J. L.; Ruhayel, R. A.; Barnard, P. J.; Baker, M. V.; Berners-Price, S. J.; Filipovska, A. *J. Am. Chem. Soc.* **2008**, *130*, 12570.

(9) Nandy, A.; Dey, S. K.; Das, S.; Munda, R. N.; Dinda, J.; Saha, K. D. *Mol. Cancer* **2014**, *13*, 57-71.

(10) Collado, A.; Gómez-Suárez, A.; Martin, A. R.; Slawin, A. M. Z.; Nolan, S. P. *Chem. Commun.* **2013**, *49*, 5541.

(11) Fürstner, A.; Alcarazo, M.; Goddard, R.; Lehmann, C. W. *Angew. Chem. Int. Ed.* **2008**, *47*, 3210.

(12) Liu, S.-T.; Lee, C.-I.; Fu, C.-F.; Chen, C.-H.; Liu, Y.-H.; Elsevier, C. J.; Peng, S.-M.; Chen, J.-T. *Organometallics* **2009**, *28*, 6957.

(13) Chartoire, A.; Nolan, S. P. In New Trends in Cross-Coupling; Colacot, T., Ed.; *RSC Catalysis Series*; Royal Society of Chemistry: Cambridge, **2014**; pp 139–227.

(14) Valente, C.; Calimsiz, S.; Hoi, K. H.; Mallik, D.; Sayah, M.; Organ, M. G. *Angew. Chem. Int. Ed.* **2012**, *51*, 3314.

(15) Gründemann, S.; Kovacevic, A.; Albrecht, M.; Faller, J. W.; Crabtree, R. H. *Chem. Commun.* **2001**, 2274.

(16) Gründemann, S.; Kovacevic, A.; Albrecht, M.; Faller, J. W.; Crabtree, R. H. *J. Am. Chem. Soc.* **2002**, *124*, 10473.

(17) Sini, G.; Eisenstein, O.; Crabtree, R. H. *Inorg. Chem.* **2002**, *41*, 602.

(18) Eguillor, B.; Esteruelas, M. A.; Oliván, M.; Puerta, M. *Organometallics* **2008**, *27*, 445.

(19) Lebel, H.; Janes, M.K.; Charette, A.B.; Nolan, S. P. *J. Am. Chem. Soc.* **2004**, *126*, 5046.

(20) Viciu, M.S.; Germaneau, R.F.; Nolan, S. P. *Org. Lett*. **2002**,*4*, 4053.

(21) He, G.; Kang, L.; Torres Delgado, W.; Shynkaruk, O.; Ferguson, M. J.; McDonald, R.; Rivard, E. *J. Am. Chem. Soc.* **2013**, *135*, 5360.

(22) Hall, D. G., *Boronic Acids: Preparation and Applications in Organic Synthesis, Medicine and Materials (Volume 1 and 2), Second Edition* - Wiley Online Library; Wiley-VCH Verlag GmbH & Co., **2011**.

(23) Viciu, M.S.; Navarro, O.; Germaneau, R.F.; Kelly, III, R.A.; Sommer, W.; Marion, N.; Stevens, E.D.; Cavallo, L.; Nolan, S. P. *Organometallics* **2004**, *23*, 1629.

(24) Dröge, T.; Glorius, F. *Angew. Chem. Int. Ed*. **2010**, *49*, 6940.

(25) Clavier, H.; Nolan, S. P. *Chem. Commun*. **2010**, *46*, 841.

(26) Poater, A.; Cosenza, B.; Correa, A.; Giudice, S.; Ragone, F.; Scarano, V.; Cavallo, L. *Eur. J. Inorg. Chem*. **2009**, 1759-1766.

(27) Wu, L.; Drinkel, E.; Gaggia, F.; Capolicchio, S.; Linden, A.; Falivene, L.; Cavallo, L.; Dorta, R. *Chem. Eur. J*. **2011**, *17*, 12886.

(28) Pangborn, A. B.; Giardello, M. A.; Grubbs, R. H.; Rosen, R. K.; Timmers, F. J. *Organometallics* **1996**, *15*, 1518.

(29) Bantreil, X.; Nolan, S. P. *Nat. Protoc*. **2011**, *6*, 69.

(30) Powers, K.; Hering-Junghans, C.; McDonald, R.; Ferguson, M. J.; Rivard, E. *Polyhedron*. DOI: 10.1016/j.poly.2015.07.070.

(31) Marion, N.; Navarro, O.; Mei, J.; Stevens, E. D.; Scott, N. M.; Nolan, S. P. *J. Am. Chem. Soc.* **2006**, *128*, 4101.

(32) Prasad, B. A. B.; Gilbertson, S. R. *Org. Lett*. **2009**, *11*, 3710.

(33) O'Brien, C. J.; Kantchev, E. A. B.; Valente, C.; Hadei, N.; Chass, G. A.; Lough, A.; Hopkinson, A. C.; Organ, M. G. *Chem. Eur. J*. **2006**, *12*, 4743.

(34) Bandari, R.; Höche, T.; Prager, A.; Dirnberger, K.; Buchmeiser, M. R. *Chem. Eur. J*. **2010**, *16*, 4650.

(35) Ackermann, L.; Potukuchi, H. K.; Althammer, A.; Born, R.; Mayer, P. *Org. Lett*. **2010**, *12*, 1004.

(36) Cahiez, G.; Chaboche, C.; Mahuteau-Betzer, F.; Ahr, M. *Org. Lett.* **2005**, *7*, 1943.

(37) Al-Rafia, S. M. I.; Ferguson, M. J.; Rivard, E.; *Inorg. Chem*. **2011**, *50*, 10543.

Chapter Four

(1) Gaillard, S.; Bosson, J.; Ramón, R. S.; Nun, P.; Slawin, A. M. Z.; Nolan, S. P. *Chem. Eur. J.* **2010**, *16*, 13729.

(2) Hickey, J. L.; Ruhayel, R. A.; Barnard, P. J.; Baker, M. V.; Berners-Price, S. J.; Filipovska, A. *J. Am. Chem. Soc.* **2008**, *130*, 12570.

(3) Díez-González, S. N-Heterocyclic Carbenes: From Laboratory Curiosities to Efficient Synthetic Tools; *Royal Society of Chemistry*, 2011.